

Fluoro-substituted prolines as structural labels
for solid state ^{19}F -NMR of polypeptides

Zur Erlangung des akademischen Grades eines

DOKTORS DER NATURWISSENSCHAFTEN
(Dr. rer. nat.)

Fakultät für Chemie und Biowissenschaften

Karlsruher Institut für Technologie (KIT) – Universitätsbereich

genehmigte

DISSERTATION

von

Volodymyr Kubyshkin

aus

Jalta

Dekan: Prof. Martin Bastmeyer

Referent: Prof. Anne S. Ulrich

Korreferent: Prof. Michael A. R. Meier

Tag der mündlichen Prüfung:

21 Dezember 2012

Table of contents

Table of contents.....	2
Acknowledgements	5
1. Introduction.....	7
1.1. Fluorine substituted amino acids and polypeptides.....	7
1.2. Studies of membrane active peptides by solid state NMR.....	7
1.2.1. Membrane active peptides.....	7
1.2.2. Solid state ¹⁹ F-NMR for investigation of peptide-membrane interaction.....	9
1.2.3. Antimicrobial peptide gramicidin S.....	11
1.2.4. Cell penetrating peptide SAP.....	12
1.3. Fluorine labeled amino acids for structural investigation of membrane active peptides.....	12
1.4. Structure and properties of proline residue in peptides and proteins.....	14
1.5. Synthesis of trifluoromethylated proline related structures.....	15
1.5.1. Proline related structures.....	15
1.5.2. Structures trifluoromethylated in position two.....	15
1.5.3. Structures trifluoromethylated in position three.....	19
1.5.4. Structures trifluoromethylated in position four.....	20
1.5.5. Structures trifluoromethylated at ω-position.....	23
1.5.6. Trifluoromethylated methanoprolines.....	24
2. Aims of this study.....	25
3. Results.....	27
3.1. Geminal difluoro-4,5-methanoproline.....	28
3.1.1. Amino acid synthesis.....	28
3.1.2. Kinetics of t-F ₂ MePro decomposition in N-protected form.....	30
3.1.2.1. Decomposition of the trifluoroacetic salt of H-t-F ₂ MePro-OMe in chloroform.....	30
3.1.2.2. Decomposition of the trifluoroacetic salt of H-t-F ₂ MePro-OH in water.....	31
3.1.2.3. Decomposition of the basic form of H-t-F ₂ MePro-OH in water.....	34
3.1.3. The 7,7-difluoro-2-azabicyclo[4.1.0]heptane system.....	34
3.2. Dipeptides with F ₂ MePro amino acid.....	34
3.2.1. Synthesis of ^D Phe-t-F ₂ MePro dipeptide.....	35
3.2.2. Synthesis of Pro-t-F ₂ MePro dipeptide.....	36
3.2.3. Configuration of the F ₂ MePro dipeptides.....	37
3.3. Miscellaneous amino acids.....	40
3.4. Peptide synthesis.....	41
3.4.1. Synthesis of proline substituted gramicidin S analogues.....	41
3.4.2. Synthesis of leucine substituted gramicidin S analogues.....	42
3.4.3. Synthesis of proline substituted SAP analogues.....	43
3.4.4. Synthesis of the peptides with F ₂ MePro.....	44
3.5. Properties of the gramicidin S analogues.....	44

3.5.1. Hydrophobicity (RP-HPLC).....	44
3.5.2. Antimicrobial activity (MIC).....	45
3.5.3. Conformation (CD).....	47
3.5.4. Hemolytic activity (HC ₅₀).....	49
3.6. Solid state NMR of GS analogues in lipid membranes.....	51
3.6.1. FPhg substituted peptides.....	51
3.6.2. II-B(t)-GS.....	53
3.6.3. I-B(t)-GS.....	56
3.6.4. II-A(c)-GS.....	56
3.6.5. II-TfmPro-GS and I-TfmPro-GS.....	57
3.6.6. II-Flp-GS.....	58
3.6.7. II-flp-GS.....	59
3.6.8. Peptides with geminal F ₂ substituent in solid state NMR.....	59
3.6.9. Influence of the GS analogues on lipid bilayers (³¹ P-NMR).....	61
3.7. Conformational analysis of SAP analogues in solution.....	64
3.8. Solid state NMR of SAP analogues in lipid membranes.....	67
3.8.1. TfmMePro substituted SAP analogues.....	67
3.8.2. TfmPro substituted SAP.....	69
3.8.3. ³¹ P-NMR spectra of oriented lipid samples with SAP analogues.....	70
4. Discussion.....	72
4.1. The antimicrobial peptide gramicidin S.....	72
4.1.1. Activity against Gram-positive strains.....	72
4.1.2. Activity against Gram-negative strains.....	73
4.1.3. Hemolytic activity.....	74
4.1.4. Understanding specific oligomerization of gramicidin S.....	75
4.1.5. Spectral populations with low molecular mobility.....	77
4.2. Cell penetrating peptide SAP.....	79
4.2.1. Conformation in solution.....	79
4.2.2. Behavior of SAP in lipids.....	82
4.3. Labeling the proline position: general remarks.....	83
4.3.1. Extrapolation of the data achieved on fluorine substituted peptides on the wild type peptides.....	83
4.3.2. Flp/flp.....	84
4.3.3. c/t-TfmMePro.....	85
4.3.4. TfmPro.....	86
4.3.5. F ₂ MePro and F ₂ Pro.....	86
5. Conclusions.....	88
6. Zusammenfassung (German).....	89
7. Experimental part.....	91
7.1. General organic synthesis.....	91
7.1.1. Procedures towards Fmoc-amino acids.....	98
7.2. Peptide synthesis.....	100
7.2.1. Synthesis of gramicidin S analogues.....	100
7.2.2. Synthesis of SAP analogues.....	100

7.3. Antimicrobial activity test.....	102
7.4. Circular dichroism measurements.....	102
7.5. Hemolysis assays.....	103
7.6. Solid state NMR studies in lipid bilayers.....	104
7.6.1. Instruments and pulses.....	104
7.6.2. Peptide-lipid sample preparation.....	105
7.6.3. Miscellaneous experimental parameters.....	105
Curriculum Vitae.....	106
References.....	108

Acknowledgements

The author acknowledges all people who supported this work on any step of its accomplishment. In particular, to

Julia Misiewicz, Eva Stockwald and Dr. Torsten Walther for their instant help in preparation of the manuscript,

Christian Weber, who helped me to stand on my own two feet in a new laboratory,

members of the analytical department in IOC for the high quality analytical expertise,

Dr. Parvesh Wadhvani for useful advice concerning synthesis,

Dr. Tamta Turtzeladze, Dr. Birgit Lange, Gabriele Buth, Claudia Weber and Anni Barwig for their help with formalities,

Markus Schmidt and the NMR team at the IBG-2 institute for child care during me while learning NMR equipment,

Dr. Joachim Bürck, Siegmund Roth and Bianca Posselt for the help with CD measurements and work on the ANKA synchrotron,

Dr. Marina Berditsch for good introduction into microbiology,

Dr. Stephan Grage for his help with adjustment of NMR experiments and discussions,

Prof. Igor Komarov and Dr. Pavel Mykhailiuk for many interesting ideas and advice, for providing with useful substances, and corrections,

Dr. Sergii Afonin for kind supervision and huge help in my work and private life,

Prof. Anne Ulrich for supervision of my work and planning it, for the inspiration and trust.

Special thanks to the referee for their impartial judgement.

Thank you!

This work was financially supported by CFN Project E1.2 and the state Baden-Württemberg (Landesgraduiertenförderung). Synchrotron Light Source ANKA is acknowledged for provision the instrument time at their beamlines.

1. Introduction

1.1. Fluorine substituted amino acids and polypeptides

Fluorine containing substances are widely used in modern chemical industry and research. About 20-25% of all drugs in the pharmaceutical market contain at least one fluorine atom¹. In agrochemicals this number is even higher ~ 30%². This reasonably high abundance of synthetic organofluorine compounds reflects³ the unique properties of fluorine and its chemical bonds. The fluorine atom possesses a small van der Waals radius (1.47 Å) similar to hydrogen (1.20 Å), meaning that it is a good substituent for hydrogen from the steric perspective. Polarity of the C-F bond is inverted in comparison to C-H, even though the molecular size remains very similar. The C-F bond is very stable against chemical modifications. The toxicity of organofluorine substances is significantly lower than of other organohalogenides.

Incorporation of fluorine into proteins for analytical purposes has also attracted significant attention^{4,5}. Fluorine labeling enables sensitive ¹⁹F-NMR studies⁶, for instance membrane protein structure investigation⁷ or even *in vivo* protein detection⁸.

Biosynthetic fluorine labeling can be done in two ways. The nucleophilicity of the side chains of cysteine, tyrosine and lysine, as well as disulfide bond formation in cysteine, enable chemical ligation of those residues with fluorine containing moieties⁹. Another opportunity is the selective biosynthetic incorporation by recombinant protein expression. Numerous fluorinated amino acids, derivatives of natural amino acids, were reported in proteins to date, of which aromatic ones are the most popular⁵.

Chemical incorporation via peptide synthesis is more straightforward and should be preferred for shorter sequences (up to 30-40 residues). Synthetic fluorine labeling requires the amino acids to be available. Recent developments of the fluorine substituted amino acids synthesis have been reviewed^{10,11,12,13}. Trifluoromethylation of the peptide backbone has been discussed separately¹⁴.

Other fluorinated so-called *fluorous* materials have been applied for numerous structural biological studies^{15,16}, in particular they were used for ¹⁹F magnetic resonance imaging in tissues¹⁷. The application of fluorine in various aspects of medicinal and pharmaceutical chemistry has also been recently reviewed in a dedicated book¹⁸.

1.2. Studies of membrane active peptides by solid state NMR

1.2.1. Membrane active peptides

Membrane active peptides (MAPs) are a class of peptides with a broad functional range, all of which involve the interaction with cell membranes as an

obligatory step. The most well studied MAPs are antimicrobial and cell penetrating peptides.

Antibacterial peptides are known since 1939 when gramicidins were first extracted from the soil bacterium *Bacillus brevis*¹⁹. Since then, peptides with bactericidal action were found in all kinds of living organisms. Small (6-59 residues) amphipathic, charged peptides (as well as protein fragments) are considered to be part of the innate immune system²⁰. For some of them the mechanism of action was elucidated. Ion-channel formation was claimed for gramicidin A²¹, oligomeric “barrel stave” pores with 3-11 parallel helices were described for alamethicin, toroidal “wormhole” pores involving lipid molecules were postulated for magainin 2²² (see Fig.1.1.). The disturbance of the membrane integrity via formation of long lived pores is the apparent reason of losing the membrane potential which is essential for ATP synthesis in prokaryotic cells. This is considered to be the prime mode of action for most cytotoxic MAPs. For many of antimicrobial peptides, for which the specific mechanism is not known, a “carpet” model was proposed²³: the amphipathic peptides possess a high affinity to lipid membranes; after binding, the peptides significantly change the biophysical properties of the target membrane and make it unstable or leaky. However, many antimicrobial peptides showed also significant damage of eukaryotic cells such as human erythrocytes. The cell selectivity (prokaryotic vs eukaryotic) is very important for clinical application and represents a significant challenge for current exploration²⁴.

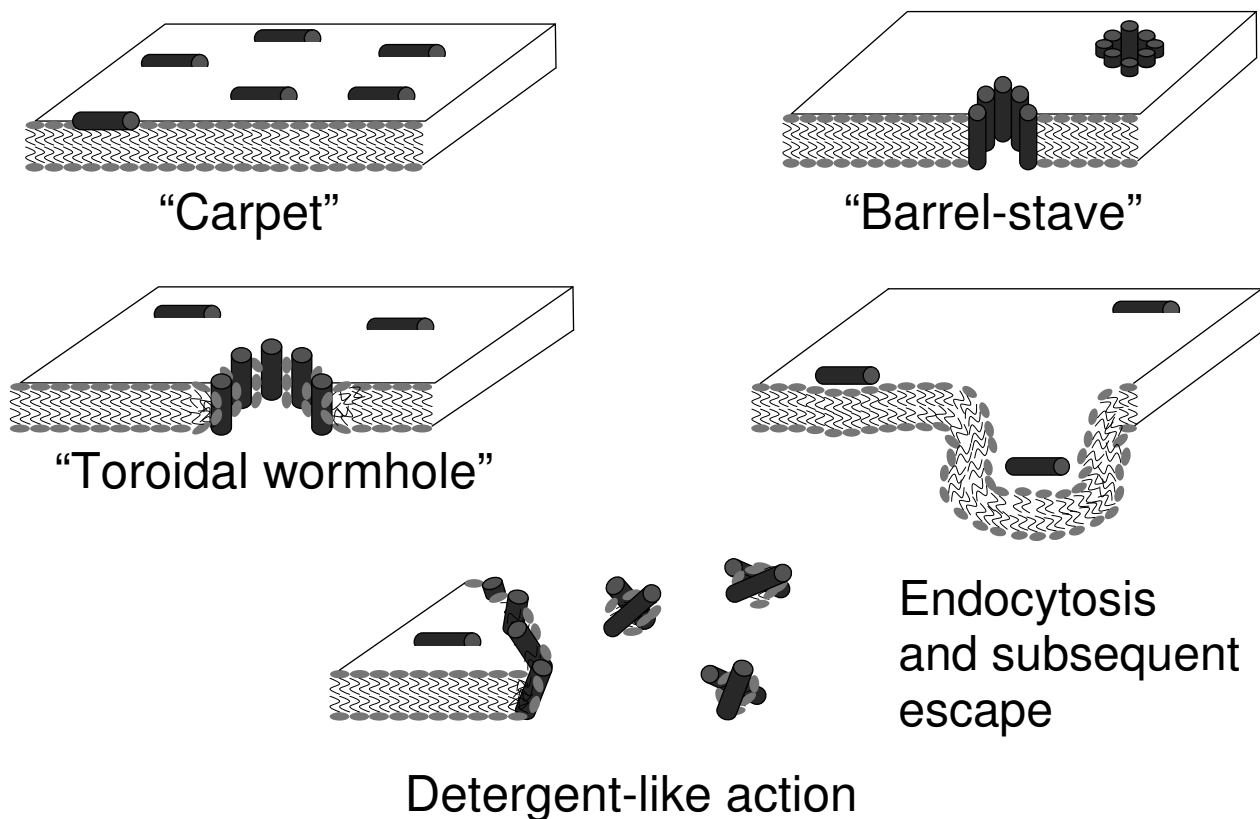


Figure 1.1. Models of action of MAPs on lipid membranes. Summarized in²⁵.

Cell penetrating peptides were discovered about 20 years ago. They can cross lipid membranes and deliver different cargos (either bound covalently or as molecular complexes) into the cell^{26,27,28}. The mechanisms of cell entry are believed to be either various endocytosis associated events or direct translocation. The latter may involve cooperative transient membrane bound structures, similar way as in antimicrobial peptides. Cell penetrating peptides are also short, positively charged and amphipathic. This suggests that both classes of MAPs are fundamentally similar and they could share same mechanism of action.

1.2.2. Solid state ¹⁹F-NMR for investigation of peptide-membrane interaction

Understanding the mechanisms of peptide-membrane interactions is an important biophysical task. It should reveal the reasons for cell selectivity as well as the structure activity relationships. The mechanism should also answer the question: how to tune a given peptide sequence to possess only the desired functionality (e.g. antimicrobial or cell penetrating)? From this perspective, solid state NMR can provide a significant insight.

Solid state ¹⁹F-NMR of peptides was successfully used for structural studies of MAPs. The method is based on specific labeling of peptide sequences with fluorine substituted amino acids, and investigation of the resulting peptides in model bilayers or even in native biomembranes^{29,30}.

The different basic mechanisms (Fig. 1.1) can be distinguished from three simple characteristics: 1) alignment of the peptide relative to the membrane normal, 2) the oligomerization state of the peptide molecules, 3) mobility of the peptides. In solid state NMR experiments these parameters can be directly measured in macroscopically oriented samples of lipid bilayers (Fig.1.2.). If the peptide is carrying a label which is rigidly attached to the backbone, the orientation of the NMR label can be determined from the spectra in a suitable NMR experiments. The data must be collected from several independent locations in the peptide secondary structure. From several orientational constants the peptide orientation can be deduced. Distances between labels can also be measured by NMR. The mobility of peptide is reflected in the NMR spectra either after corresponding data analysis (e.g. getting S_{mol} parameter) or by observation of the relaxation rate (T_1 , T_2 , $T_1\rho$ constants as well as the line widths).

Among the different NMR labels that could be applied for peptides, ²H, ¹³C, ¹⁵N and ¹⁹F nuclei are normally used. Even though the fluorine atom is not present in natural peptides, ¹⁹F labeling has several significant advantages: the high NMR sensitivity of the ¹⁹F nucleus (0.94 of the ¹H magnetogyric ratio), 100% natural abundance of the ¹⁹F isotope, and no natural background. Thus, the solid state NMR measurements can be performed fast and with a very low concentration of label in the sample. High sensitivity of ¹⁹F-NMR leads to significant shortening of the total spectral acquisition time compared to other labels. Qualitative changes in the peptide state cause qualitative changes in the resulting NMR spectra, which can

be easily observed. Because of the latter two reasons, ^{19}F -NMR enables fast, high quality biophysical investigations under various conditions.

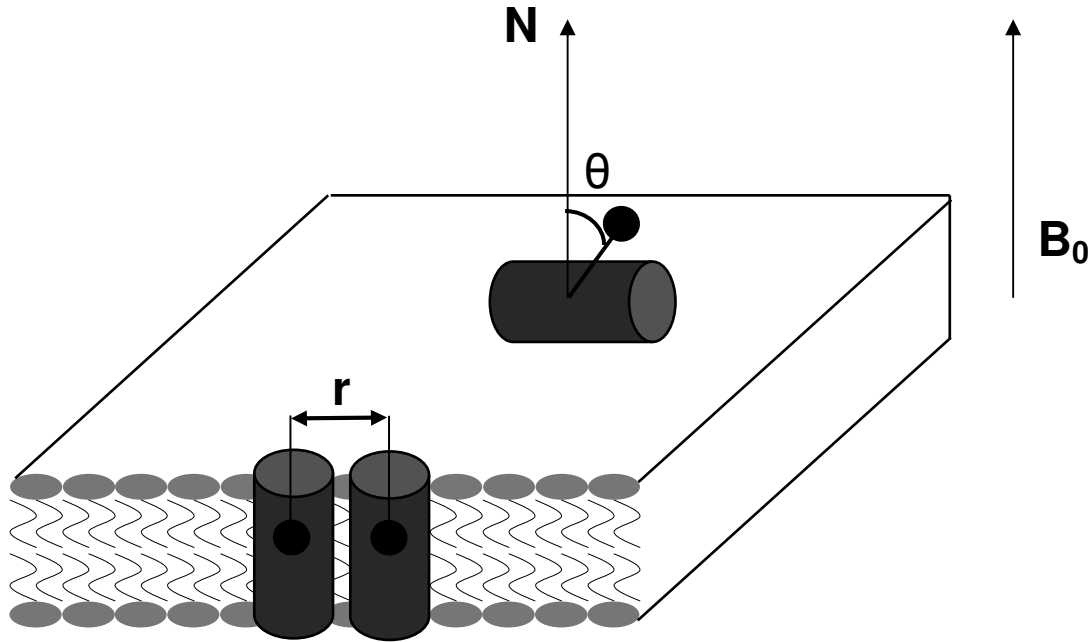


Figure 1.2. Solid state NMR parameters used for characterizing MAPs in oriented membrane samples. The spectrometer magnetic field direction is shown as B_0 . The membrane normal is shown as N . The angle between the label and the bilayer normal (θ) and the inter-label distance (r) can be determined by the NMR experiments²⁹.

Furthermore, the spectral parameters can be converted into quantitative values for characterizing the peptide mobility and orientation. The resonance frequency of the label with a spin of $\frac{1}{2}$ is defined by the total Hamiltonian (\hat{H}_{res}) with several contributious (eq. 1): isotropic chemical shielding (\hat{H}_{δ}), indirect dipolar coupling (\hat{H}_J), chemical shift anisotropy (\hat{H}_{CSA}) and direct dipolar coupling (\hat{H}_D). The first two are present in solution NMR, and the last two ones additionally appear in solid state NMR and dominate the spectra in the case when anisotropy is present in the sample.

$$\hat{H}_{\text{res}} = \hat{H}_{\delta} + \hat{H}_J + \hat{H}_{\text{CSA}} + \hat{H}_D \quad (\text{equation 1})$$

If the membrane bound peptide is labeled with a fluorine atom, the chemical shift depends on the label orientation (chemical shift anisotropy). The chemical shift in this case is composed of the isotropic and anisotropic contributions, where the latter is governed by the label tensor (spatial orientation). For instance, in the case of a trifluoromethyl group the chemical shift depends on the macroscopical orientation in the magnetic field of the spectrometer. In this case the additional interaction, dipolar coupling, will lead to an appearance of three spectral components (triplet), where the coupling constant depends also on the orientation, according to eq. 2, as further illustrated in Fig. 1.3:

$$\Delta_{CF_3} = S_{\text{mol}} \Delta_{CF_3}^0 \frac{3\cos^2 \theta - 1}{2}, \quad (\text{equation 2})$$

where $\Delta_{CF_3}^0$ is the maximum dipolar splitting of the trifluoromethyl group (15.8 kHz), and S_{mol} is the molecular wobbling parameter ($1 \geq |S_{mol}| \geq 0$).

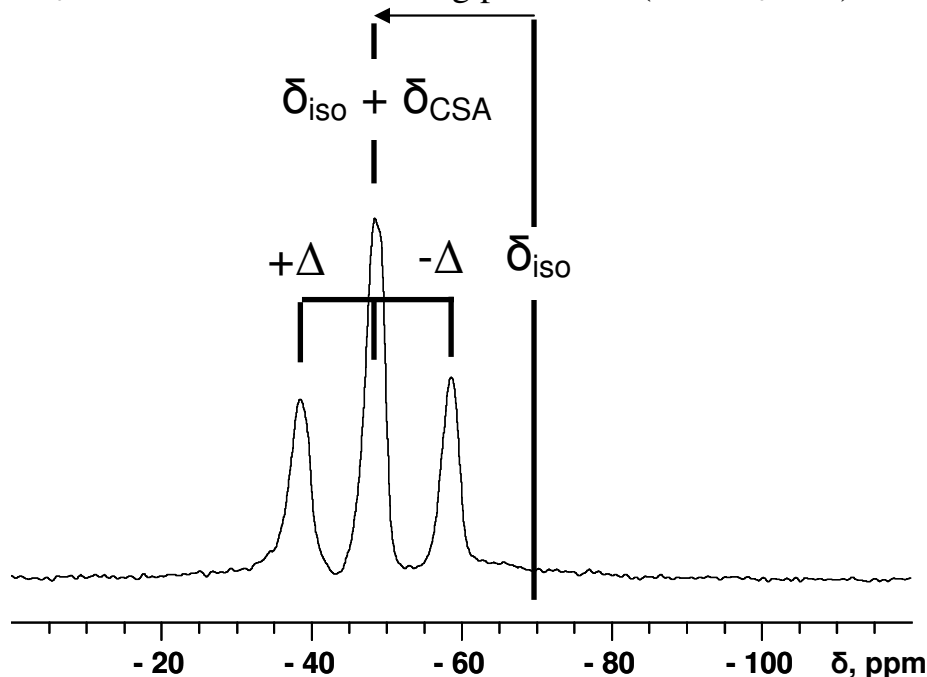


Figure 1.3. Typical signal of a trifluoromethyl group in ^{19}F -NMR in macroscopically oriented samples containing CF_3 -labeled peptide. The chemical shift anisotropy component (δ_{CSA}) moves the signal away from the isotropic position (δ_{iso}). The signal is a triplet with an orientation dependent splitting Δ due to the dipolar coupling between the three chemically equivalent fluorine atoms.

1.2.3. Antimicrobial peptide gramicidin S

Gramicidin S (GS) is an antimicrobial peptide first isolated in 1943 from the soil bacterium *Aneurinibacillus migulanus* (former *Bacillus brevis*)³¹. It possesses high activity against Gram-positive bacteria, and is modestly active against Gram-negative bacteria as well some fungi^{32,33}. It shows also high hemolytic activity, which prevents its broad use in medicine. GS is one of the well-studied antimicrobial peptides, as by the year of 2012 the number of papers referring to gramicidin S exceeds 1000.

The structure of gramicidin S is *cyclo*[Val-Orn-Leu-^DPhe-Pro]₂ as shown on Fig. 1.4. Kato and Izumiya postulated that the amphiphilic *sidedness* of GS is essential for its membrane binding³⁴: leucine and valine residues constitute the hydrophobic face, and charged ornithine residues the hydrophilic side of the molecule. This amphipathic structure correlates with the amphipathic profile of lipid membranes and was indeed experimentally confirmed^{35,36}. In GS the Pro-^DPhe sequences form two β -turn type-II structure, which enables the molecule to become cyclic. The two Val-Orn-Leu chains form an antiparallel β -sheet, where Val and Leu form four intra-molecular hydrogen bonds.

The mechanism of the toxic action is still not quite clear, and optimization of its cell selectivity is still a subject of discussion in many biophysical^{37,38,39} and chemical^{40,41,42,43} studies.

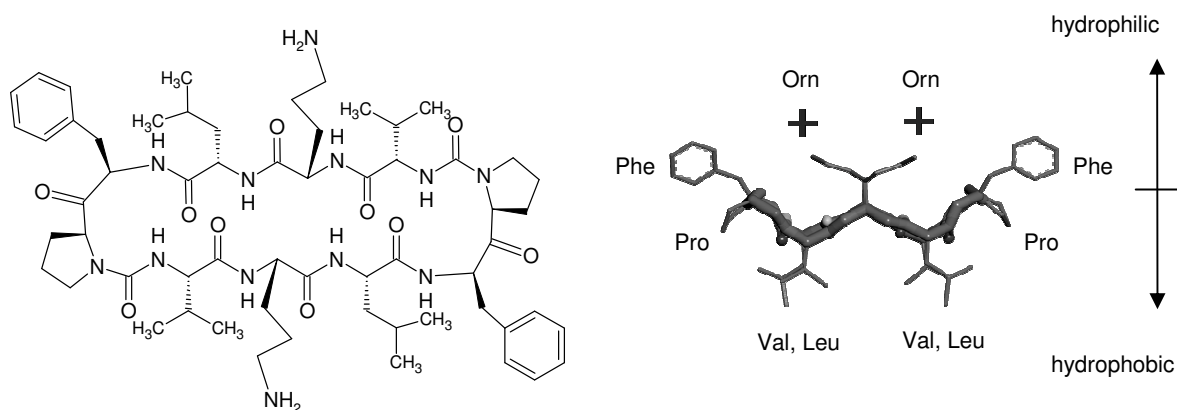


Figure 1.4. Structure of gramicidin S: chemical (left), spatial (right), illustrating the sidedness of the amphipathic molecule.

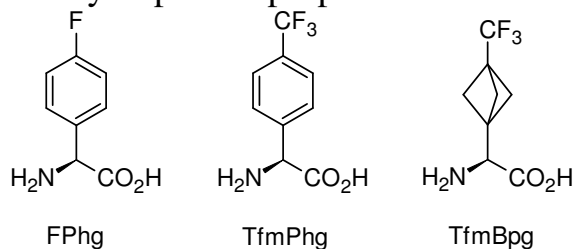
1.2.4. Cell penetrating peptide SAP

The cell penetrating peptide SAP (“sweet arrow peptide”) was designed in 2004⁴⁴. The sequence of the N-terminal repetitive domain (Val-His-Leu-Pro-Pro-Pro)₈ of the maize γ -zein protein was taken as a template, and the hydrophilic residues as well as the peptide length were varied in a systematic study. The sequence (Val-Arg-Leu-Pro-Pro-Pro)₃ showed the highest uptake by HeLa cells and no cytotoxicity up to very high concentrations (about 1 mM). Thus, this sequence (named SAP) was postulated to be an optimal cell penetrating peptide.

SAP belongs to the proline-rich peptide family⁴⁵, which undergoes an equilibrium in solution between a poly-L-proline type II helix (PPII) and random coil conformations. When SAP is structured as PPII, the three arginines are located on the same face of the helix such that the molecule gets amphipathic. At high concentrations PPII helices can assemble to cylindrical micelles. This kind of assembly is also important for the parent zein protein for the protein body biogenesis⁴⁶.

1.3. Fluorine labeled amino acids for structural investigations of membrane active peptides

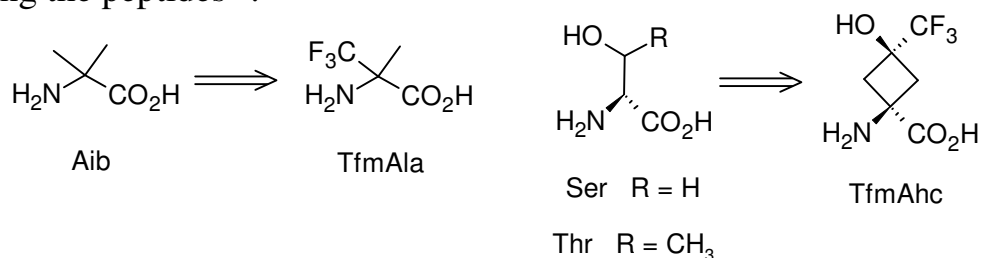
To determine the structures of MAPs in lipid membranes, the fluorine labeled amino acids should be introduced into the peptide sequence with the least possible perturbations. Several hydrophobic ¹⁹F-substituted amino acids have been applied for labeling Leu, Ile, Val, Ala and Met. They represent different generations with successfully improved properties as ¹⁹F-NMR reporters.



First, 4-fluorophenylglycine (FPhg) was applied^{47,48}. This amino acid has a phenyl ring serving as a linker between the α -carbon and the fluorine atom. The linker provides a rigid attachment of the label to the peptide backbone, which is a fundamental prerequisite for the method to work. However, the chemical shift of the fluorine atom in this case depends not only on the macroscopic orientation of the C-F bond, but also on the rotameric state of the phenyl ring. Also, precise chemical shift referencing in solid state NMR is a tough task⁴⁹.

Such complications were overcome by changing the reporter from a single fluorine to a trifluoromethyl group, by introducing trifluoromethylphenylglycine (TfmPhg)⁵⁰. The trifluoromethyl group undergoes fast rotation along the C-CF₃ bond, thus any conformational changes in the side chain do not contribute to the label anisotropy. The dipolar splitting of a CF₃-group delivers the same information as the CSA, but it does not require referencing. Unfortunately, phenylglycine residues suffer from significant racemization during Fmoc peptide synthesis (normally Hünig base is employed for amino acid couplings).

The racemization problem was solved by changing the linker type, as bicyclo[1.1.1]pentane was taken instead of the phenyl ring. The amino acid TfmBpg was specially designed and synthesized for such structural studies⁵¹. Chemically, it behaves like a normal α -amino acid, without significant increase of the α -CH acidity, and thus no racemization. Hence, it was successfully used for labeling the peptides⁵².



Several other amino acids were also used for specific labeling of peptides. Trifluoromethylalanine (TfmAla)⁵³ was used for labeling in place of aminoisobutyric acid (Aib) in the Aib-rich peptide alamethicin⁵⁴. Incorporation of these amino acids imposes a synthetic challenge. Both TfmAla and Aib are quaternary amino acids. Also, in TfmAla both functional groups suffer from significant deactivation in peptide synthesis due to the electron withdrawing nature of the CF₃-group. Introduction of this amino acid into a peptide was not a trivial task but it was solved in the following way. The TfmAla residue was first incorporated in the middle position of a tripeptide, which was used as a building block in the solid state peptide synthesis (SPPS) of alamethicin analogues. Both (R)- and (S)-forms of TfmAla were applied, since the parent amino acid Aib is non-chiral. This trick provided some additional information in solid state NMR studies (twice more labels).

Another amino acid, trifluoromethyl-aminohydroxycyclobutanecarboxylic acid (TfmAhc), was recently developed as a ¹⁹F-label to replace serine (Ser) and threonine (Thr). It was used in place of serine in the antimicrobial peptide temporin

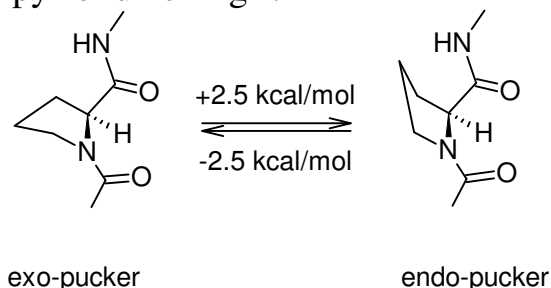
A⁵⁵, as well as in antimicrobial peptides from the magainin family (PGLa and magainin 2)⁵⁶.

Recently the labeling of peptides with trifluoromethylated amino acids, including their synthesis and solid state ¹⁹F-NMR results, was discussed in a comprehensive review⁵⁷. It is also worth mentioning that peptide labeling has to be done with caution: non-natural structures are introduced into peptide sequences eventually delivering peptides different from the original one. Conformational and activity studies should therefore be done for each of the labeled peptide analogues in order to ensure that the wild type peptide structure and function are maintained.

1.4. Structure and properties of proline residue in peptides and proteins

Among all proteinogenic amino acids, proline (Pro) possesses several unique properties. In fact, it is an imino acid with very different propensities for secondary structures than common α -amino acids^{58,59}. Namely, it does not support an α -helix and therefore is most often being found in turns (kinks and loops), in polyproline II structures, as well as at the ends of regular α -helices and β -strands.

Proline ring is already conformationally restricted such that the ϕ angle is fixed around -60° . A proline conformation is normally described in terms of exo- and endo-puckers of the pyrrolidine ring⁶⁰.



Substituents in the ring can significantly shift the equilibrium between the two puckers,^{61,62} such that an anchoring can be achieved. This fact has significant impact on the *cis-trans* isomerization rate of the corresponding amide bond, a significant issue for protein folding in general^{63,64,65} and specifically for the stability of the polyproline II helix in collagen^{66,67}. *Cis-trans* isomerization of prolyl residues plays a key role in protein folding because of the enormously low reaction rate of this process (much slower as for any other natural amino acid). In contrast to the rest of canonical α -amino acids, proline enables *cis*-peptide bonds to occupy up to 5-50% of the total population in unstructured protein parts⁶⁸.

In nature the peptide bond isomerization of an N-acylated proline is controlled by chaperone of the class peptidyl prolyl *cis/trans* isomerases (PPIase)⁶⁹. These enzymes attract significant attention. For instance, Pin1 mediates phosphorylation dependent signaling and is supposed to play a pivotal role in the development of cancer, Alzheimer and other age related human diseases⁷⁰. PrsA was shown to be essential in the biosynthesis of penicillin binding proteins in *Bacillus subtilis*⁷¹. In the plant *Arabidopsis thaliana*, over-expression of the ROF2

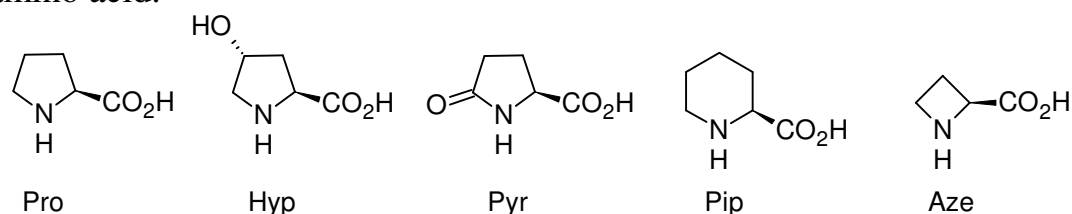
enzyme significantly modulates intracellular pH and causes tolerance of the cell to various inorganic toxic ions⁷².

1.5. Synthesis of trifluoromethylated proline related structures

1.5.1. Proline related structures

Several amino acids reported in the literature can be proposed for a proline substitution in peptides. First of all, commercially available 4-fluoroprolines can be used to label a peptide with fluorine. However, it was already mentioned that the use of a CF₃-group rather than a single fluorine offers significant advantage for the solid state NMR methodology. Also, the conformational restriction in the amino acid side chain has to be considered. Significant rigidity is an essential property to be able to calculate the peptide orientation from the NMR spectral parameters. Hence various trifluoromethylated prolines or *proline related structures* (the closest structural analogues) should be considered as the labels of choice. Also the size of the CF₃-moiety makes it a good anchor for fixing the pyrrolidine cycle in one particular conformation.

This chapter discusses the current literature concerning the synthesis of different trifluoromethylated prolines and similar structures. Five related skeletons will be considered: proline (Pro), hydroxyproline (Hyp), pyroglutamic (Pyr), pipercolic acid (Pip) and azetidincarboxylic acid (Aze). A few of these were found to occur in natural peptide sequences as well as Pro. Transformation of Hyp and Pyr in proline can be done synthetically and/or enzymatically. Pipercolic (homoproline) and azetidincarboxylic (norproline) acids can be considered as substituents for proline, both being the closest structurally related analogues of this amino acid.

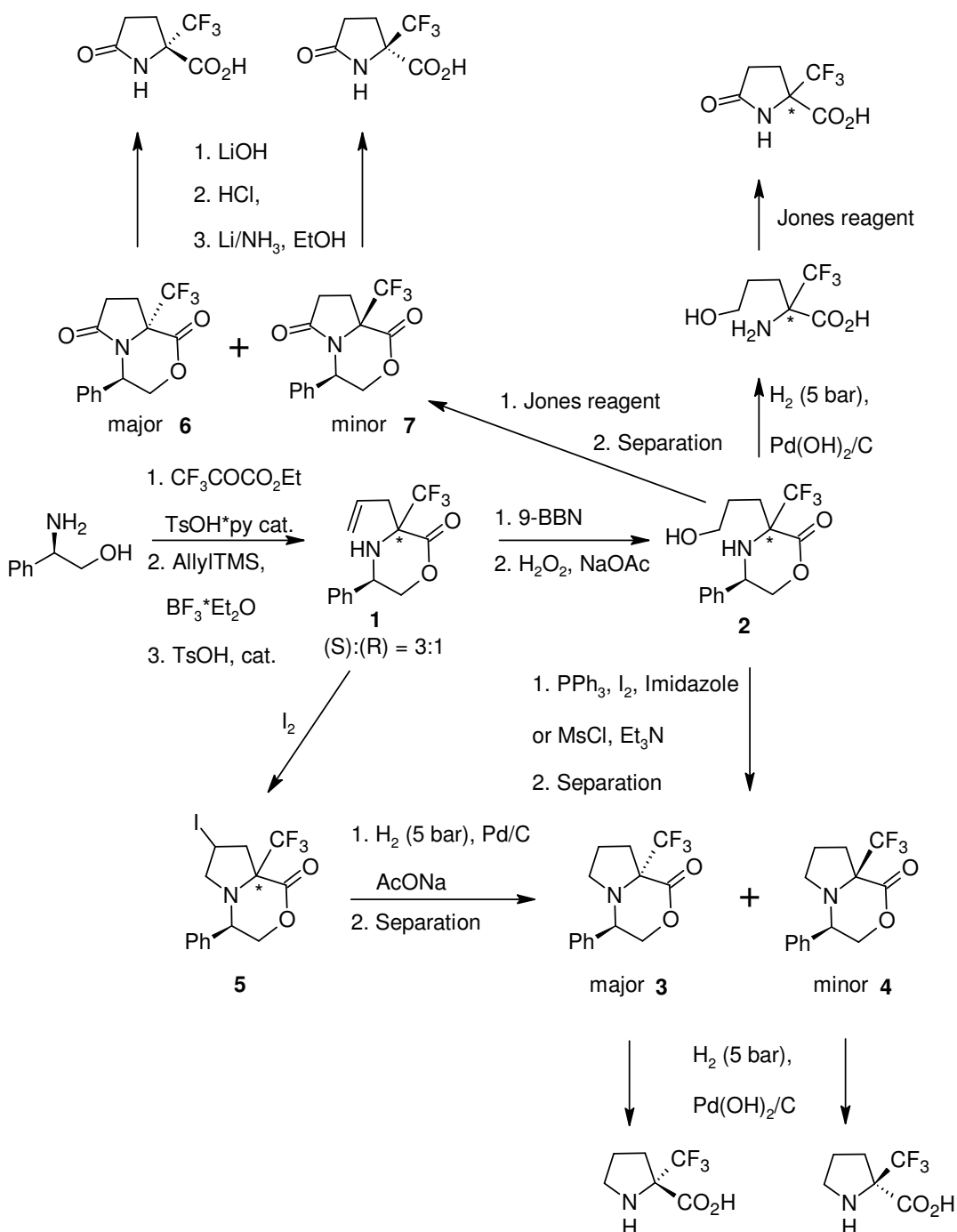


1.5.2. Structures trifluoromethylated at position two

The synthetic approaches are mostly based on the synthesis of linear α -trifluoromethylated structures, followed by formation of the C(5)-N bond to achieve cyclization to the proline 5-membered ring.

2-Tfm substituted proline (2-TfmPro) was first reported in 2006⁷³ (Scheme 1.1). The key intermediate was the corresponding allylated morpholinone **1**, which first was synthesized from N-Boc-(R)-phenylglycinol in a multigram scale with 67% yield and a diastereomeric ratio (R,S):(R,R) = 3:1. The allyl substituent was transformed into the terminal alcohol **2** in 90% yield by oxidative hydroboration. The cyclization was achieved either by substitution with iodine or by mesyl

activation. The resulting diastereomeric bicyclic products were separated by silica gel column chromatography to give two (S)- and (R)-isomers **3** and **4** in 45% and 15% (with iodine) or 64% and 14% (with mesyl activation) yields, respectively.



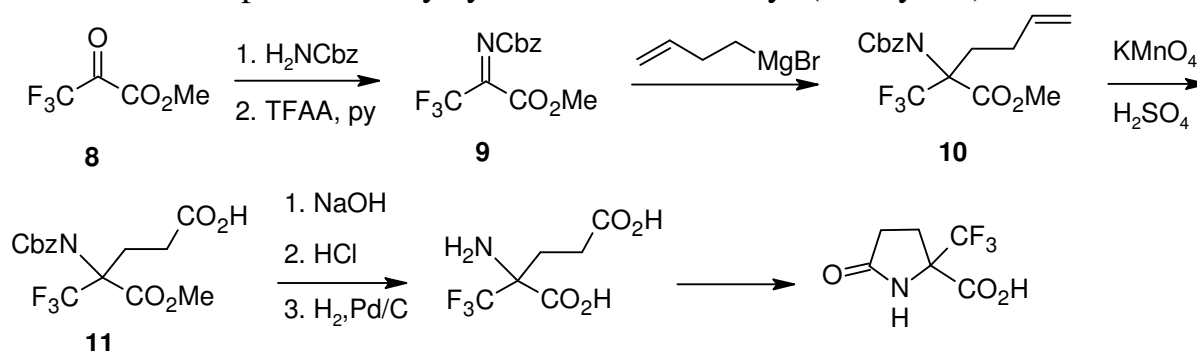
Scheme 1.1. Synthesis of 2-TfmPro and 2-TfmPyr in chiral forms.

Another method of proline ring closure upon iodocyclization was described by the same group later⁷⁴. Treatment with iodine under optimized conditions (in pure dichloromethane) gave the four stereoisomers **5** (87% total yield), which were then separated. The iodine atom was removed by hydrogenolysis with palladium catalysis in 52% and 25% yields for the (S)- and (R)-derivatives **3** and **4**,

respectively. The amino acids were eventually obtained upon stronger hydrogenolysis to yield enantiomerically pure (S)- and (R)-2-TfmPro (68% and 45% yields).

The same terminal alcohol intermediate **2** was used to get α -trifluoromethylated pyroglutamic acid as well. Remove of the protecting group, followed by Jones oxidation, gave 2-TfmPyr in 31% yield and with the same 50% *ee*. The inverted procedure allowed resolution of the diastereomers prior to oxydation by selective crystallization. This procedure gave 61% yield for (R,S)-**6** and 20% for (R,R)-**7**. The compounds were hydrogenated and isomeric (S)- and (R)-TfmPyr were obtained in 49% and 69% yields, respectively. These residues were later introduced into dipeptides at the N-terminal position using an optimized protocol⁷⁵, demonstrating the use in peptide synthesis.

Racemic 2-TfmPyr was first described in 1990⁷⁶ (Scheme 1.2.). Methyl trifluoropyruvate **8** was transformed into the corresponding imine **9** (60% yield), followed by a Grignard reaction with but-3-enylmagnesiumbromide (73% yield). Oxidation of the terminal double bond in **10** by acidic permanganate gave 96% of methyl ester **11**, which was then saponificated (99% yield). After hydrogenolysis, the 2-TfmGlu spontaneously cyclized into 2-TfmPyr (70% yield).

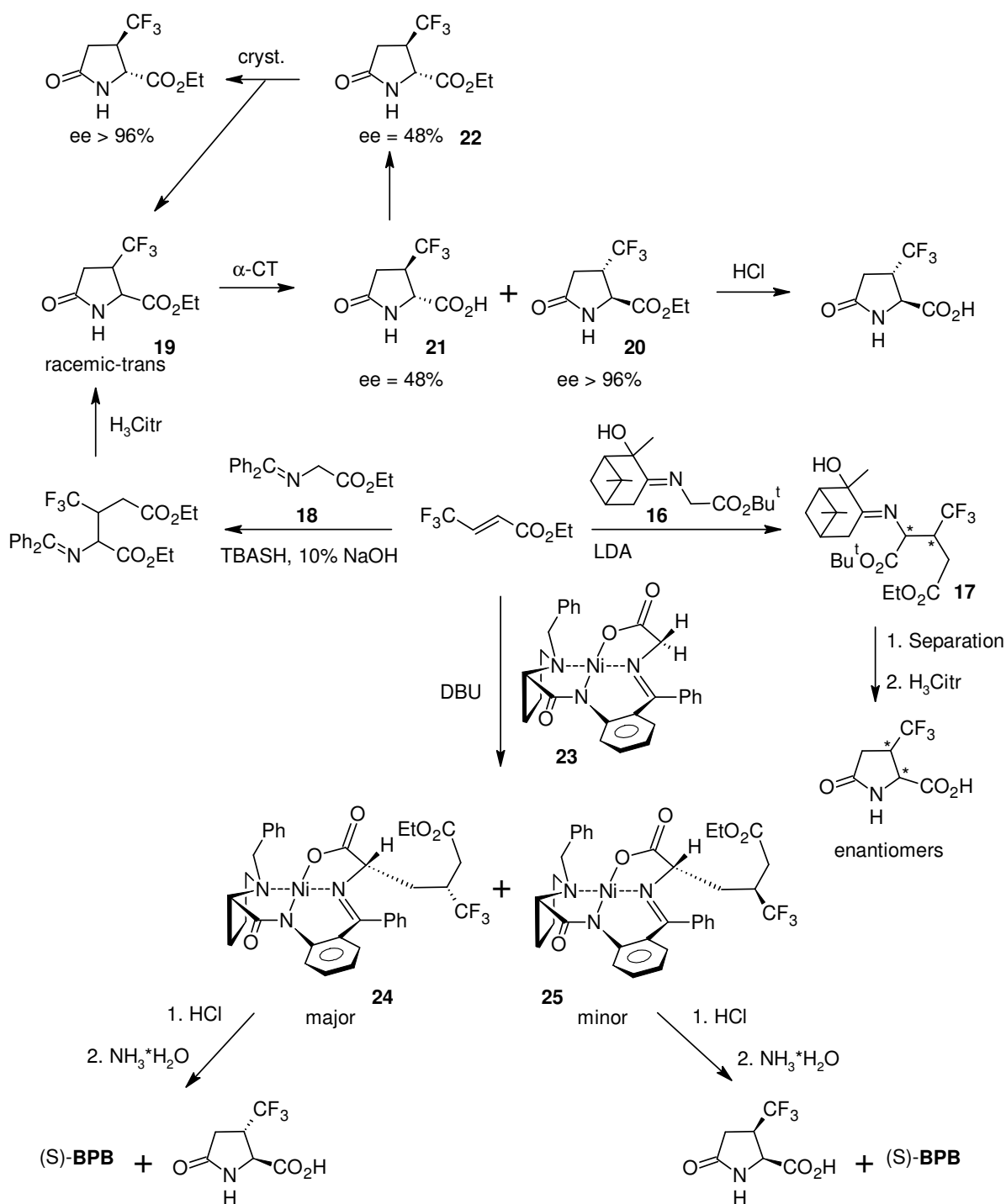


Scheme 1.2. Synthesis of 2-TfmPyr in the racemic form.

The resulting 2-TfmPyr has been used for synthesis of tripeptides, where the amino acid was introduced at the N-terminal position⁷⁷. The activity of the carboxylic group in α -alkylated peptides is known to be reduced. The synthesis was therefore performed with prolonged reaction time and with 4-5 fold excess of the amino acid at the coupling step.

The synthetic pathway towards racemic 2-TfmHyp is shown in Scheme 1.3⁷⁸. Product of the cycloaddition reaction **12** gave the desired amino acid upon hydrolysis in 68% yield.

The synthesis of the dehydro analogues of 2-TfmPro and 2-TfmPip in nonchiral forms is presented in scheme 1.4⁷⁹. The Grignard reaction (54-75% yields) followed by alkylation of the nitrogen atom using sodium hydride in DMF (55-81% yields) and the ring closure methathesis reaction, gave the protected amino acids **13** with 5-membered ($n = 0$, $m = 1$) ring in 45-50% and 6-membered ($n = m = 1$) in 93-98% yields, respectively.



Scheme 1.6. Synthetic approaches towards isomeric 3-TfmPyr.

The first approach⁸¹ used the pinen derivative **16** which gave the Michael adduct **17** as mixture of four isomers, with the ratio 52(*cis*):31(*trans*):13(*cis*):4(*trans*) and 63% overall yield. The first two diastereomers were successfully separated by column chromatography.

The second approach⁸² with the benzophenone derivative **18** yielded in an optimized procedure (with sodium hydroxide in the condensation and citric acid on the hydrolysis steps) only the racemic *trans*-diastereomer (95% overall yield). The enantiomeric mixture was resolved by an α -chemotrypsin (α -CT) assisted

hydrolysis of the ethyl esters (65% conversion), giving the (2S,3S)-isomer **20** in high and the (2R,3R)-isomer **21** in medium purity. The latter substance was finally purified by crystallization of its ethyl ester (17% chemical yield). Hydrolysis of the corresponding ethyl ester **22** gave the free (2R,3R)-amino acid (95% yield).

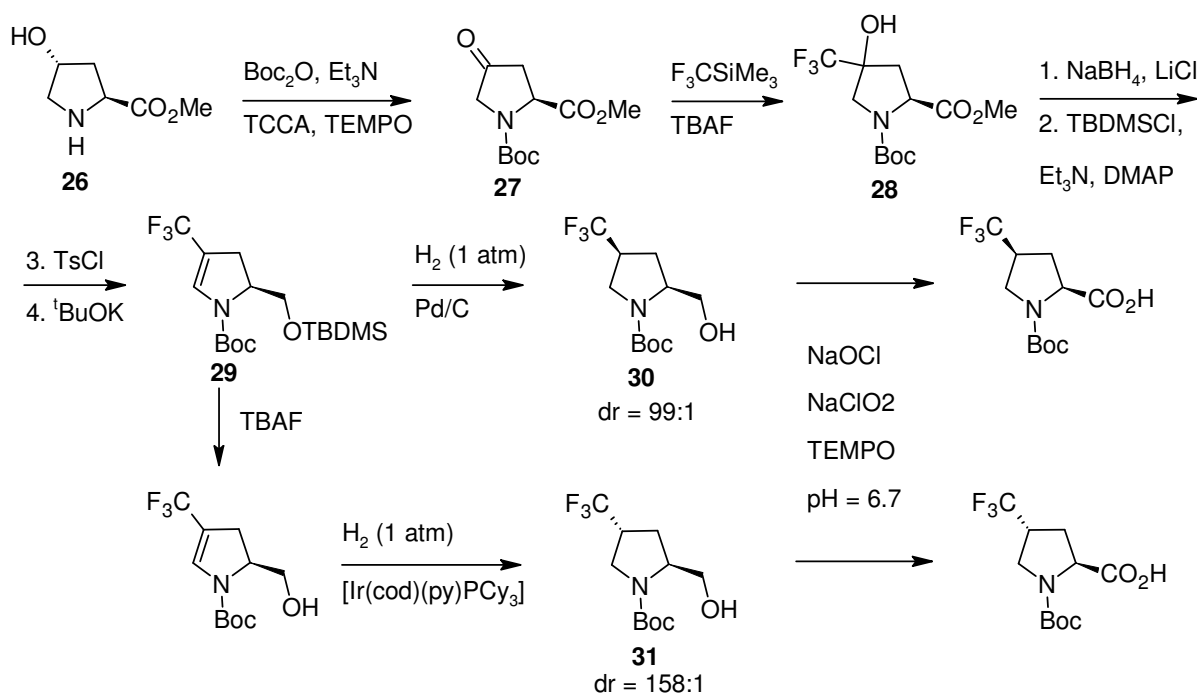
The third approach⁸³ used the chiral complex **23** of Ni(II) with the Schiff base of glycine and (S)-o-[N-(N-benzylpropyl)amino]benzophenone ((S)-**BPB**). The Michael addition was done in dimethylformamide using 1,8-diazobicycloundec-7-ene (DBU) as a base. The resulting adducts showed only the (S)-configuration of the 2-C atom. Two epimers of the position 3, **24** and **25** in a ratio 5.6:1.0, were obtained as a mixture (78% yield). From the mixture the (S)(2S,3S)-isomer **24** was obtained in pure form in 65% yield simply by washing with diethyl ether. The ether fraction was chromatographically separated to give (S)(2S,3R)-**25** and (S)(2S,3S)-**24** in 11% and 5% isolated yields, respectively. Hydrolysis of the ethyl esters gave the corresponding 3-TfmPyr isomers (85-87% yields). The chiral auxiliary (S)-**BPB** was extracted with chloroform from the obtained amino acids; the recovery was 93-95%.

1.5.4. Structures trifluoromethylated in position four

All three structures, 4-TfmPro, 4-TfmPyr and 4-TfmHyp, are well known and some of them can be cross-converted.

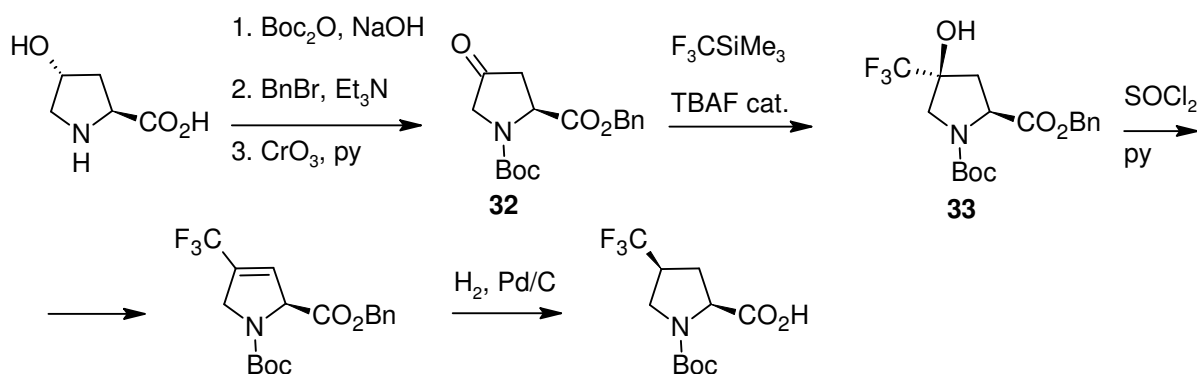
The synthesis of 4-TfmHyp and its conversion into 4-TfmPro is shown on Scheme 1.7⁸⁴. First, the methyl ester of *trans*-Hyp **26** was protected with a Boc group, and the hydroxyl was oxidized with trichloroisocyanuric acid (TCCA) using TEMPO ((2,2,6,6-tetramethylpiperidin-1-yl)oxyl) free radical catalysis (88% yield). The protected prolinone **27** was treated with the Ruppert-Prakash reagent to give the 4-TfmHyp derivative **28** as a single diastereomer in 56% yield. The carboxyl group was reduced with sodium borohydride (94% yield). The resulting carbinol was protected with a silyl type protection group (89% yield) and dehydrated (76% yield). The key enamide intermediate **29** was then hydrogenated under palladium for the double bond reduction (78% yield) to give only the *cis*-isomer **30** in > 98% *de*. Finally, the hydroxymethyl group was oxidized (94% yield) to give Boc-4-*cis*-TfmPro.

The key enamide **29** was also deprotected (85% yield) and reduced with an Ir-cyclooctadiene complex to give **31** (91% yield). This procedure enabled inversion of the reaction diastereoselectivity. Boc-4-*trans*-TfmPro was obtained after oxidation of the carboxymethyl group (96% yield).



Scheme 1.7. Synthesis of the isomeric N-Boc 4-Tfm-(S)-Pro.

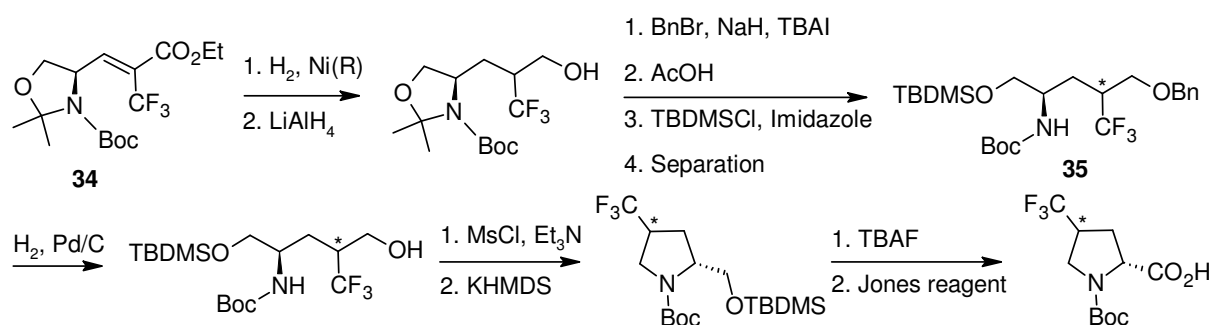
A similar but shorter procedure was used for the synthesis of 4-*cis*-Tfm-(S)-Pro⁸⁵ (Scheme 1.8.). The protected prolinone **32** was obtained in 38% overall yield starting from Hyp. It was treated with the Ruppert-Prakash reagent to yield 81% of the 4-TfmHyp derivative **33**. Dehydration (78% yield) followed by hydrogenation of the resulting double bond under palladium (90% yield) gave Boc-4-*cis*-Tfm-(S)-Pro as a single product.



Scheme 1.8. Synthesis of chiral N-Boc 4-*cis*-Tfm-(S)-Pro.

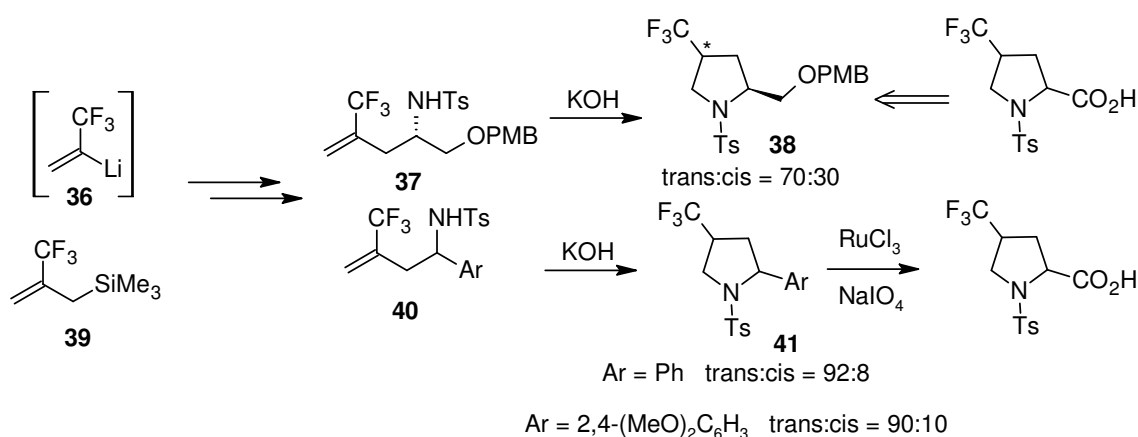
A completely different approach towards 4-Tfm-(R)-Pro was published by the same authors⁸⁶ (Scheme 1.9.). Here, the trifluoromethyl group was installed first, and then the proline ring was constructed. First, the trifluoromethylated acroleate derivative **34** was synthesized from Garner's aldehyde in two steps (not shown). The double bond was reduced by hydrogenolysis (94% yield), the protection groups were changed in three steps (64% overall yield), and two

diastereomers **35** were separated chromatographically to give the pure (2R,4R)- and (2R,4S)-isomers in the ratio of 4:3. After deprotection (91% and 99% yields, respectively) the proline ring was constructed by an energetically favorable 5-*exo-tet* intramolecular alkylation (80% and 83% yields), the silyl-protection group was removed quantitatively. Finally, the hydroxymethyl group was oxidized with the Jones reagent (68% and 56% yields) to give the corresponding (2R,4R)- and (2R,4S)-isomers of Boc-4-TfmPro.



Scheme 1.9. Synthesis of the isomeric 4-Tfm-(R)-Pro.

Another method which involves the intramolecular cyclization is presented in Scheme 1.10⁸⁷. 1-Trifluoromethylvinyl lithium **36** was reacted with para-methoxybenzyl (PMB) protected (*S*)-hydroxymethyloxirane. The hydroxyl group was exchanged to tosylamine (45% yield in four steps). The resulting compound **37** underwent an intramolecular unfavorable 5-*endo-trig* cyclization by heating with potassium hydroxide in ethyleneglycol (68%). The product **38** was enriched with the *trans*-isomer (40% *de*) and could be transformed to the corresponding amino acid derivative.



Scheme 1.10. Synthesis of the N-tosylated 4-TfmPro.

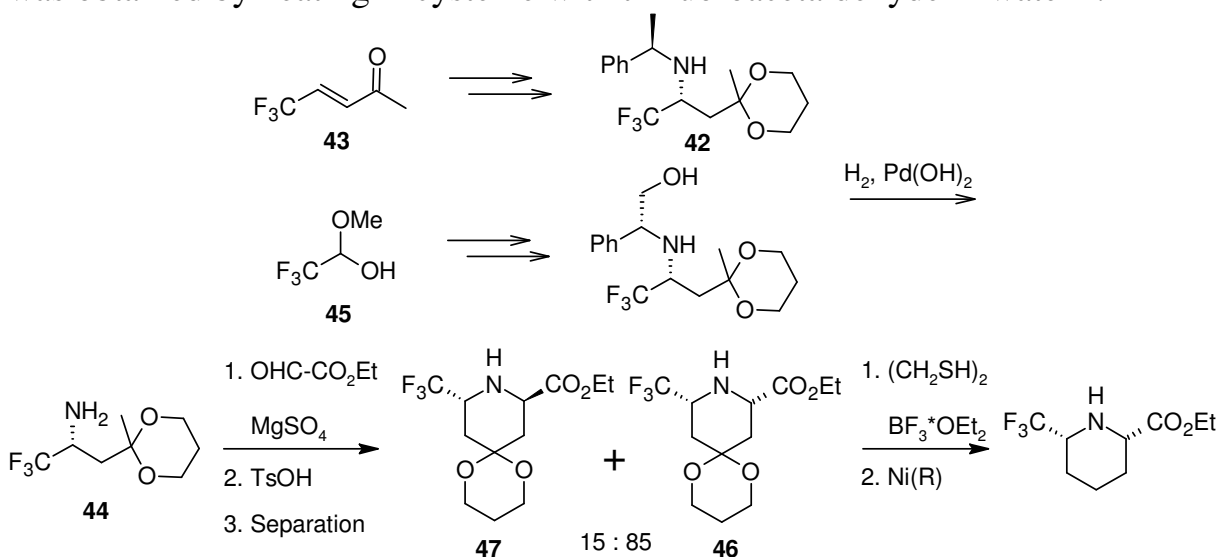
The organolithium reagent **36** also reacted with aryl-oxiranes as well as the trimethylsilyl derivative **39** with aryl-aldehydes, and eventually the aryl derivatives **40** were cyclized in the same way. The *de* was 86 and 80 for phenyl and 2,4-

dimethoxyphenyl pyrrolidines, respectively (85% and 74% chemical yields). The aryl groups in **41** were oxidized in 45% and 72% yield to give the non-chiral diastereomerically enriched Ts-TfmPro.

Oxydation of 4-TfmPro to the corresponding 4-TfmPyr with sodium periodate/ruthenium (IV) oxide was also described⁸⁸. Type of the functional group protection played a key role in this case.

1.5.5. Structures trifluoromethylated at ω -position

5-Tfm-thioproline (2-(trifluoromethyl)-1,3-thiazolidine-4-carboxylic acid) was obtained by heating L-cysteine with trifluoroacetaldehyde in water⁸⁹.



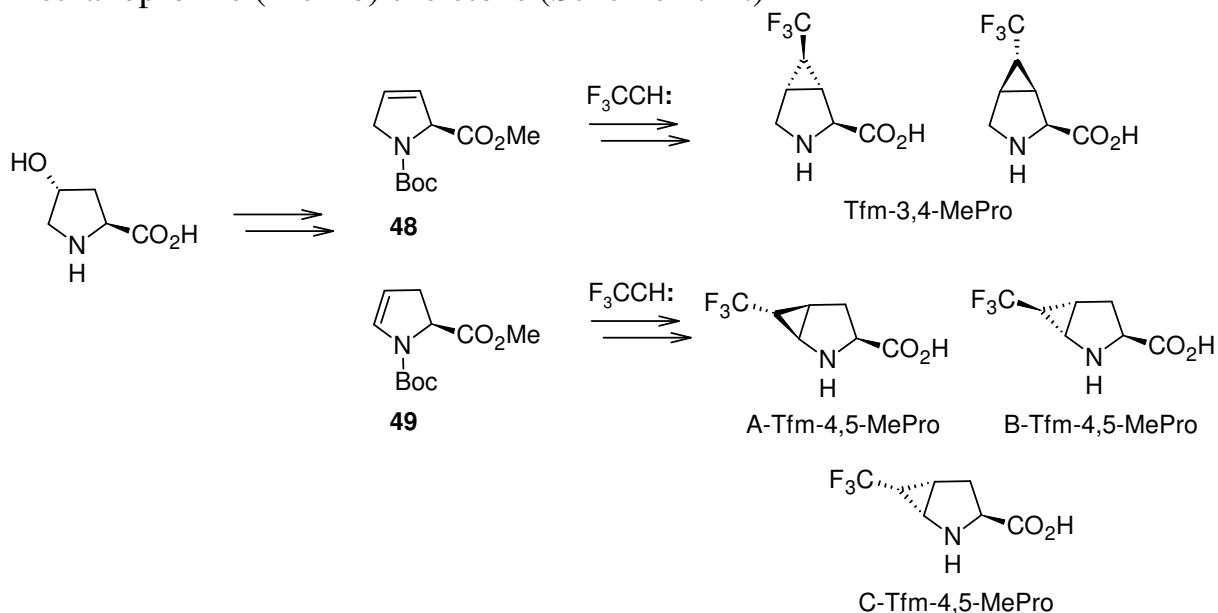
Scheme 1.11. Synthetic approach towards 6-Tfm-(S)-Pip.

6-TfmPip (ω -Tfm-homoproline) was synthesized recently⁹⁰ (Scheme 1.11.). The key intermediate β -amino ketal **42** was obtained starting from ω,ω,ω -trifluoropent-3-en-2-one **43** and (+)-phenylethylamine in 57% yield as an equimolar mixture of diastereomers. However, the chiral substituent enabled the separation of the isomers on silica gel. The benzyl protection group was removed by hydrogenolysis (95% yield). The formed (R) -amine **44** was also synthesized alternatively, starting from trifluoroacetaldehyde methyl hemiacetal **45** in four steps (52% overall yield). This intermediate was condensed with ethyl glyoxalate, giving the mixture of *cis*- and *trans*-cyclic amino acids **46** and **47** in 70% *de* and 65% chemical yield. The 1,3-dioxin ring in **46** was transformed into a methylene group by consecutive dithioketolation (96% yield) and desulfurization of the dithiolane with Raney nickel (90% yield).

4-*cis*-TfmAze was described recently⁹¹. The synthesis was based on the cyclization of ω,ω,ω -trifluoromethyl- β -aminobutyric acid. The carboxylic group was constructed in the place of the keto group in four steps.

1.5.6. Trifluoromethylated methanoprolines

A few structures were specifically developed to place a CF₃-label onto proline in peptides⁹². They are based on the corresponding 3,4- and 4,5-methanoproline (MePro) skeletons (Scheme 1.12.)



Scheme 1.12. Synthetic approach towards isomeric TfmMePro.

The key step was in both cases a trifluoromethylation of the corresponding dehydroprolines **48** and **49** with trifluorodiazomethane. Isomeric Tfm-3,4-MePro was obtained in relatively poor chemical yield, whereas the Tfm-4,5-MePro synthesis was more successful. Three isomers, the so-called A- B- and C-Tfm-4,5-MePro, were obtained. Finally, A-Tfm-4,5-MePro was introduced into the cell penetrating peptide SAP by standard SPPS, where it demonstrated prominent stabilization of the polyproline type-II secondary structure.

2. Aims of this study

The main aim of this work was to examine the conformational influence of different proline analogues when placed into peptides. This included some amino acids with only minor modifications (like monofluoroprolines) but covered also some rather complex structures (like different methanoprolines). At the same time, rather simple commercially available compounds were used, as well as a few of synthetically highly demanding novel structures.

Proline is never inert towards modifications. Any changes in its structure will influence the conformational and functional properties of the resulting peptides. In order to reveal these changes and understand the risks of proline labeling, the present study systematically compares a wide range of available and novel analogues.

Two different peptide structures were chosen as templates for the proline substitution. In the antimicrobial peptide gramicidin S (*cyclo*[VOL^DFP]₂) proline is rigidly enclosed in a β -turn. The cell penetrating peptide SAP ([VRLPPP]₃), on the other hand is conformationally very sensitive to amino acid substitutions, because a random coil to PPII equilibrium takes place. Gramicidin S is only modestly water soluble, thus its functionality is highly sensitive to unspecific changes in hydrophobicity. In contrast, the highly charged SAP is perfectly water soluble. The amino acid position 11 in SAP, where proline was systematically substituted, is located on the hydrophilic face of the amphipathic PPII structure. Therefore, unspecific effects of the proline analogues unlikely to play a role in the aggregation and assembly of this peptide.

In summary, the aims of this work were as follows:

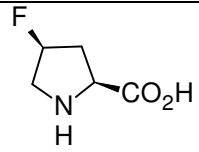
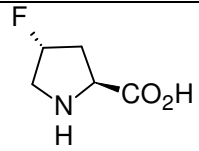
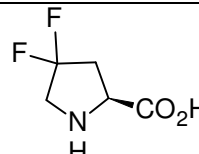
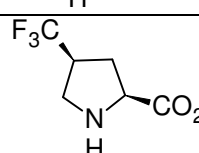
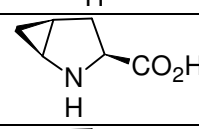
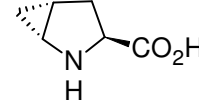
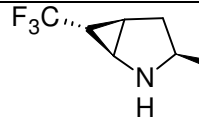
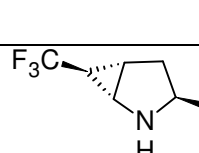
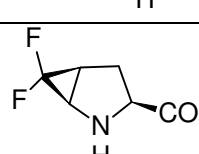
- To synthesize various proline analogues in a suitable form for peptide synthesis. To verify, and if needed to modify the available synthetic procedures for this purpose;
- To synthesize the linear peptide SAP and the cyclic peptide gramicidin S with the proline analogues. To check the compatibility of the chosen amino acids with the common solid phase peptide synthesis protocol and (for gramicidin S) other synthetic steps;
- To perform a thorough conformational analysis of the resulting peptides using circular dichroism;
- To perform biological activity tests with the antimicrobial gramicidin S analogues, in order to reveal and understand the unspecific and specific impacts of the different proline substitutions;
- To study the fluorine-labeled MAPs using solid state NMR in oriented lipid samples and answer the questions: how does the spectral response look like for different peptides labeled with different ¹⁹F-NMR reporter groups? Which experimental protocol is better, and how to perform the most informative spectral analysis?

- To understand whether there is a relationship between peptide function and conformation, and what may cause such response;
- To come to a final conclusion on how to choose a suitable proline analogue for labeling a peptide with a ^{19}F -NMR reporter group? Which amino acids are recommended, and what is the optimal protocol to incorporate them? How to minimize the conformational and functional impact in the study of native peptide structures? Or how to maximize these effects in the design of novel peptide structures?

In the following sections 3 (Results) and 4 (Discussion), a comprehensive answer on the above questions will be given. Step by step, from method to method the findings will be assembled, in order to give a final complete picture. Eventually, a recommendation on proline substitution will be formulated.

3. Results

First a number of different amino acids were chosen for incorporation into peptides instead of proline. The list of the amino acids and used nomenclature are summarized in Table 3.1. Chemical synthesis of the amino acids in the form suitable for the peptide synthesis will be described in the chapters 3.1-3.3. Chapter 3.4. will be dedicated to the synthetic incorporation of the amino acids into gramicidin S and SAP. Studied properties of the resulting peptides will be described in the chapters 3.5-3.6. (GS) and 3.7.-3.8. (SAP).

#	amino acid	name*	structure
1	4- <i>cis</i> -fluoroproline	flp	
2	4- <i>trans</i> -fluoroproline	Flp	
3	4,4-difluoroproline	F ₂ Pro	
4	4- <i>cis</i> -trifluoromethylproline	TfmPro (4- <i>cis</i> -(S)-Pro)	
5	<i>cis</i> -4,5-methanoproline	c-MePro	
6	<i>trans</i> -4,4-methanoproline	t-MePro	
7	(1R,3S,5R,6R)-6-trifluoromethyl-2-azabicyclo[3.1.0]hexane-3-carboxylic acid	c-TfmMePro (A-TfmMePro)	
8	(1S,3S,5S,6S)-6-trifluoromethyl-2-azabicyclo[3.1.0]hexane-3-carboxylic acid	t-TfmMePro (B-TfmMePro)	
9	(1R,3S,5S)-6,6-difluoro-2-azabicyclo[3.1.0]hexane-3-carboxylic acid	c-F ₂ MePro	

* the marks “c-” and “t-” indicate relative configuration of the methano unit in various methanoprolines used.

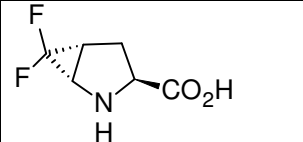
10	(1S,3S,5R)-6,6-difluoro-2-azabicyclo[3.1.0]hexane-3-carboxylic acid	t-F ₂ MePro	
----	---	------------------------	---

Table 3.1. Amino acids used in this study for proline substitution.

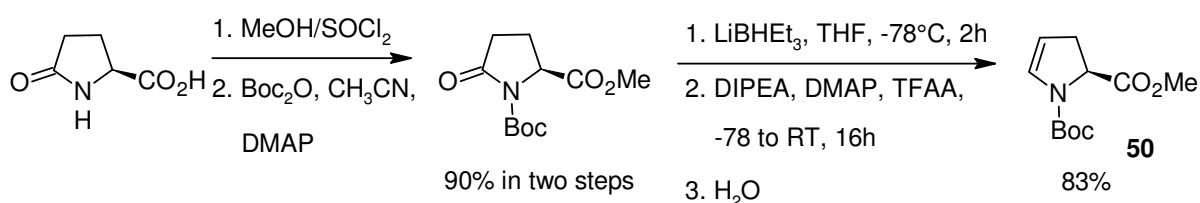
Few rows for further comparison can be extracted out of the full amino acids list:

- 1) different degree of conformational restriction (flp/Flp vs TfmPro; TfmPro vs TfmMePro; F₂Pro vs F₂MePro);
- 2) different stereochemistry (flp vs Flp; c-MePro vs t-MePro; c-TfmMePro vs t-TfmMePro; c-F₂MePro vs t-F₂MePro);
- 3) different degree of fluorination (MePro vs flp/Flp vs F₂Pro/F₂MePro vs TfmPro/TfmMePro);
- 4) different electronic effects of the substituents (MePro vs TfmMePro vs F₂MePro).

3.1. Geminal difluoro-4,5-methanoproline

3.1.1. Amino acid synthesis

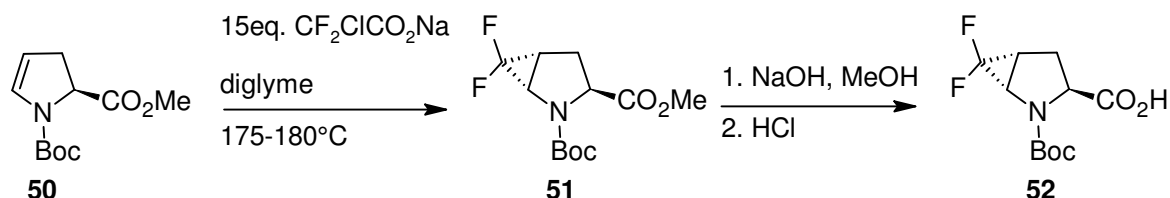
The novel amino acid t-F₂MePro was synthesized starting from 4,5-dehydroproline derivative **50** which was obtained in three steps starting from pyrrolidone (Scheme 3.1)⁹³.



Scheme 3.1. Synthesis of the protected 4,5-dehydroproline (**50**).

Difluorocyclopropanation was done using thermal decomposition of ClF₂CO₂Na salt in refluxing diglyme⁹⁴. Temperature in bath was kept strictly in the range 175-180°C (overheat above 185°C led to decomposition of the material) for 20-45 min reaction time, the solvent was then removed in vacuum and the crude material was subjected directly to silica gel separation (Scheme 3.2). Single compound was obtained. Only traces of the starting dehydroproline were detected. The yield varied depending on how the salt was added: 31% in the case when 7 eq. of the salt was added to the enamide before heating, 58% when only 1/3 of the same 7 eq. was added before heating and the rest 2/3 was added already at the high temperature, and 71% when 15 eq. of the salt was added at once at the high temperature. Resulting Boc-t-F₂MePro-OMe **51** was then saponificated giving the Boc-amino acid Boc-t-F₂MePro-OH **52**. The crystal structure (Fig. 3.1) determined **52** being *trans*-methano isomer.

It turned out that Boc-deprotection of both the methyl ester Boc-t-F₂MePro-OMe and the acid Boc-t-F₂MePro-OH with trifluoroacetic acid in dichloromethane at room temperature led to full decomposition of the material. There was no major product detected in the orange water soluble residue formed. Decomposition of geminal F₂-aminocyclopropane system was expected⁹⁵ but not at such conditions: already at room temperature in acidic medium. This effect was further investigated.



Scheme 3.2. Synthesis of Boc-t-F₂MePro-OH.

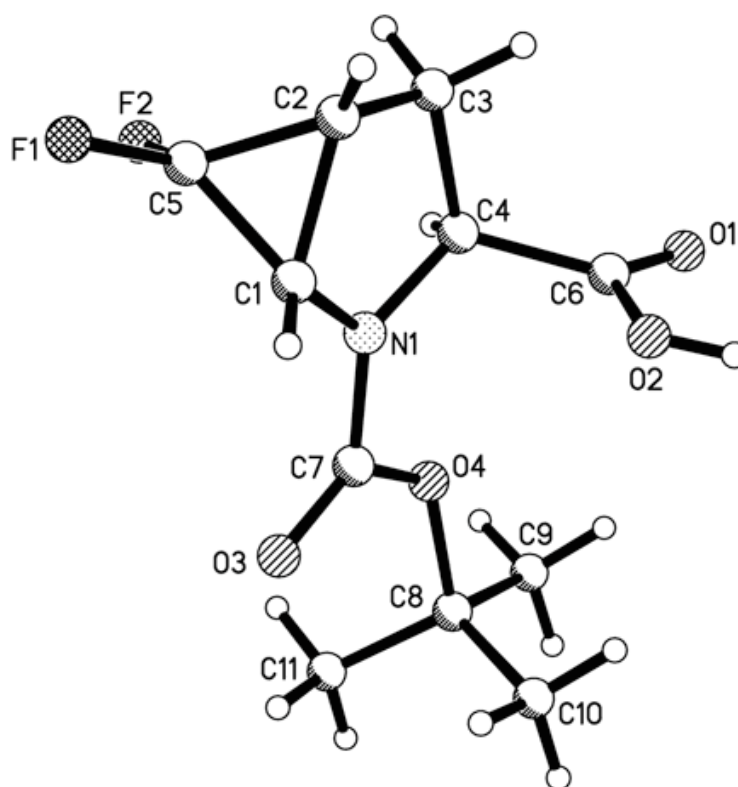


Figure 3.1. X-ray molecular structure of Boc-t-F₂MePro-OH.

In order to estimate the stability of free amino acid acetylation was done. Treatment of Boc-t-F₂MePro-OMe with TFA/CH₂Cl₂ cocktail for 30 min, followed by quick (within 5 min) evaporation of volatilities and adding of acetic anhydride gave Ac-t-F₂MePro-OMe in reasonably low 9% yield. For instance, for the same derivative of proline similar procedure⁹⁶ yielded 85% of the acetylated product. This fact was indicating significant degree of decomposition along the performed procedure.

Resulting derivative Ac-t-F₂MePro-OMe (as well as the starting Boc-t-F₂MePro-OMe) was stable at room temperature at least for several months.

3.1.2. Kinetic of t-F₂MePro decomposition in N-protected form

Three substances were generated and followed by ¹⁹F/¹H-NMR: TFA*H-t-F₂MePro-OMe (in CDCl₃), TFA*H-t-F₂MePro-OH and H-t-F₂MePro-OH (both in D₂O).

3.1.2.1. Decomposition of the trifluoroacetic salt of H-t-F₂MePro-OMe in chloroform

Boc-t-F₂MePro-OMe was treated with trifluoroacetic acid in CHCl₃ (1:2 vol) for 15 min. The time delay between addition of TFA and the spectra acquisition was 30 min.

The spectrum at the beginning showed presence of both TFA*H-t-F₂MePro-OMe salt and the starting Boc-t-F₂MePro-OMe in the ratio ~ 5:1*. The intensities of the two characteristic doublets seen in the ¹⁹F-NMR spectra at -129.2 (exo-F) and -148.0 ppm (endo-F†) with J_{F-F}= 178Hz were steady decreasing along the time as presented on Fig. 3.2. Linearization in the coordinates lnI-time and 1/I-time (where I is the intensity value of the exo-F signal) gave correlation coefficient square 0.979 and 0.958 respectively. Therefore it was concluded that the order of the reaction was not an integer number. The half life time τ_{1/2} was about 110 min and the practical disappearance of the salt signals was committed after about 24 hours of the observation.

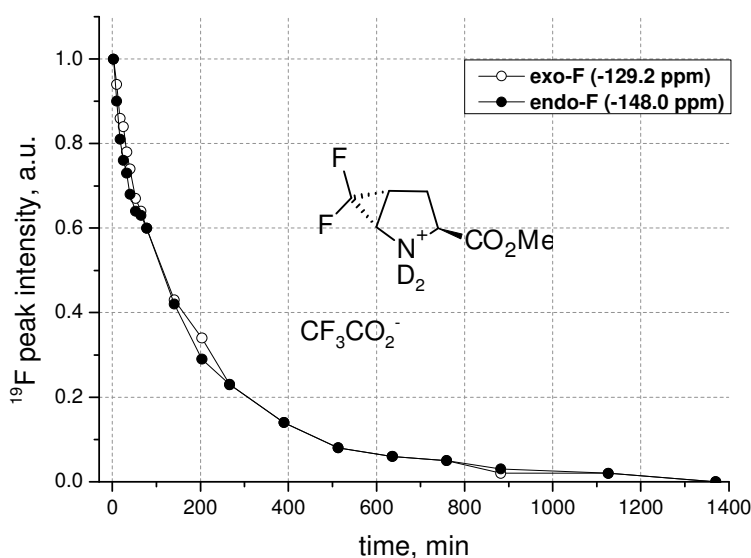


Figure 3.2. Decomposition of TFA*H-t-F₂MePro-OMe in CDCl₃ at 23°C observed by ¹⁹F-NMR.

* when the cocktail treatment time was only 5 min the ratio was lower, ~ 4:3.

† the assignment was assumed basing on the additional splitting on protons characteristic for the down field fluorine signal as well as the chemical shift values themselves (see chapter 3.2.3).

No (prominent) product was identified in the mixture in both ^1H - and ^{19}F -NMR spectra. Presumably, eventual evolution of F^- ions during decomposition process in the slightly acidic medium was leading to a reaction of hydrofluoric acid with the glass material of the NMR tube. This explains why the total ^{19}F -signal was practically disappearing. The bands in the ^1H -NMR spectra of the final mixture were broad and not resolved, presumably due to various condensation reactions happening.

3.1.2.2. Decomposition of the trifluoroacetic salt of H-t-F₂MePro-OH in water

In order to generate the free amino acid salt Boc-t-F₂MePro-OH was treated with the TFA/ CDCl_3 cocktail for 15 min and the residue was extracted with CDCl_3 . The spectrum of the extract showed almost pure starting substance. The non-soluble in chloroform part was dissolved in deuterium oxide and a $^1\text{H}/^{19}\text{F}$ -NMR time series was launched. These operations were done within the next 25 min, the total time before the series start was 40 min. Two doublets attributed to the product TFA*H-t-F₂MePro-OH in the ^{19}F -NMR spectrum were at -129.8 (exo-F) and -148.3 (endo-F) with $J_{\text{F-F}} = 178\text{Hz}$. The ^1H -NMR spectrum of this substance is presented on Fig.3.3.

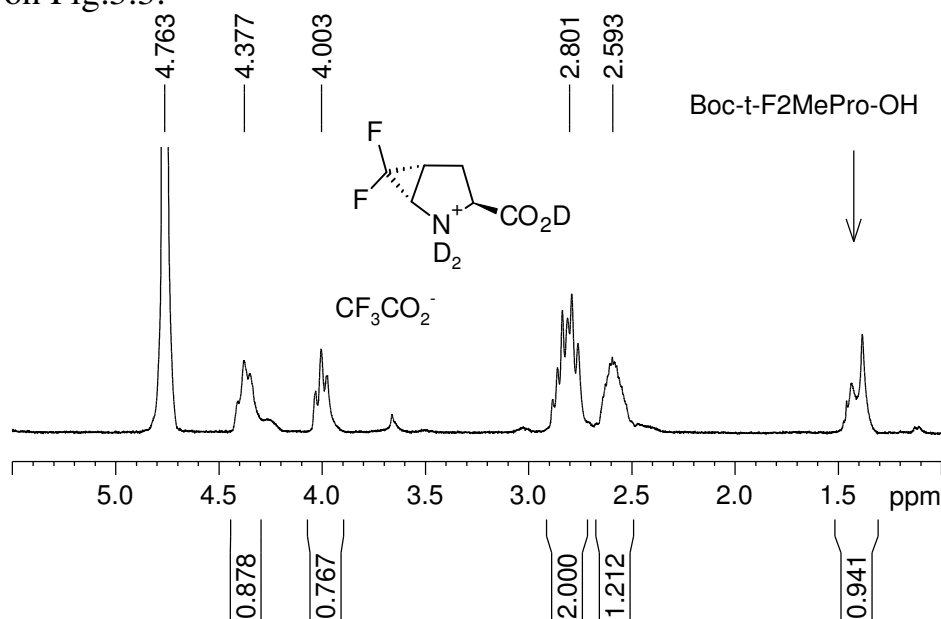


Figure 3.3. ^1H -NMR spectrum of H-t-F₂MePro-OH in D_2O at the beginning of the time series. Two singlets of the residual starting substance (Boc-rotamers) are indicated by an arrow.

The ratio of the product to the starting Boc-form was $\sim 10/1$ at the beginning of the series. Corresponding signals in the fluorine spectrum decayed as presented on Fig. 3.4. Linearization in coordinates $\ln I$ -time and $1/I$ -time (where I is the peak intensity of the exo-F signal) gave the correlation coefficient square 0.999 and 0.847 respectively, indicating the first order of the decomposition process (Fig. 3.5.). The half life time $\tau_{1/2}$ was 39 min, and the signal was completely vanishing after ~ 200 min of observation.

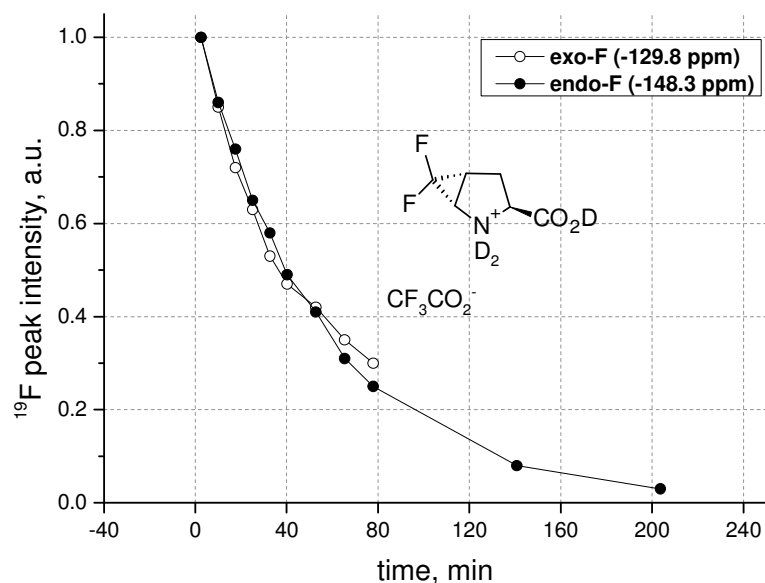


Figure 3.4. Decomposition of TFA*H-t-F₂MePro-OH in D₂O.

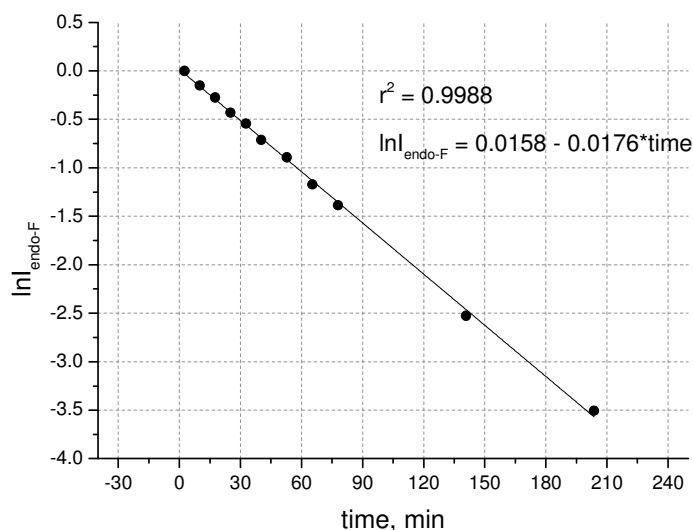


Figure 3.5. Linearization curve for the endo-F signal intensity of TFA*H-t-F₂MePro-OH in D₂O as seen in ¹⁹F-NMR.

It was not possible to figure out the composition of the resulting mixture after 24 hours. However, few prominent signals were observed in the spectra during the series. Few of them showed the same evolution along the time: in ¹H-NMR d, J= 19Hz at 9.21 ppm, dt J= 32 and 7Hz at 6.31 ppm, t, J= 7Hz at 4.26 ppm, m at 3.02 ppm and in ¹⁹F-NMR dd J= 32 and 19Hz at -131.1 ppm. Signals in characteristic spectral regions enabled me to deduce the structure of the additive being **54** (Fig. 3.6.*). The maximum of the aldehyde additive **54** population corresponds to the time point of disappearance the starting amino acid salt signals.

* slight difference between ¹⁹F and ¹H curvatures on Fig. 3.6 is caused by the complicated baseline shape in ¹⁹F spectra

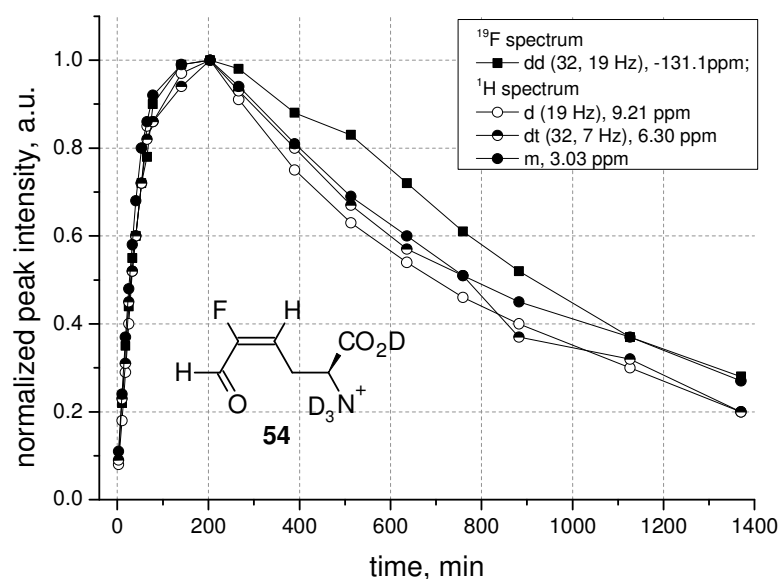
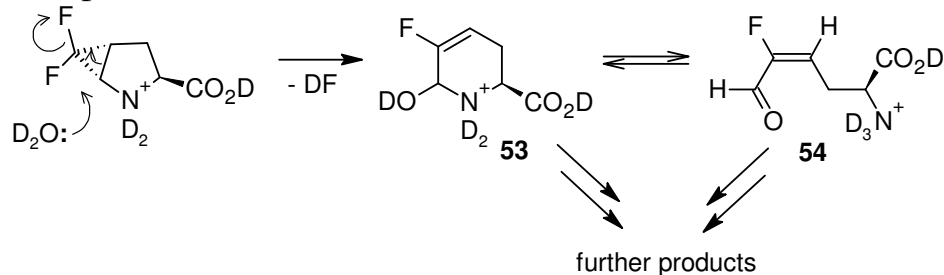


Figure 3.6. Evolution of the additive signal in the TFA*H-t-F₂MePro-OH decomposition series and its proposed structure (**54**).

Basing on the observations a mechanism of the F₂MePro ring opening was proposed (Scheme 3.3.). High electrophilic atom in position 1 of the bicycle is being attacked by a water molecule, resulting hemiaminal **53** gives the observed high reactive aldehyde **54**. The aldehyde as well as the hemiaminal has few theoretical reaction possibilities: condensation, oxidation, cycloaddition. Eventually complicated mixture was formed.



Scheme 3.3. Proposed mechanism of TFA*H-t-F₂MePro-OH decomposition in D₂O.

Such decomposition mechanism explains the first order of the degradation in excess of water. In the case of TFA*H-t-F₂MePro-OMe the only one nucleophile present in CDCl₃ solution was trifluoroacetic acid, which was in about 3-4 fold excess*. This explains complex order of the degradation in this case.

3.1.2.3. Decomposition of the basic form of H-t-F₂MePro-OH in water

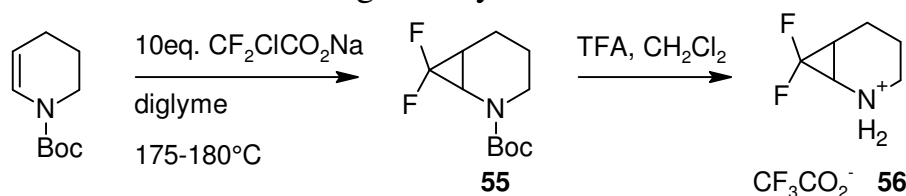
However, whether the protonated forms were unstable because of the acidic medium or deprotected form was unstable intrinsically was not clear. In order to

* the ratio was estimated from the ¹⁹F-NMR spectrum at the starting point.

check the stability of the base form Boc-t-F₂MePro-OH was deprotected and the starting compound was extracted as described above. Now the salt was extra treated with the Hünig base (DIPEA) before the NMR executions. The total time from the addition of trifluoroacetic acid until the ¹⁹F-NMR spectrum was taken was the same 40 min as for the trifluoroacetic acid salt. There were no characteristic doublet signals in the expected for geminal F₂ ranges neither from the basic amino acid nor from the TFA salt. Moreover, the major lines in the spectrum were the trifluoroacetic acid signal and a singlet at -122.2 ppm attributed to fluoride ions. This fact clearly showed that the decomposition was caused not by the acidic medium, but from other reasons.

3.1.3. The 7,7-difluoro-2-azabicyclo[4.1.0]heptane system

In order to understand the role of the bicyclic system an analog of the desired amino acid with a nitrogen locked in a wider six-membered ring was synthesized according to scheme 3.4. Resulting Boc-amine **55** was synthesized in 73% yield and then deprotected. The salt with trifluoroacetic acid **56** was stable in deuteriochloroform for several months. In deuterium oxide no traces of decomposition was observed during 1.5 days of careful NMR observation.



Scheme 3.4. Synthesis of the 7,7-difluoro-2-azabicyclo[4.1.0]heptane.

Moreover, the salt can be transformed into corresponding amine by shaking with potassium carbonate solution. This free amine was stable for recording the basic NMR spectra. Detailed investigation of the amine stability was not provided. However, it was already clear that the decomposition of t-F₂MePro was caused by the bicyclic system. Apparently, the [3.1.0]heptane system becomes unstable after the nitrogen changes its hybridization from sp² in the Boc- or Ac-protected to sp³ in deprotected form.

3.2. Dipeptides with F₂MePro amino acid

In order to overcome the synthetic complications and incorporate F₂MePro amino acid into peptides, the N-deprotected form of this amino acid must be completely avoided in the peptide synthesis. For this purpose difluorocyclopropanation was carried out with the dipeptides where the future peptide bond between the preceding amino acid and dehydroproline was already created before the CF₂ carbene installation.

3.2.1. Synthesis of ^DPhe-t-F₂MePro dipeptide

For incorporation into gramicidin S, the corresponding dipeptide with ^DPhe residue was designed and synthesized as presented on Scheme 3.5. Pyroglutamic acid was esterified with isobutylene (82% yield), this protection was used to make the final remove of the protecting groups Bu^t and Boc in one step. ^DPhe residue was coupled to the pyroglutamate⁹⁷ (89% yield) and the amide group in the resulting dipeptide **57** was reduced and dehydrated giving the dipeptide of 4,5-dehydroproline **58** (76% yield). The regioselectivity of this reduction was rather poorly discussed in literature⁹⁸, however in this work it gave only the desired 4,5-dehydroproline derivative.

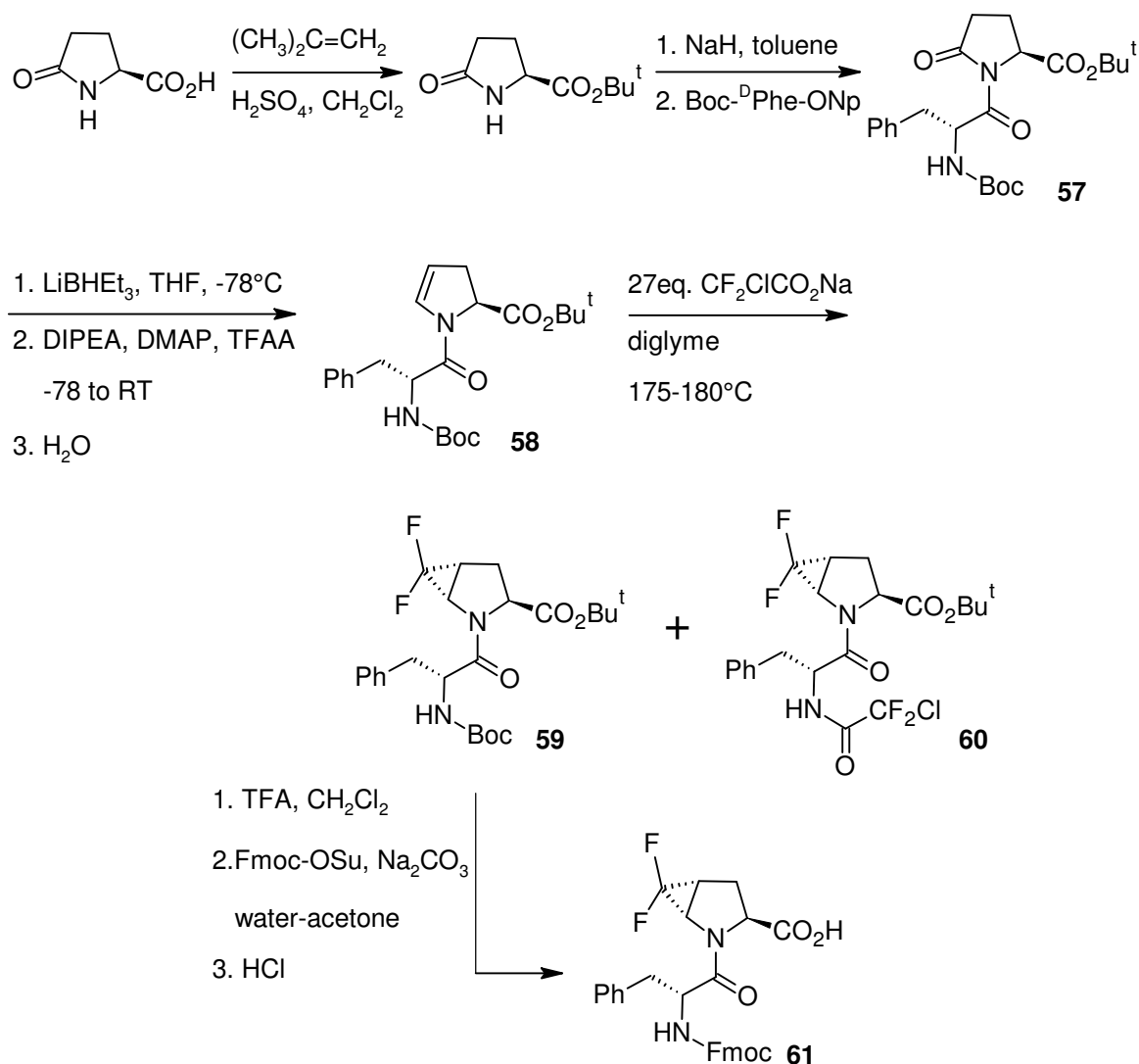
This dipeptide was difluorocyclopropanated with sodium chlorodifluoroacetate. The enamide conversion turned out to be a critical point. Use of 15 equivalents gave mixture of the starting material and the product with the ratio ~ 1:1*. This mixture was practically impossible to separate by common silica gel chromatography. Shaking this mixture with potassium permanganate enriched the product content to ~ 4:1. Such purity was still not good enough for introduction into peptides. Use of 25 equivalents of the salt on the cyclopropanation step finally gave full conversion, this lead however to formation of a side product. The yields were 29% for the desired dipeptide **59** and 7% for the additive **60**.

Structure of the additive was deduced from the NMR data. In the ¹H-NMR spectrum of Boc-^DPhe-t-F₂MePro-OBu^t the two tert-butyl groups were presented and the substance showed two prominent Boc-rotamer forms. In contrast, the additive spectrum contained only one tert-butyl group and showed marginal amount of rotameric forms. In the ¹³C-NMR spectrum of the additive normal Boc carbonyl signal at ~155 ppm was absent, but two new triplets were present instead at 158.3 (J= 31Hz) and 118.8 ppm (J= 301Hz). In the ¹⁹F-NMR an additional singlet was at -63.8 ppm (2F). The NMR data of the additional signals was in complete agreement with the literature for the ClF₂C(=O)-NH group⁹⁹. The configurations of the product and of the additive were the same as was judged from heteronuclear NOE experiments (see chapter 3.2.3.).

Apparently excess of the reacting salt acetylated the NH group in ^DPhe residue followed by elimination of the butoxycarbonyl protection. Such side reaction has never been reported in the literature.

The dipeptide **59** was transformed in two steps into the corresponding Fmoc-form **61** (in 82% yield) ready for use in the peptide synthesis. Analytical HPLC with UV detection of the Fmoc-^DPhe-t-F₂MePro-OH revealed purity of 89% (at 220 nm) with no major additives. This substance was pure enough for the further gramicidin S synthesis.

* this was not expected since in the case of the amino acid synthesis (chapter 3.1.1) any attempts towards **51** gave only barely detectable amounts of the starting substance **50**.



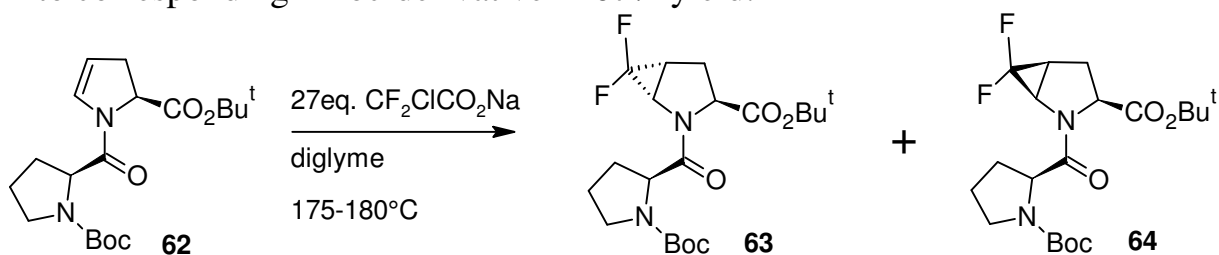
Scheme 3.5. Synthesis of Fmoc-^DPhe-t-F₂MePro-OH.

3.2.2. Synthesis of Pro-t-F₂MePro dipeptide

For the incorporation into SAP in position 11 the dipeptide Pro-F₂MePro was synthesized analogously to the ^DPhe dipeptide. Boc-proline was coupled to the tert-butyl pyroglutamate in 83% yield. Reduction-dehydration reaction gave corresponding 4,5-dehydropyroline derivative in 70% yield.

This dipeptide **62** was difluorocyclopropanated according to the procedure established for ^DPhe-dipeptide with 27 equivalents of the salt (Scheme 3.5). In this case two isomers with t-F₂MePro **63** (48% yield) and c-F₂MePro **64** (10%) were obtained. The configuration of the isomers was determined using heteronuclear NOE experiments (*vide infra*). Quantitative separation was done by the preparative RP-HPLC. The dipeptides were transformed into the corresponding Fmoc-dipeptides according to Scheme 3.4. Fmoc-Pro-t-F₂MePro-OH was obtained with 94% yield and 80% purity without any major admixture. The minor Boc-Pro-c-F₂MePro-OBu^t **64** was obtained as ~ 9:1 mixture with the major isomer (estimated

from the ^{19}F -NMR spectra) in the preparative RP-HPLC. It was then transformed into corresponding Fmoc-derivative in 67% yield.



Scheme 3.5. Synthesis of the Boc-Pro-c/t- $\text{F}_2\text{MePro-OBu}^t$ dipeptides.

3.2.3. Configuration of F_2MePro dipeptides

In order to distinguish *cis*- and *trans*-isomeric forms of methano units in the difluorocyclopropanation products, heteronuclear $^1\text{H} \leftrightarrow ^{19}\text{F}$ NOE experiments were carried out. Eventually, the experiment with ^1H irradiation and ^{19}F observation was sensitive to distances up to $\sim 3\text{\AA}$ and the inverse experiment with ^{19}F irradiation and ^1H observation – up to $\sim 4\text{\AA}$ respectively. This latter type of transfer was chosen for the proceeding. Efficiency of the ^{19}F -NMR signal suppression was always checked by the homonuclear ^{19}F NOE of the same suppression power level.

Analysis of the crystal structures available for *cis*- and *trans*-methano Boc-4,5-MePro-OH in the Cambridge Structural Database showed that the distance between endo-H in methano unit and the H-2 atom should be 3.80 and 3.11 \AA respectively¹⁰⁰. This fact led to the expectation of a relative strong correlation endo-F \leftrightarrow H-2 in *trans*- and relative weak in *cis*-methano isomer of F_2MePro .

The distance H-2 \leftrightarrow H-5 in *cis*- and *trans*-4,5-MePro is 3.83 and 3.96 \AA respectively. The difference between these type homonuclear distances in the two methano-isomers is rather small. Presence of some correlation between the two protons was observed already in t- F_2MePro derivatives in NOESY indicating that $^1\text{H}^1\text{H}$ NOESY experiment in this case can be misleading. Eventually, only $^1\text{H} \leftrightarrow ^{19}\text{F}$ NOE enabled clear distinguish of the isomers.

The ^{19}F -NMR spectrum of the CF_2 unit of all F_2MePro derivatives showed a downfield doublet at $\sim 126\text{-}132$ ppm with additional splitting on protons (4-15 Hz) and an upfield doublet at $\sim 148\text{-}155$ ppm with no additional splittings. For Boc-t- $\text{F}_2\text{MePro-OH}$ the molecular structure and full assignment of the ^1H -NMR spectrum* were known. In the X-ray molecular structure (Fig 3.1.) the distances from exo-fluorine atom to H-4 and H-5 are 2.65 and 2.63 \AA respectively[†], whereas to the rest of the protons in the range 3.86-4.84 \AA . When the downfield fluorine was suppressed the corresponding ^1H difference spectrum contained two strong correlations with H-4 and H-5 with relative intensities 1.3 and 1.0 respectively. Thus this fluorine was the exo. The endo-fluorine atom is close to almost all protons of the 5-membered ring, the distances to H-2, 3(endo), 3(exo), 4 and 5 are

* from $^1\text{H}^1\text{H}$ -COSY and $^1\text{H}^{13}\text{C}$ -HMQC NMR spectra.

† all the X-ray molecular structure distances should be taken into consideration with the warning that X-ray structures show distances between centers of the electron densities and NMR shows distance between nuclei.

3.22, 2.59, 3.77, 3.23 and 3.25 Å respectively. Corresponding relative integrals in ^1H difference NOE were 0.93, 0.92, 0.27, 0.88 and 1.00. The strong correlation between H-2 and endo-F was expected for the *trans*-methano isomer. It was indeed observed. The assignment of exo/endo-fluorine atoms was extrapolated for all F_2MePro containing compounds basing on their similar patterns in the corresponding ^{19}F -NMR spectra: an upfield pure doublet for endo-F and a downfield doublet of doublets for exo-F.

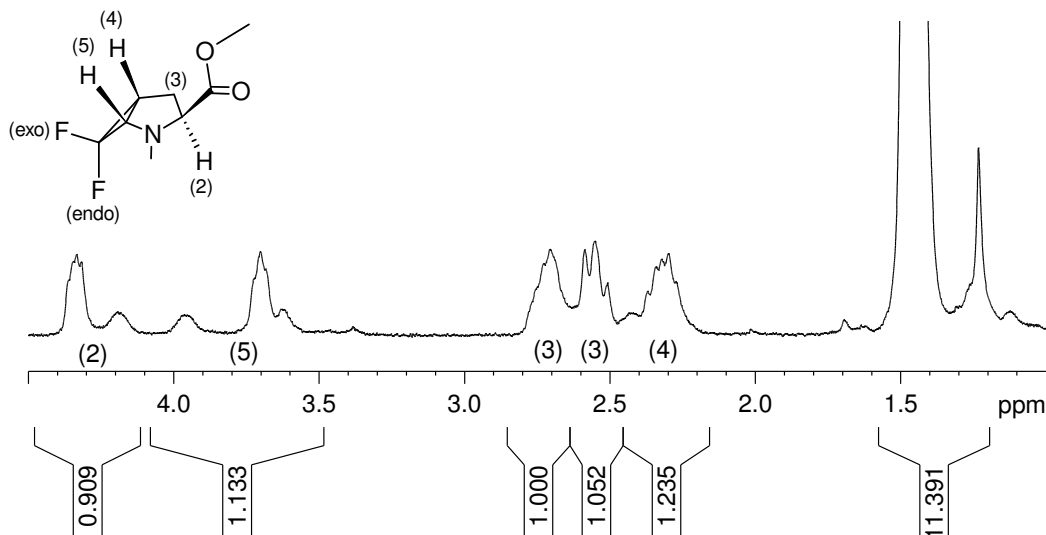


Figure 3.7. ^1H -NMR spectrum of Boc-*t*- $\text{F}_2\text{MePro-OH}$ with assignment. The spectrum shows presence of rotameric forms.

Compound		relative integral		
		α -CH	H-5	H-4
Boc- <i>t</i> - $\text{F}_2\text{MePro-OH}$	exo-F	-	1.00	1.28
	endo-F	0.93 (2)	1.00	0.64
Boc-Pro-(<i>t</i>)- $\text{F}_2\text{MePr-OBu}^t$ Major	exo-F	-	1.00	1.45
	endo-F	1.27	1.00	3.66
Boc-Pro-(<i>c</i>)- $\text{F}_2\text{MePr-OBu}^t$ Minor	exo-F	0.05	1.00	1.07
	endo-F	0.21	1.00	1.27
Pro-(<i>t</i>)- $\text{F}_2\text{MePr-OBu}^t$ Major	exo-F	-	1.00	1.43
	endo-F	0.91 (2)	1.00	5.01
Pro-(<i>c</i>)- $\text{F}_2\text{MePr-OBu}^t$ Minor	exo-F	-	1.00	1.71
	endo-F	-	1.00	1.66
Boc- $^{\text{D}}$ Phe-(<i>t</i>)- $\text{F}_2\text{MePro-OBu}^t$	exo-F	-	1.00	1.48
	endo-F	0.96 (2)	1.00	3.99
$\text{ClF}_2\text{C(=O)-}^{\text{D}}$ Phe-(<i>t</i>)- $\text{F}_2\text{MePro-OBu}^t$	exo-F	-	1.00	1.27
	endo-F	1.02 (2)	1.00	3.91
Fmoc-Pro-(<i>t</i>)- $\text{F}_2\text{MePro-OH}$ Major	exo-F	0.14	1.00	1.14
	endo-F	2.38	1.00	3.77
Fmoc- $^{\text{D}}$ Phe-(<i>t</i>)- $\text{F}_2\text{MePro-OH}$ Major	exo-F	-	1.00	1.21
	endo-F	2.11	1.00	4.86

Table 3.2. Relative integral values in the ^1H -NMR difference spectra recorded with irradiation of the corresponding fluorine atom and without. The integral value for the full α -CH range are given, unless (2) marks the integrals only for α -CH in F_2MePro residue (H-2). Few large values for endo-F \leftrightarrow H-4 correlation are caused by overlap of this signal with other signals that experienced NOE.

The heteronuclear NOE difference spectra (Table 3.2) of Boc-Pro-F₂MePro-OBu^t showed integrals 1.45 and 1.00 for the major and 1.42 and 1.00 for the minor isomer for H-4 and H-5 in the case of *exo*-F irradiation. These values can be considered to be practically the same since the geometry of the cyclopropane ring is expected to be the same in both isomers. Correlation in the case of *endo*-fluorine irradiation with the protons from the α -CH range was 1.27 and 0.20 respectively if correlation with H-5 was taken as 1.00. This was a prominent difference, it indicated that the major isomer was *trans* and the minor was *cis*.

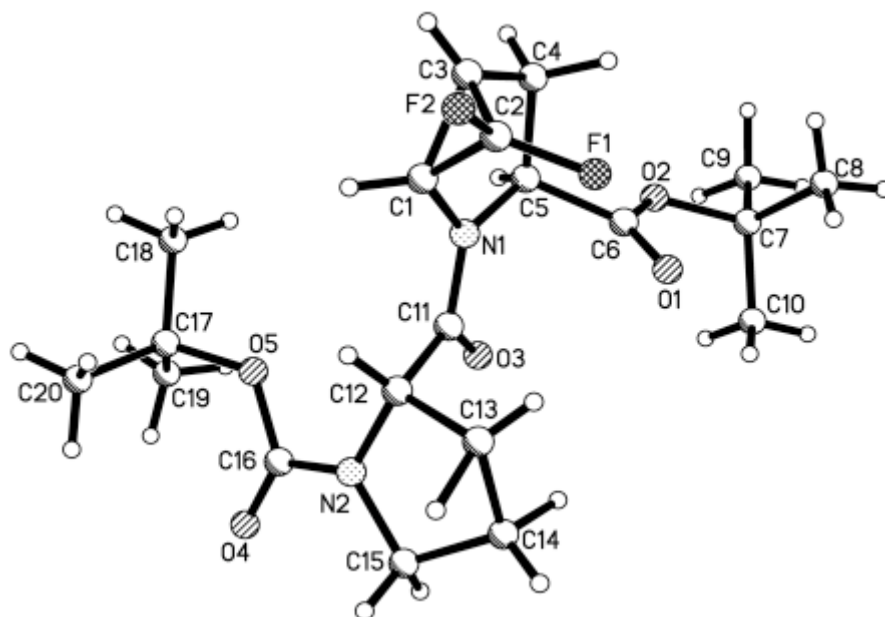


Figure 3.8. Molecular structure of the minor isomer Boc-Pro-*c*-F₂MePro-OBu^t.

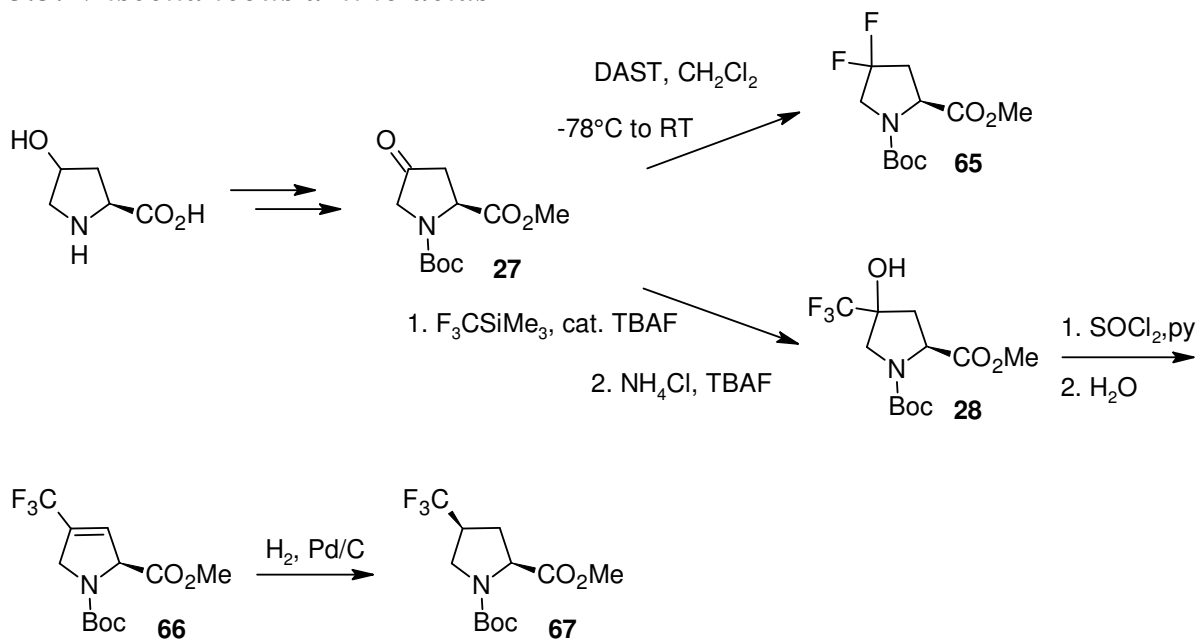
Despite an additional correlation was found between the *endo*-F atom and CH-2 of the proline residue, the absence of a strong correlation in the α -CH spectral region with *endo*-F, in the case of the minor isomer proofs, it being the *cis*-isomer. Finally those conclusions were confirmed with the X-ray molecular structure analysis of the minor Boc-Pro-*c*-F₂MePro-OBu^t (Fig. 3.8).

This prominent difference in the correlations between *endo*-F and α -CH was also found for Pro-F₂MePro-OBu^t dipeptides which were obtained after partial deprotection of the Boc-protected dipeptides.

In contrast to the proline dipeptide, both products of the ^DPhe dipeptide synthesis showed the same strong correlation between *endo*-F and H-2. The observation confirmed them possessing the same configuration. Finally the major dipeptides in the Fmoc-form showed similar strong correlation *endo*-F \leftrightarrow H-2.

It is worth mentioning that the conclusions of the substances configurations were consistent with the $[\alpha]_D$ values. Namely, all *cis*-methano isomers showed prominent shift towards positive values in comparison with the values from the corresponding *trans*-methano derivatives.

3.3. Miscellaneous amino acids



Scheme 3.6. Syntheses of Boc-F₂Pro-OMe and Boc-TfmPro-OMe starting from hydroxyproline.

Incorporation of amino acids into peptide sequences with manual Fmoc SPPS strategy requires corresponding amino acids in Fmoc-Xaa-OH form. flp and Flp were bought already as Fmoc-protected. Boc-F₂Pro-OMe **65** was synthesized according to¹⁰¹ starting from hydroxyproline (Scheme 3.6.). Boc-TfmPro-OMe was obtained starting from the same compound according to synthetic protocol at Scheme 1.8. which was however modified as shown on Scheme 3.6. First 4-oxoproline derivative **27** was obtained from hydroxyproline in two steps in 73% yield. It was treated with the Ruppert-Prakash reagent to give the adduct **28** in 77% yield. Water molecule was eliminated with thionyl chloride in pyridine giving **66** in 77% yield. Finally, hydrogenolysis under palladium catalyst gave desired protected amino acid **67** (94% yield).

The two TfmMePro amino acids were synthesized according to Scheme 1.13. starting from protected dehydroproline (Scheme 3.1.) by cyclopropanation with trifluorodiasoethane. Despite the procedure was performed according to the protocol and conversion of the dehydroproline was full, problems on the chromatographic separation step appeared. Only two A- and B-forms (c- and t-) of Boc-TfmMePro-OMe were eluted from the column with 8.9 and 8.5% yields respectively. That was about 3 fold less in comparison to the original protocol. However, amount of the c- and t-TfmMePro in Boc-Xaa-OMe forms was enough to provide further syntheses.

The rest of the amino acid was available as Boc-*cis*-MePro and HCl**trans*-MePro. All the amino acids were successfully transformed in the Fmoc-protected form according to common procedures (Scheme 3.7.).

the TFA based cocktail, precipitated and RP-HPLC purified. In this case the product was already quite clean and easier to separate.

To avoid the unexplored cyclization ^DPhe-**Xaa**, for the double substituted GS the synthesis was started from Val such that the cyclization was a more predictable.

Precipitation at the end of the synthesis was also not very efficient since reasonable amount of the material was dissolved in ether. For the most hydrophobic peptides, amount of compounds in ether fraction was higher than was precipitating. Both, the residue and the ether solution were taken for purification.

Full list of the synthesized GS analogues and their nomenclature are given in Table 3.3.

name	Sequence
I-flp-GS	<i>cyclo</i> [Val-Orn-Leu- ^D Phe- flp -Val-Orn-Leu- ^D Phe-Pro]
II-flp-GS	<i>cyclo</i> [Val-Orn-Leu- ^D Phe- flp -Val-Orn-Leu- ^D Phe- flp]
I-Flp-GS	<i>cyclo</i> [Val-Orn-Leu- ^D Phe- Flp -Val-Orn-Leu- ^D Phe-Pro]
II-Flp-GS	<i>cyclo</i> [Val-Orn-Leu- ^D Phe- Flp -Val-Orn-Leu- ^D Phe- Flp]
I-F ₂ Pro-GS	<i>cyclo</i> [Val-Orn-Leu- ^D Phe- F₂Pro -Val-Orn-Leu- ^D Phe-Pro]
II-F ₂ Pro-GS	<i>cyclo</i> [Val-Orn-Leu- ^D Phe- F₂Pro -Val-Orn-Leu- ^D Phe- F₂Pro]
I-c-MePro-GS	<i>cyclo</i> [Val-Orn-Leu- ^D Phe- c-MePro -Val-Orn-Leu- ^D Phe-Pro]
II-c-MePro-GS	<i>cyclo</i> [Val-Orn-Leu- ^D Phe- c-MePro -Val-Orn-Leu- ^D Phe- c-MePro]
I-TfmPro-GS	<i>cyclo</i> [Val-Orn-Leu- ^D Phe- TfmPro -Val-Orn-Leu- ^D Phe-Pro]
II-TfmPro-GS	<i>cyclo</i> [Val-Orn-Leu- ^D Phe- TfmPro -Val-Orn-Leu- ^D Phe- TfmPro]
I-A(c)-GS	<i>cyclo</i> [Val-Orn-Leu- ^D Phe- c-TfmMePro -Val-Orn-Leu- ^D Phe-Pro]
II-A(c)-GS	<i>cyclo</i> [Val-Orn-Leu- ^D Phe- c-TfmMePro -Val-Orn-Leu- ^D Phe- c-TfmMePro]
I-B(t)-GS	<i>cyclo</i> [Val-Orn-Leu- ^D Phe- t-TfmMePro -Val-Orn-Leu- ^D Phe-Pro]
II-B(t)-GS	<i>cyclo</i> [Val-Orn-Leu- ^D Phe- t-TfmMePro -Val-Orn-Leu- ^D Phe- t-TfmMePro]
I-t-F ₂ MePro-GS	<i>cyclo</i> [Val-Orn-Leu- ^D Phe- t-F₂MePro -Val-Orn-Leu- ^D Phe-Pro]

Table 3.3. List of the proline synthesized substituted GS analogues.

3.4.2. Synthesis of leucine substituted gramicidin S analogues

In order to provide the material for further planned investigations of GS behavior in lipid membranes, few other analogues were synthesized. Namely, phenylglycine (Phg) and para-fluorophenylglycine (FPhg) were introduced at leucine positions, from which the first was used for double substitution only and the second for both single and double (Table 3.4.).

The amino acids were bought as zwitter-ions in racemic forms (as the racemization along the synthesis was assumed to be very likely) and transformed into corresponding Fmoc-derivatives suitable for the peptide synthesis using Fmoc-Cl reagent. The peptide synthesis was done the same way as described in the previous chapter starting from ^DPhe-preloaded chlorotrytyl resin. The peptides were synthesized in a mixture of D- and L-labeled forms which were then separated on the preparative RP-HPLC. Assignment of the chromatogram was done according to the observation that each one ^DFPhg causes significant shift of the retention time to lower values⁴⁸. The assignment was consistent with the circular

dichroism measurements of obtained fractions (D-amino acids invert the ellipticity and thus decrease the absolute signal intensity).

name	Sequence
I- ^D FPhg-GS	<i>cyclo</i> [Val-Orn- ^D FPhg - ^D Phe-Pro -Val-Orn-Leu- ^D Phe-Pro]
I- ^L Phg-GS	<i>cyclo</i> [Val-Orn- ^L FPhg - ^D Phe-Pro -Val-Orn-Leu- ^D Phe-Pro]
II- ^{D,D} FPhg-GS	<i>cyclo</i> [Val-Orn- ^D FPhg - ^D Phe-Pro -Val-Orn- ^D FPhg - ^D Phe-Pro]
II- ^{D,L} FPhg-GS	<i>cyclo</i> [Val-Orn- ^D FPhg - ^D Phe-Pro -Val-Orn- ^L FPhg - ^D Phe-Pro]
II- ^{L,L} FPhg-GS (LGS)	<i>cyclo</i> [Val-Orn- ^L FPhg - ^D Phe-Pro -Val-Orn- ^L FPhg - ^D Phe-Pro]
II- ^{D,D} Phg-GS	<i>cyclo</i> [Val-Orn- ^D Phg - ^D Phe-Pro -Val-Orn- ^D Phg - ^D Phe-Pro]
II- ^{D,L} Phg-GS	<i>cyclo</i> [Val-Orn- ^D Phg - ^D Phe-Pro -Val-Orn- ^L Phg - ^D Phe-Pro]
II- ^{L,L} Phg-GS	<i>cyclo</i> [Val-Orn- ^L Phg - ^D Phe-Pro -Val-Orn- ^L Phg - ^D Phe-Pro]

Table 3.4. List of the synthesized leucine substituted GS analogues.

3.4.3. Synthesis of proline substituted SAP analogues

A row of SAP analogues was synthesized (Table 3.5.), where proline residue in position 11 was substituted with the artificial amino acids. The synthesis was performed according to⁴⁴, starting from proline preloaded chlorotrytyl resin. Arginine was loaded in the Pbf-protected form. The only change in the reactants was the coupling reagent 6Cl-HOBt instead of HOAt.

Name	Sequence	cleavage
SAP-TfmPro	VRLPPPVRLLP- TfmPro -PVRLPPP	HFIP
SAP-c-MePro	VRLPPPVRLLP- c-MePro -PVRLPPP	HFIP
SAP-t-MePro	VRLPPPVRLLP- t-MePro -PVRLPPP	TFA
SAP-flp	VRLPPPVRLLP- flp -PVRLPPP	TFA
SAP-Flp	VRLPPPVRLLP- Flp -PVRLPPP	TFA
SAP-A(c)	VRLPPPVRLLP- c-TfmMePro -PVRLPPP	*
SAP-B(t)	VRLPPPVRLLP- t-TfmMePro -PVRLPPP	HFIP
SAP-t-F ₂ MePro	VRLPPPVRLLP- t-F₂MePro -PVRLPPP	TFA
SAP-c-F ₂ MePro	VRLPPPVRLLP- c-F₂MePro -PVRLPPP	HFIP

Table 3.5. List of the synthesized SAP analogues. The last column represents the cocktail type used for cleavage of the peptide from the resin. Asterisk indicates the peptide synthesized previously by Dr. Mykhailiuk¹⁰⁴.

For the first few synthesized analogues the cleavage and the deprotection steps were separated in order to make a proper monitoring. First the linear peptide was cleaved from the resin with hexafluoroisopropanol/dichloromethane cocktail and the tris-Pbf-protected peptide was treated with the TFA-water mixture in the volume ratios 95:5 and 80:20¹⁰⁵.

According to the HPLC monitoring, the first employed cocktail showed absence of all protection groups after one hour and the second one gave not complete deprotection even after 2 hours of treatment. After this observation the cleavage from the resin for the rest of peptides was done with the TFA-water 95:5

cocktail directly. The full list of the synthesized analogues is presented in the Table 3.5.

3.4.4. Synthesis of the peptides with F_2MePro

Both I-t- F_2MePro -GS and SAP-t- F_2MePro were synthesized as usual. The Fmoc-dipeptides were taken as 2 eq, whereas the rest of the amino acids as 4 eq (for GS) and 6 eq (for SAP). Normal 2 hour coupling time was prolonged for the dipeptide coupling to 4-5 h and for the next amino acid to 3 h. However careful HPLC monitoring showed that such prolongation was even not necessary. Cyclization of the GS analogue was done as usual. Resulting peptides were obtained in pure forms in 20% and 34% yields for I-t- F_2MePro -GS and SAP-t- F_2MePro respectively.

Synthesis of SAP-c- F_2MePro was done the same way as for the corresponding *trans*-analogue, except of the 3 times less loading and the lower purity of the starting Fmoc-dipeptide (see chapter 3.2.2.). Here the coupling was complete after 3 hours. After coupling of the next amino acid (Pro) and at the end of the sequence grow the chromatogram showed two main products. Previously few diastereomeric SAP peptides labeled with rac-FPhg were not possible to separate on corresponding D- and L- forms with RP-HPLC¹⁰⁶. The peaks on the chromatogram are usually broad. Hence the strategy was changed.

First the linear tris-Pbf peptide was cleaved from the resin with the HFIP cocktail, the compound in contrast to the deprotected form was rather hydrophobic than amphiphilic, thus showed narrower peaks in chromatogram. The two products were separated by RP-HPLC, deprotected with the TFA-water (95:5 vol) cocktail* and purified by RP-HPLC again. The major peptide obtained this way was pure (7% yield) and showed characteristic ¹⁹F-NMR spectrum with two doublets different by chemical shifts than of the t- F_2MePro substituted peptide (see Table 7.2).

3.5. Properties of the gramicidin S analogues

3.5.1. Hydrophobicity (RP-HPLC)

First the GS analogs were systematically compared by retention times in analytical RP-HPLC. This is a normal part of the purity characterization of the peptides after the synthesis. However, the retention time reflects also the hydrophobicity of the corresponding substances.

Systematic analysis of the retention time values showed few tendencies (Fig. 3.9.). For the proline substituted analogues, each single fluorination (Flp and flp substitution) decreases the hydrophobicity of resulting peptides, whereas trifluoromethylation (TfmPro, c/t-TfmMePro) increases it. The rest of the peptides

* the deprotection was complete within 30-60 min period according to the HPLC monitoring.

from this group (substituted with F₂Pro, c-MePro, t-F₂MePro) showed only slight increase of this parameter.

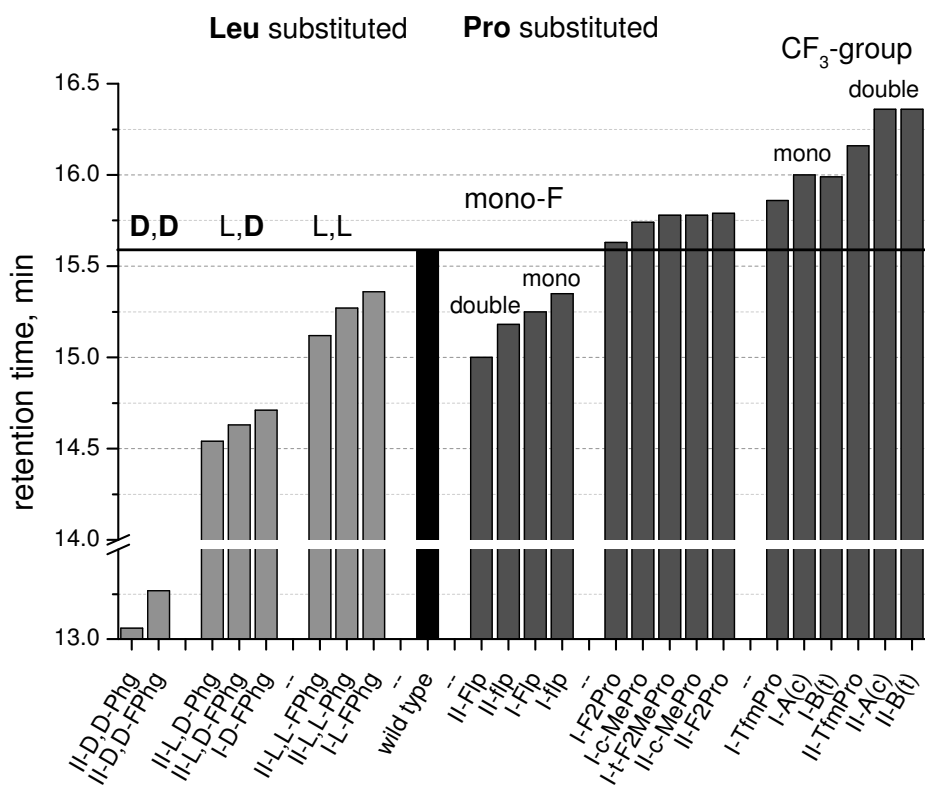


Figure 3.9. RP-HPLC retention times of the studied GS analogues.

The influence of the proline substituent is rather non-specific in contrast to the leucine substitution. Introduction of a phenylglycine residue decreases the hydrophobicity and exceed impact of fluorination. Inversion of L-PHg or FPHg to respective D-configuration has the strongest effect, causing dramatic reduction of the retention times. This effect can be easily explained as disruption of the amphipathic profile of the molecule.

3.5.2 Antimicrobial activity (MIC)

Antimicrobial activity of the GS analogues was compared in serial 2-fold broth dilution test with both Gram-positive and Gram-negative bacterial strains¹⁰⁷. This test shows the ability of the substances to inhibit the bacterial grow in a given medium. The bacteriostatic activity correlates with the ability of the tested peptides to kill bacterial cells. Gravimetrically determined peptide concentration is known to be not very accurate. Therefore the peptide amounts were calibrated on HPLC and then corrected by aliquotizing from the stock solutions with known concentrations. The values of minimal inhibitory concentration (MIC) obtained thereafter are presented in Table 3.6.

All the synthesised GS analogues maintain the antimicrobial activity with differend degree of decrease. In the case of proline substitution few tendencies can be extracted from the MIC data. Single fluorination (flp and Flp) retains the

activity almost on the level of the wild type peptide. In contrast, trifluoromethylation (TfmPro, c/t-TfmMePro) decreases the activity especially in the case of double substitution. Double F₂Pro substitution does it as well. The rest of the proline substituted GSs showed values of the activity 1-3 dilution less than the wild type.

For leucine labeling decrease of the antimicrobial activity against Gram-positive strains is caused by introduction of D-residue (main effect) and a Phg/FPhg instead of leucine (minor effect).

GS analogue	strain / MIC, g/l			
	Gram-positive		Gram-negative	
	<i>S. aureus</i> DSM 1104	<i>E. faecalis</i> DSM 2570	<i>E. coli</i> DSM 1103	<i>P. aeruginosa</i> DSM 1117
wild type	≤0.5	2	16	64
Pro substitution				
II-Flp	1	8	16	128
II-flp	1	4	32	128
I-Flp	1	8	16	128
I-flp	≤0.5	2	16	128
I-F ₂ Pro	1	2	32	256
I-c-MePro	1	4	32	128
I-t-F ₂ MePro	1	2	32	128
II-c-MePro	2	4	64	128
II-F ₂ Pro	8	16	256	128
I-TfmPro	2	4	64	128
I-A(c)	4	4	128	128
I-B(t)	8	8	256	128
II-TfmPro	16	16	> 256	256
II-A(c)	64	32	> 256	128
II-B(t)	64	64	> 256	> 256
Leu substitution				
II- ^{D,D} Phg	64	64	128	128
II- ^{D,D} FPhg	64	> 64	128	64
II- ^{D,L} Phg	32	32	64	128
II- ^{D,L} FPhg	8	32	64	128
I- ^D FPhg	8	64	32	256
II- ^{L,L} FPhg	2	4	64	256
II- ^{L,L} Phg	2	8	128	> 256
I- ^L FPhg	1	2	16	64

Table 3.6. Minimal inhibitory concentration (MIC) of the GS analogues determined in the serial broth dilution test.

3.5.3. Conformation (CD)

Circular dichroism (CD) is a versatile spectroscopic method widely used to study conformation of peptides in solution^{108,109}. Gramicidin S is cyclic and therefore possesses a relatively rigid secondary structure. The structure is additionally stabilized by four intermolecular hydrogen bonds. The CD spectra in a hydrogen bond preserving solvent such as trifluorethanol (TFE) and in a protic solvent such as water might be different. This is indeed observed (Fig. 3.10.). The spectrum contains two prominent negative bands: at 206 and 223 nm¹¹⁰. The band ratio changes upon changing the solvent as shown at Fig. 3.11.

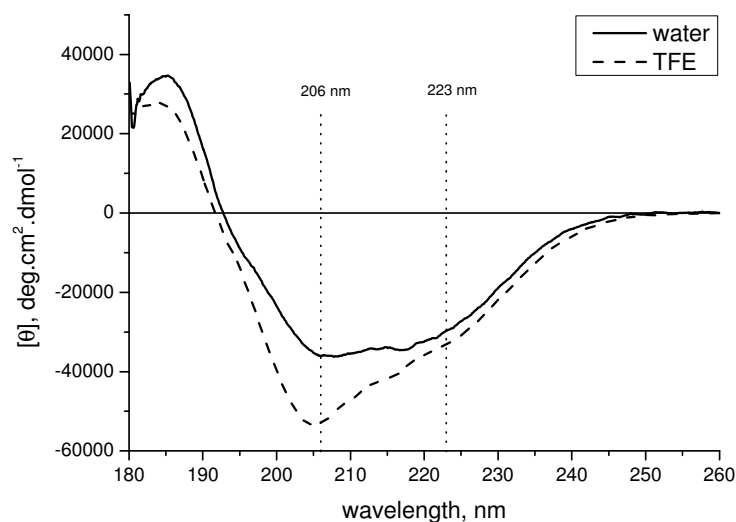


Figure 3.10. Circular dichroism spectra of the wild type gramicidin S in water (solid line) and trifluorethanol (dashed line) at 25°C.

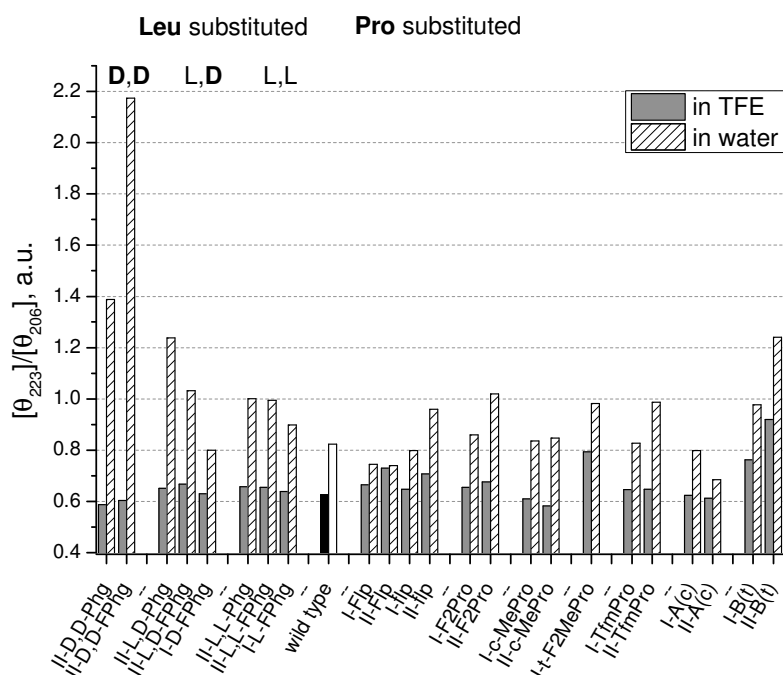


Figure 3.11. $[\theta]_{223}/[\theta]_{206}$ ellipticity ratios determined in CD spectra of the gramicidin S analogues in trifluorethanol (grey boxes) and water (white patterned boxes) at 25°C.

The leucine substituted analogues showed the largest differences between the ellipticity ratios in the two solvents when the D-residues content was increased. The GS structure is significantly affected by D-amino acids content.

For the group of proline substituted peptides additional measurements were done in (12:0/12:0)PC (DLPC) unilamellar vesicles. First the wild type peptide was measured in phosphate buffer (PB) and in PB-methanol mixture (1:1 vol). The ellipticity at 215 nm was taken as the value to indicate the signal intensity.

GS is a peptide modestly soluble in water. The signal intensity in PB was only 0.27 of that in PB-methanol. The intensity rose to about 0.8 of the PB-methanol value when the peptide was mixed to DLPC liposomes. It remained practically the same when the lipid and the peptide were codissolved before the vesicles preparation rather than mixed. This apparent equality indicates high affinity of GS to an amphipathic lipid interface.

The most hydrophobic analogues II-A(c)-GS and II-B(t)-GS showed no spectrum in PB meaning they are not soluble in this solvent at all. The binding to the DLPC liposomes led to transfer of the peptide in solution and increase of the signal. The observed signal increase was slow (Fig. 3.12.). Measured instantly after mixing the signal intensity was only 0.1 of the signal intensity in reconstituted samples for both II-A(c)-GS and II-B(t)-GS. Being monitored over prolonged time the intensity steady increased during few hours of observation (Fig 3.12.) and after 10 h reached 0.9 intensity of the reconstituted sample.

For the most hydrophobic ones II-Flp-GS and II-flp-GS this ratio was 0.9 already after mixing with the liposomes indicating immediate immobilization as was for the wild type. For the rest of the proline substituted peptides the starting intensity ratio value was varying in the range 0.4 ÷ 0.7.

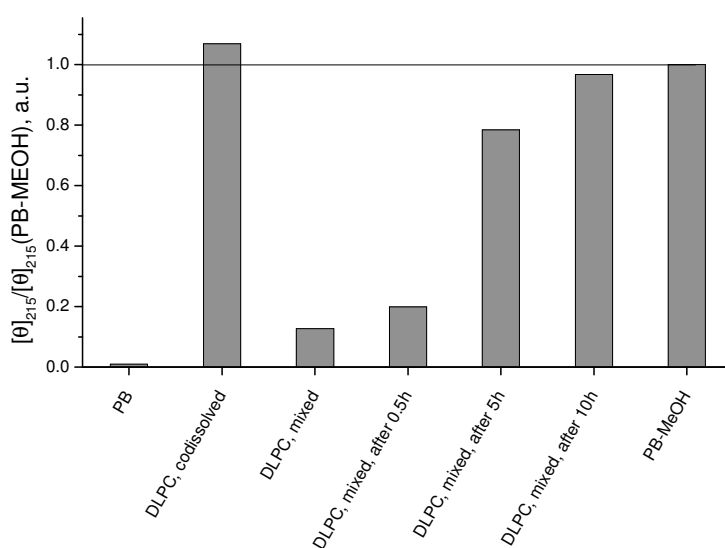


Figure 3.12. Intensity of the signal at 215 nm in the CD spectrum of hydrophobic II-A(c)-GS in various environments related to the intensity in PB-methanol solution (taken as 1.0) at 30°C and 37 mM nominal peptide concentration. In DLPC samples the peptide to lipid ratio was 1/40.

It was said that the ellipticities ratio $[\theta]_{223}/[\theta]_{206}$ for the wild type GS in water was substantially increased (0.82) in comparison to TFE (0.63). In lipid vesicles this ratio was even higher 0.92. In PB-methanol this ratio was practically the same as in water. The ratio $[\theta]_{223}/[\theta]_{206}$ in this solvent mixture was compared against the band ratio in DLPC reconstituted samples as shown on Fig. 3.13. The peptides with methanoprolines in *trans*-configuration (I-t-F₂MePro-GS, I-B(t)-GS and II-B(t)-GS) demonstrated systematically higher $[\theta]_{223}/[\theta]_{206}$ values. Moreover for all of them as well as for II-flp-GS the ratio remained almost the same in solution and in the liposomes suggesting the same conformation assumed in both conditions.

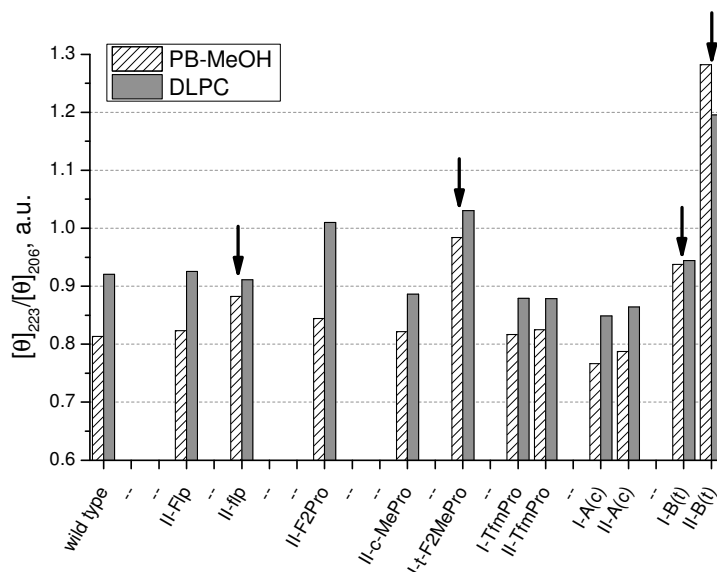


Figure 3.13. $[\theta]_{223}/[\theta]_{206}$ ellipticities ratios in CD spectra of the gramicidin S analogues in PB-methanol solution (white patterned) in presence of DLPC vesicles (grey) at 30°C and 37 mM nominal peptide concentration. The peptide to lipid ratio was 1/40.

All the other amino acids were showing rather moderate and less systematic levels of conformational changes. However, all the gramicidin S peptides showed similar shapes of the CD spectra, showing that the rigid GS structure was not significantly disturbed.

3.5.4. Hemolytic activity (HC_{50})

Lytic activity against human erythrocytes of selected GS analogues was measured. The 50% hemolytic concentrations for the proline substituted GS peptides are illustrated at Fig. 3.14. For all peptides containing single fluorinated amino acids the level of hemolysis decreased whereas for the rest of the amino acids the effect was opposite. The highest hemolysis was observed for double trifluoromethylated peptides. The degree of hemolysis was higher for II-A(c)-GS < II-TfmPro-GS < II-B(t)-GS.

GS analogues containing two FPhg residues were previously investigated¹¹¹. It was shown that hemolysis decreased in the order L,L > wild type GS >> L,D >>

D,D. Here the effect of a single leucine with FPhg replacement was studied (Fig. 3.15.). The activity decreased in the order $II^{-L,L}FPhg \geq II^{-L,L}Phg > I^{-L}FPhg >$ wild type GS. Thus data is consistent with the previous observation that $II^{-L,L}FPhg-GS$ possesses higher hemolytic activity then the wild type peptide. On the other hand the activity was almost the same for $II^{-L,L}Phg-GS$ and $II^{-L,L}FPhg-GS$ suggesting no special effect from a fluorine atom.

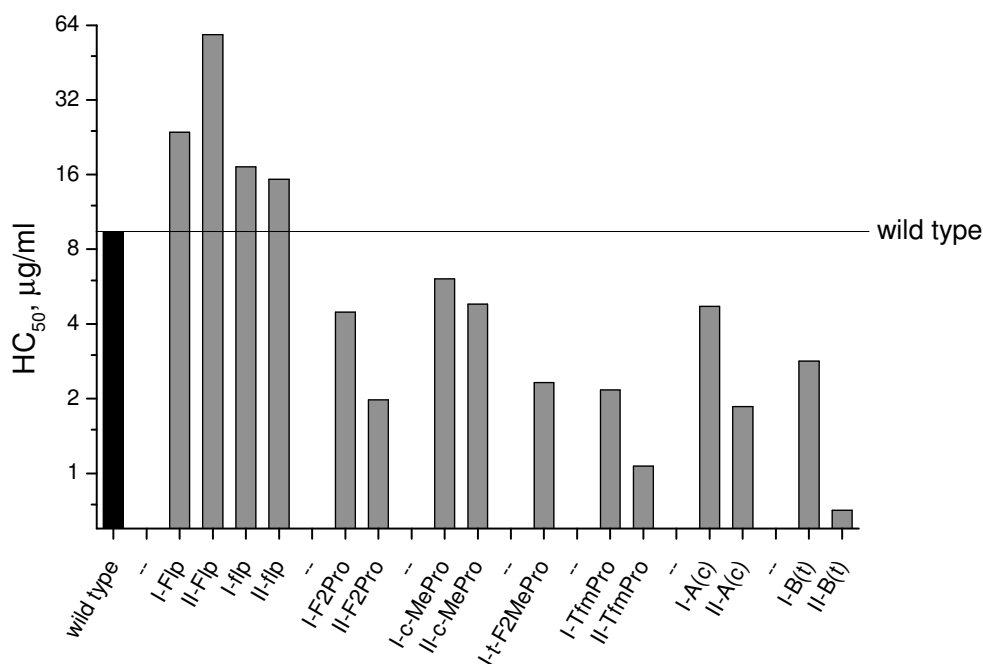


Figure 3.14. 50% hemolytic concentrations determined for the proline substituted GS analogues.

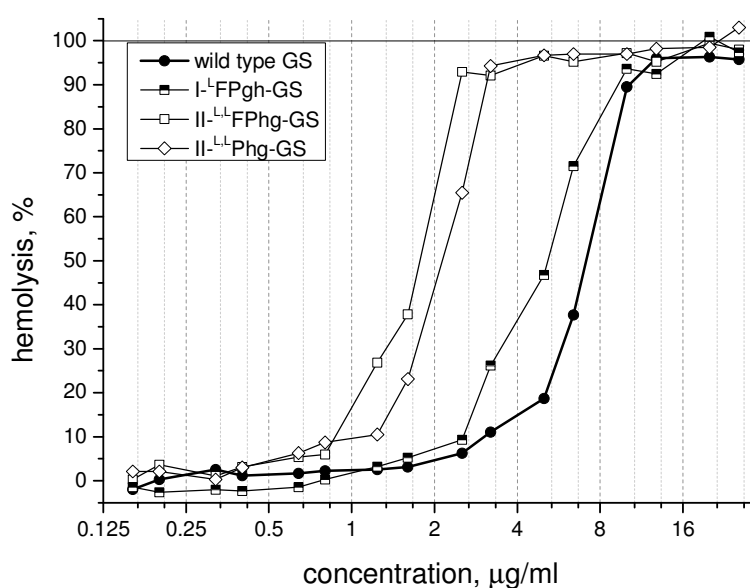


Figure 3.15. Hemolytic activity of leucine substituted GS analogues containing L-epimers.

3.6. Solid state NMR of GS analogues in lipid membranes

Solid state NMR of the GS analogues in macroscopically oriented lipid bilayers was done. Herein orientational behavior of selected peptides is described. In the following description the oriented samples were aligned parallel to the magnetic field unless other stated.

3.6.1. FPhg substituted peptides

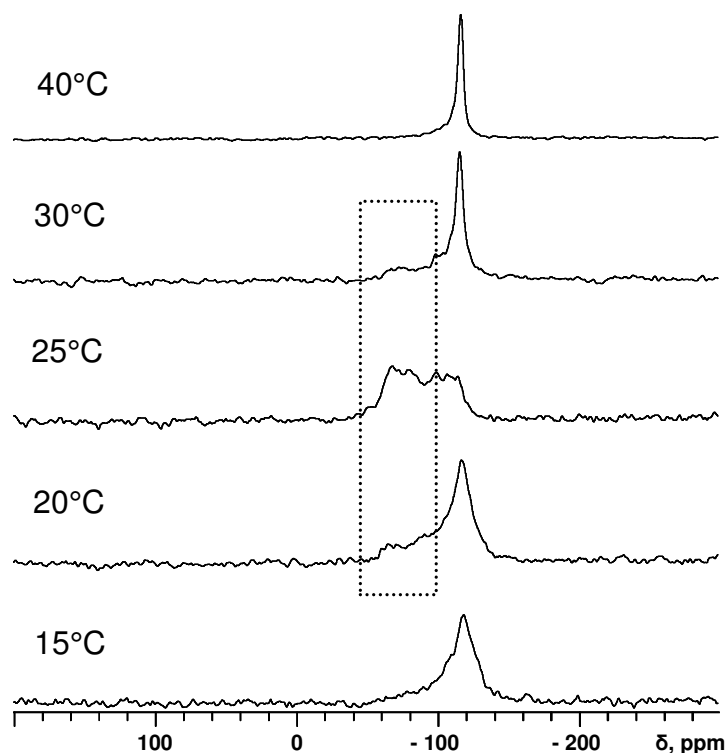


Figure 3.16. Solid state ^{19}F -NMR spectra of II- L,L FPhg-GS in (14:0/14:0)PC at $p/l = 1/40$. Dotted square indicates the re-aligned signals.

As was already described in the literature II- L,L FPhg-GS (denoted LGS by the authors) demonstrated a specific orientational behavior in (14:0/14:0)PC (DMPC) at peptide to lipid ratio (p/l) up to $1/80$ ¹¹². In a temperature dependent series of ^{19}F -NMR spectra, at the temperatures far from the main gel-to-liquid-crystalline lipid phase transition (T_m) the fluorine signal was at the upfield side of the CSA tensor and at the temperature close to the main phase transition ($T_m \sim 23^\circ\text{C}$) new signals appeared at the downfield side, regardless of whether the temperature was changed in cooling or heating mode. After the analysis the upfield singlet was attributed to the surface peptide alignment and the downfield (so-called re-aligned) signal was assigned as a state when the GS molecule is immersed in the lipid bilayer. The same re-alignment of LGS was observed in this work as shown on Fig. 3.16.

An analysis was proposed¹¹³ in which different regions of the spectra were integrated and the normalized integrals were plotted against the temperature (as shown on Fig. 3.17.). It turned out that corresponding mono substituted peptide I-

L FPhg-GS showed barely visible degree of re-alignment at the same conditions where II - L,L FPhg-GS showed almost 80% of the re-aligned state.

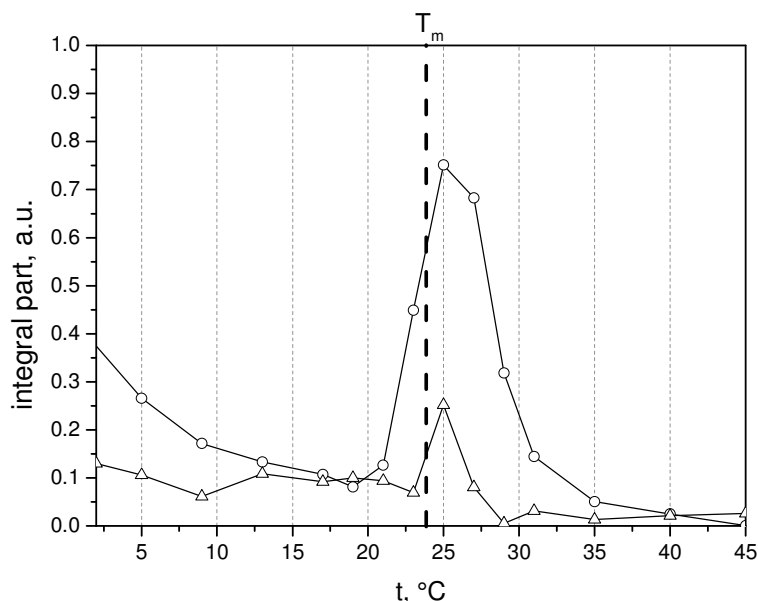


Figure 3.17. Analysis of II - L,L FPhg-GS and I - L FPhg-GS re-alignment in DMPC ($p/l = 1/40$). Circles – the re-aligned fraction (-67; -104ppm) in the 19 F-NMR spectra (-67; -136ppm) of II - L,L FPhg-GS, triangles – the re-aligned fraction (-75; -102ppm) in the spectra (-75; -131ppm) of I - L FPhg-GS.

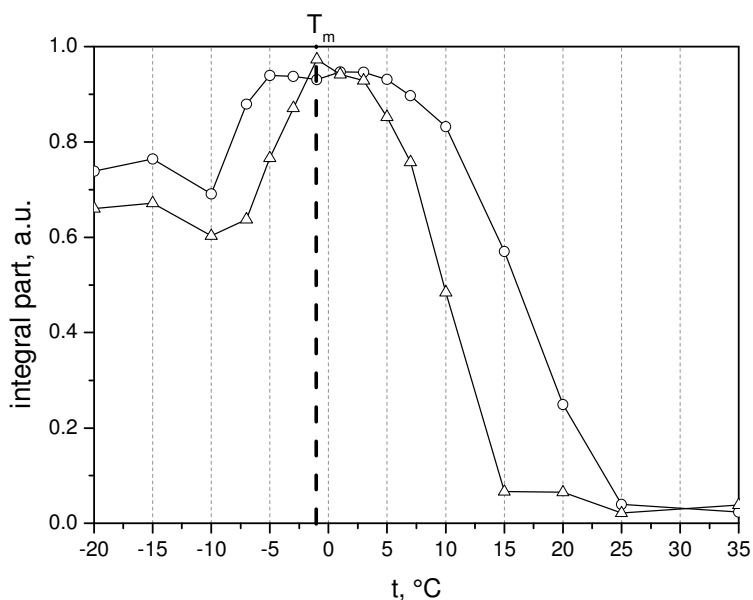


Figure 3.18. Analysis of II - L,L FPhg-GS and I - L FPhg-GS re-alignment in DLPC at $p/l = 1/40$. Circles – the re-alignment fraction (-62; -100ppm) in the 19 F-NMR spectra (-62; -125ppm) of II - L,L FPhg-GS, triangles – the re-aligned fraction (-63; -101ppm) in the spectra (-63; -125ppm) of I - L FPhg-GS.

In a shorter DLPC lipid the degree of the re-orientation and the corresponding temperature range was known to be higher and broader for LGS. The main thermotropic phase transition in this lipid takes place at -2°C the re-

alignment of LGS happened in the temperature range $+25 \div -10^\circ\text{C}$. For the mono labeled molecule I-^LFPhg-GS this range was smaller $+15 \div -7^\circ\text{C}$ (Fig. 3.18.).

Finally, II-^{D,D}FPhg-GS in DMPC oriented bilayers showed two peaks in the spectrum above the phase transition (35°C) at -105 (sharp) and -114 ppm (broad). This indicated completely different mode of alignment with two states of the fluorine orientation in this case.

3.6.2. II-B(t)-GS

Few samples of II-B(t)-GS in DMPC at $p/l = 1/40$ were investigated within both heating and cooling series with a step of 1°C in the focus (phase transition) temperature range. Corresponding ¹⁹F-NMR spectra showed broad $+5.5$ kHz triplet at the lower temperatures and narrow $+4.6$ kHz triplet at the higher temperatures with a transition around 25°C (Fig. 3.19., left stack). Apparently, there was no re-aligned state detected upon these conditions. The peptides mobility was different in the gel and fluid lipid bilayer phases. In the fluid phase the triplet becomes 1 kHz smaller and the components become resolved and narrow.

At higher concentration $p/l = 1/20$ two additional signals appear from both sides of the main triplet at the temperature close to the lipid phase transition (Fig. 3.19., central stack). Addition of cholesterol (5%) caused appearance of the same signals already in the lamellar ordered state, and at $\sim 25^\circ\text{C}$ only an additional non-resolved component at the higher field remained (Fig. 3.19., right stack).

In mixture with non-fluorinated analogue of LGS (II-^{L,L}Phg-GS) the proline substituted II-B(t)-GS showed much higher degree of re-orientation as illustrated on Fig. 3.20. The total p/l ratio was taken as $1/30$ and then the peptides ratio was varied. At the peptides ratio 1:1 (left spectrum) the re-oriented signal was a triplet with the constant -6.7 kHz (dashed square), its population at 22°C was 37% of the total signal. In the sample where II-^{L,L}Phg-GS dominated (peptides ratio 4:1) the intensity of this signal reached 49% (right spectrum). In a parallel sample where II-B(t)-GS was mixed with the wild type GS as 1:1 (the p/l ratio was the same $1/30$) no additional triplets were observed.

In contrast to the DMPC situation, in DLPC II-B(t)-GS completely re-aligned in the temperature range $+7 \div -4^\circ\text{C}$ (Fig. 3.21., left stack). At higher temperatures there was one triplet $+4.6$ kHz, the re-aligned signal was a single -3.7 kHz triplet and at the lower temperatures the splitting was $+5.7$ kHz. This behavior independent from the direction of the temperature change (cooling or heating) was observed if the lowest temperature in the series did not reach -10°C .

If the series when a pre-incubation at -20°C preceded the acquisition series in the heating mode, the data showed prominent hysteresis (Fig. 3.21., right stack). In the range $-10 \div -20^\circ\text{C}$ the signal had powder-like shape. Upon heating at $-5 \div +1^\circ\text{C}$ the signal was composed by two triplets with -3.0 kHz and $+12$ kHz splittings.

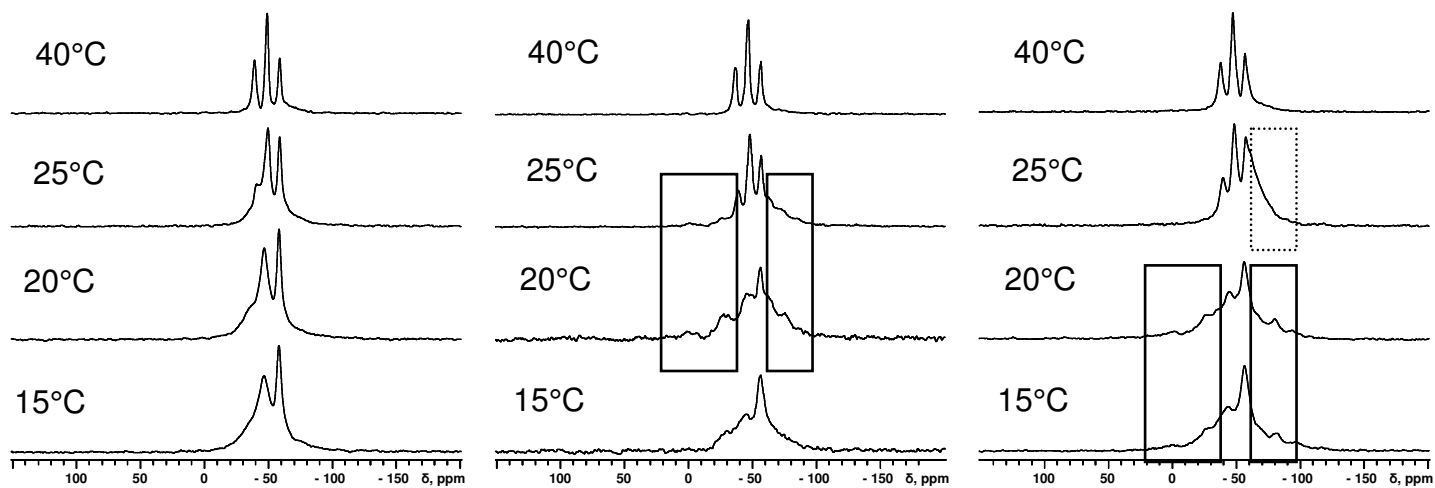


Figure 3.19. Solid state ^{19}F -NMR spectra of II-B(t)-GS in oriented lipid bilayers within heating temperature series: left stack – in DMPC at $p/l = 1/40$, central stack – in DMPC at $p/l = 1/20$, right stack – in DMPC with 5% (mol.) cholesterol.

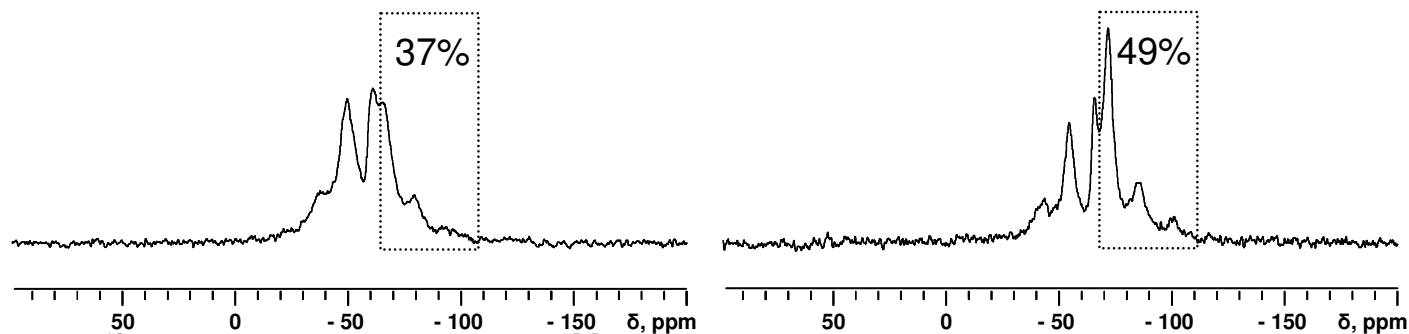


Figure 3.20. Solid state ^{19}F -NMR spectra of II-B(t)-GS: II- L,L Phg-GS: DMPC mixtures at 22°C: left spectrum 1:1:60 mixture, right spectrum 1:4:150 mixture.

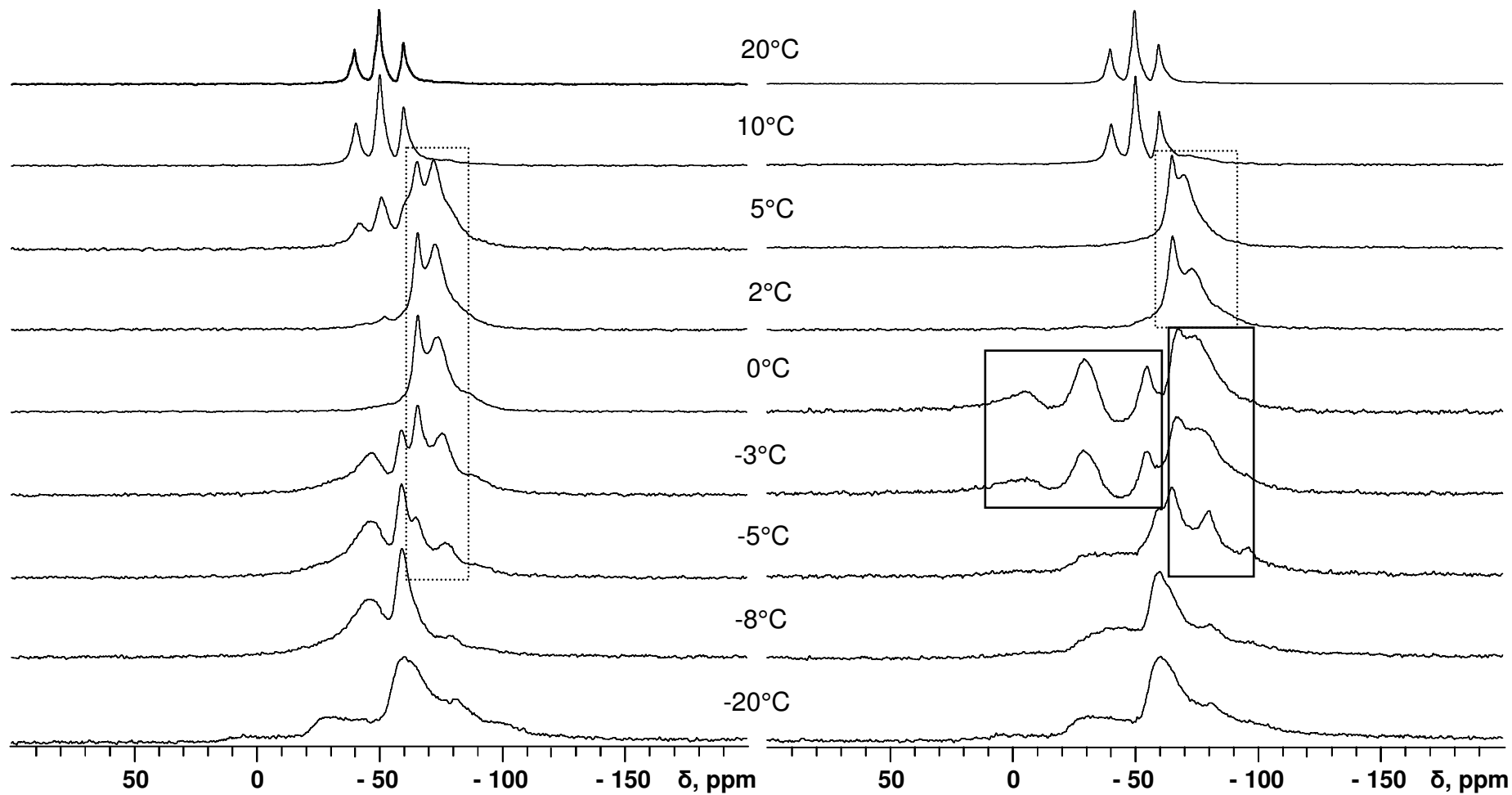


Figure 3.21. Solid state ^{19}F -NMR spectra of II-B(t)-GS in DLPC oriented bilayers ($p/l = 1/40$) at different temperatures upon cooling (left stack) and heating (right stack).

After reaching +1°C the spectral become the same as was in the cooling cycle: -3.7 kHz splitting persisted up to 5°C followed by the triplet +4.6 kHz.

The re-alignment in DLPC was concentration dependent. The threshold concentration was estimated as $p/l = 1/400$. At $p/l = 1/500$ the signal evolution was devoid of the re-aligned state, resembling the situation observed previously in DMPC: single triplets 5.7 and 4.6 kHz below and above 1°C respectively. The re-aligned signal in diluted samples with $p/l = 1/200$ or $1/400$ was slightly different and better resolved with the constant -4.5 kHz.

3.6.3. I-B(t)-GS

Corresponding mono substituted analogue I-B(t)-GS was measured in DMPC and DLPC samples at $p/l = 1/40$. In DMPC at lower temperatures the ^{19}F -NMR spectrum contained one triplet +5.5 kHz. This splitting value remained unchanged upon crossing gel to liquid crystalline phase transition of the lipid.

In DLPC the triplet at higher temperatures (+20°C) was +5.5 kHz, upon cooling the re-aligned state appeared as triplet with -4.3 kHz constant. At -20°C the signal was powder like and upon heating the state with two triplets +13 and -7.4 kHz was observed first, then after 1°C the signal was ~ -3 kHz triplet and after further heating the +5.6 kHz triplet restored. In diluted sample in DLPC ($p/l = 1/400$) the re-oriented signal was -4.7 kHz.

The only difference observed in the spectra of I-B(t)-GS in comparison with its double substituted analogue was the splitting at high temperatures which in this case remained the same as in gel, around +5.5 kHz.

3.6.4. II-A(c)-GS

II-A(c)-GS in DMPC at $p/l = 1/40$ showed no re-alignment. The only one triplet observed in the ^{19}F -NMR spectrum was +5.5 kHz in gel (+10 ÷ +24°C) and +4.6 kHz in the fluid phase (up from +25°C).

In DLPC at $p/l = 1/40$ in the cooling series there was only one triplet +4.7 kHz at higher temperatures (+20 ÷ +7°C). The re-aligned state was a triplet -4.8 kHz (+5 ÷ +1°C). Down from this temperature a triplet +5.5 kHz was present until -10°C, and at even lower temperatures the broad powder-like spectrum was observed. In the heating series a triplet -6.5 kHz appeared first (at -5 ÷ 0°C) and up to +5°C it drifted to -4.2 kHz, then up from 7°C the spectrum contained purely the high temperature triplet +4.6 kHz.

In corresponding diluted sample in DLPC ($p/l = 1/400$) the triplet of the re-aligned state was -4.5 kHz.

The splitting data for all TfmMePro substituted GS peptides is summarized in Table 3.7. The spectra at 90° orientation of the sample to the magnetic field showed that in the fluid lipid phase the peptides were fast rotating along the membrane normal, and in the gel states they were not.

GS analogue	DMPC		DLPC					
	gel state	fluid state	cooling series			heating series after pre-incubation < -10°C		
			gel state	re-aligned state	fluid state	re-aligned below 0°C	re-aligned above +1°C	fluid state
II-B(t)	+5.5	+4.6	+5.7	-3.7 (-4.5)	+4.6	+12& -3.0	-3.7	+4.6
I-B(t)	+5.5	+5.5	+5.5	-4.3 (-4.7)	+5.5	+13& -7.4	~ -3	+5.6
II-A(c)	+5.5	+4.6	+5.5	-4.8 (-4.5)	+4.6	-6.5	-4.2	+4.6
I-A(c)	+5.9	+5.7	~ +6	-4.8	+5.7	-6.5	-4.4	+5.5

Table 3.7. Splitting constants in ^{19}F -NMR spectra of GS analogues substituted with TfmMePro in DMPC and DLPC at $p/l = 1/40$ (in parentheses the values for diluted samples, $p/l = 1/400$) at different peptide states.

3.6.5. II-TfmPro-GS and I-TfmPro-GS

Both TfmPro substituted GS peptides were investigated in the above mentioned lipids. The splitting constants of the triplet signals for both peptides are given in Table 3.8.

I-TfmPro-GS in DMPC ($p/l = 1/40$) showed a singlet shape below the phase transition temperature and a triplet above the phase transition with the splitting constant $+2.8 \text{ kHz} \div +3.2 \text{ kHz}$ at $+30 \div +45^\circ\text{C}$. In DLPC ($p/l = 1/40$) in the cooling cycle the triplet well above the phase transition ($+20^\circ\text{C}$) was $+3.2 \text{ kHz}$, in the re-oriented state -1.7 kHz and in gel there was a singlet-like shape.

GS analogue	DMPC			DLPC					
	gel state	fluid state		cooling series			heating series		
		30°C	40°C	gel state	re-oriented state	fluid state	re-aligned below 0°C	re-aligned above +1°C	fluid state
I-TfmPro	0	+2.8	+3.2	0	-1.7	+3.2	(-5)	-1.7	+3.1
II-TfmPro	0	+1.6	+2.2	0	-6.3	+2.3	-7	-6.1	+2.3

Table 3.8. Splitting constants for triplets in ^{19}F -NMR spectra of GS analogues substituted with TfmPro in DMPC and DLPC at $p/l = 1/40$ within different temperature series.

In the heating cycle there was a powder-like spectral shape in the frozen state ($-20 \div -10^\circ\text{C}$), which then transformed into a not resolved triplet with $\sim -5\text{kHz}$ constant. After $+1^\circ\text{C}$ the signal become a normal re-oriented triplet with the -1.7kHz constant and finally at high temperatures ($+20^\circ\text{C}$) there was only the triplet $+3.1\text{kHz}$.

3.6.6. II-Flp-GS

The most hydrophilic of the proline substituted GS analogues II-Flp-GS showed in general quite similar behavior to the other proline substituted peptides. However it took a while before the correct read out was invented.

In the FPgh substituted peptides the fluorine chemical shift changed in a substantially big range. This enabled use of the normalized integrals for quantification of the acquired data assuming different spectral ranges for different peptide states. In Flp substituted peptides this was not possible. It turned out that the signals of the high temperature and the re-aligned states differed only slightly, within ~ 8 ppm. This value lays in the order of the band width. Therefore, the chemical shift change was analyzed rather than the integral intensity. The spectra were acquired in corresponding temperature series with small temperature steps, the data was processed using high line broadening (1.5 kHz) and the main chemical shift was plotted against the temperature as shown on Fig. 3.22.

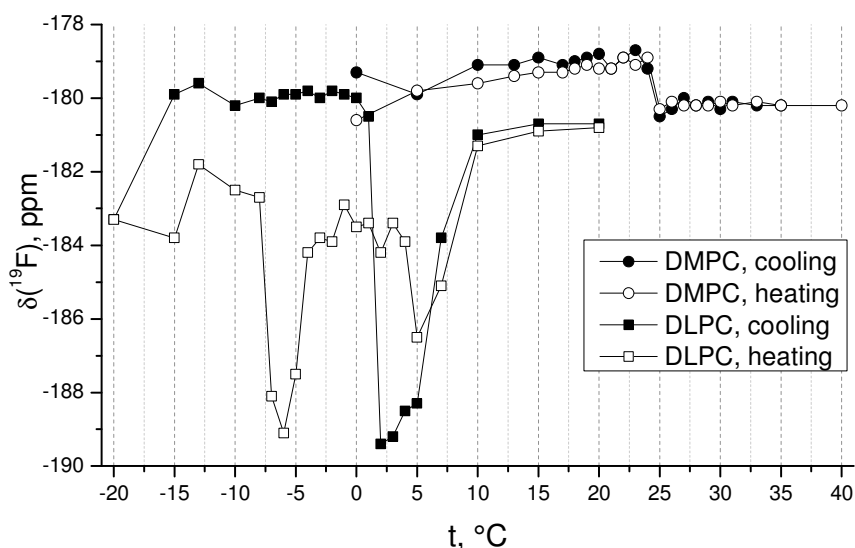


Figure 3.22. Temperature dependence of the chemical shift in the solid state ^{19}F -NMR spectra of II-Flp-GS reconstituted in DMPC (circles) and DLPC (squares) at $p/l = 1/40$ samples in cooling (filled dots) and heating (empty dots) series.

In DMPC the signal changed slightly at 24-25°C upon gel to liquid crystalline phase transition of the lipid without any re-oriented state in both cooling and heating performed series. In DLPC in the cooling cycle the re-orientation was in the same width temperature range $+7 \div +1^\circ\text{C}$, shifted from that demonstrated by the CF_3 -labeled peptides, presumably, due to the other type of the analysis. After reaching -20°C in the heating series the signal showed complicated development meaning the hysteresis observed previously for the other peptides.

3.6.7. II-flp-GS

The flp double substituted peptide II-flp-GS in DLPC possessed even less different chemical shift (≤ 3 ppm) in the re-aligned state in comparison to the signal in the fluid lipid phase (high temperatures). The spectral acquisition and analysis were done the same way as was described for II-Flp-GS. Two curves for the II-flp-GS/DLPC 1/40 sample are shown on Fig. 3.23.

In the cooling temperature series the re-aligned state appeared as a slight downfield shift of the signal in the $+7 \div 0^\circ\text{C}$ temperature range. Below, in the gel state of the lipid, the ^{19}F -NMR band was very broad, the band width on the half high was > 5 kHz, which correspond to ~ 10 in ppm units. The chemical shift read out becomes not accurate in gel, such that the chemical plotting is no longer reliable in this lipid phase. The same broad signal was observed upon heating from -20°C up to 4°C . Up from this temperature the chemical shift development resembled corresponding situation in the cooling series (shown on Fig. 3.23. as “end of hysteresis”).

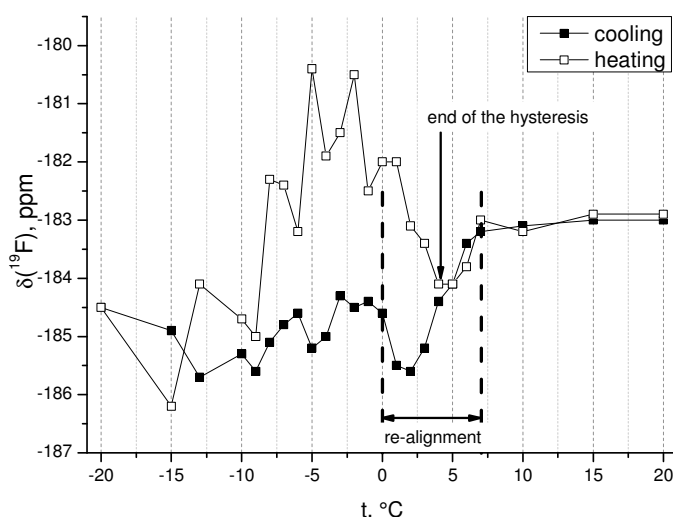


Figure 3.23. Solid state ^{19}F -NMR main chemical shift of II-flp-GS in DLPC at $p/l = 1/40$, dependence from the temperature in cooling (filled squares) and heating (empty squares) cycles.

3.6.7. Peptides with geminal F_2 system in solid state NMR

Non-rotating geminal difluor system was complicated for observation in solid state ^{19}F -NMR experiments, such that the spectral acquisition and the data analysis became not trivial. Due to the presence of a strong geminal coupling between unequivalent fluorine nuclei and strong interaction with the ^1H nuclei in corresponding proline cycles, the free induction decay of the ^{19}F signal was complete in less than 1 ms in the fluid lipid and 200 μs in the gel lipid phase. The spectral lines were broad and therefore the number of scans was substantially increased in order to get the spectra of the same quality as for a CF_3 labeled

peptide. Other acquisition parameters such as spectral window and the pulse if not optimized caused significant distortion of the spectral line shape.

Upon adjusted conditions, II-F₂Pro-GS in both DLPC and DMPC showed a good resolved characteristic spectrum only above the phase transition (fluid phase). In gel as well as in the re-aligned state conditions the spectrum was very broad (the band width at the half high was > 80kHz) and not resolved (Fig. 3. 24., left stack), such that the analysis was impossible. The same behavior showed its mono substituted analogue I-F₂Pro-GS (not shown).

¹⁹F-NMR spectra of I-F₂MePro-GS with two fluorine atoms rigidly attached to the amino acid were narrower and better resolved. As shown on Fig. 3.24. (right stack) the signal in gel and fluid lipid phases appears at the same spectral position whereas the re-aligned spectrum appeared at the upfield side of the CSA tensor with the band width at the half high ~ 25 kHz.

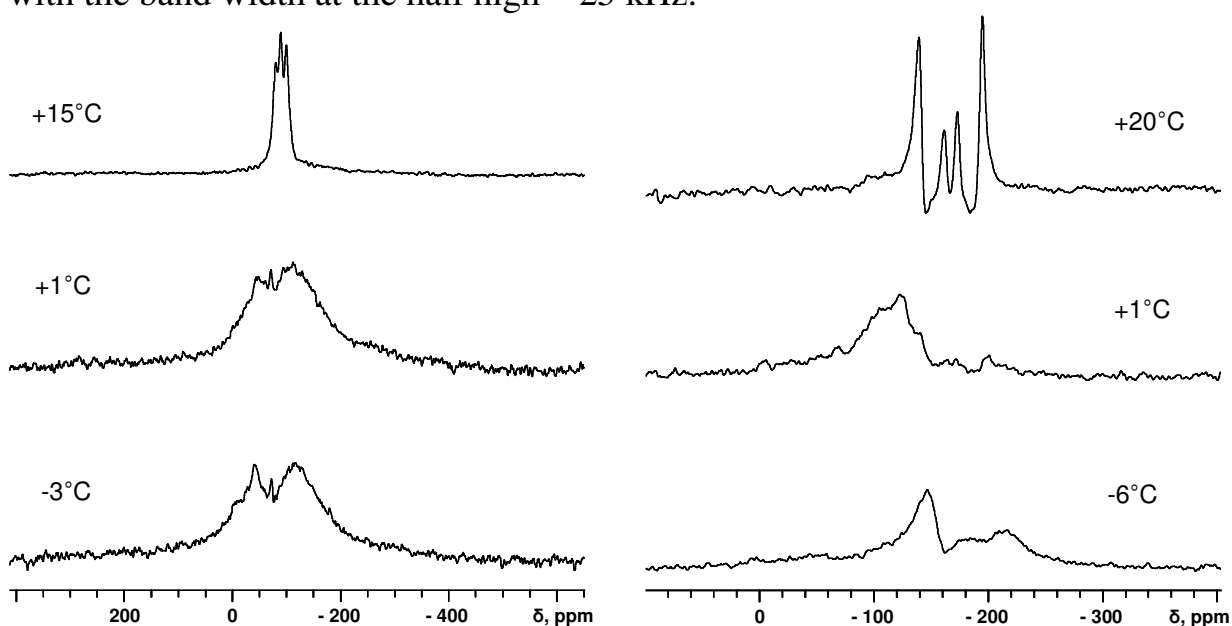


Figure 3.24. Solid state ¹⁹F-NMR spectra of II-F₂Pro-GS (left stack) and I-t-F₂MePro-GS (right stack) in DLPC oriented bilayers at p/l = 1/40.

The line shape in the ¹⁹F-NMR spectra at high temperature (fluid lipid phase) can be considered as two doublets originating from the two nonequivalent fluorine atoms of the CF₂ groups. In the ¹⁹F-NMR of F₂MePro residue (Fig. 3.25.) the two signals stand 33 ppm apart (in solution the distance between two ¹⁹F-NMR resonances was 25 ppm), strong dipole dipole interaction between that two fluorines causes the doublet shape for each of them with the 10 kHz coupling constant. The doublet shape is distorted such that the inner components have lower intensity as the outer. This secondary effect can be called “inverted roof”: if the two fluorine atoms had the same chemical shift the two signals would merge in a doublet in solid state NMR, in contrast to liquid state NMR where the merge will lead to a singlet line shape causing the common roof effect.

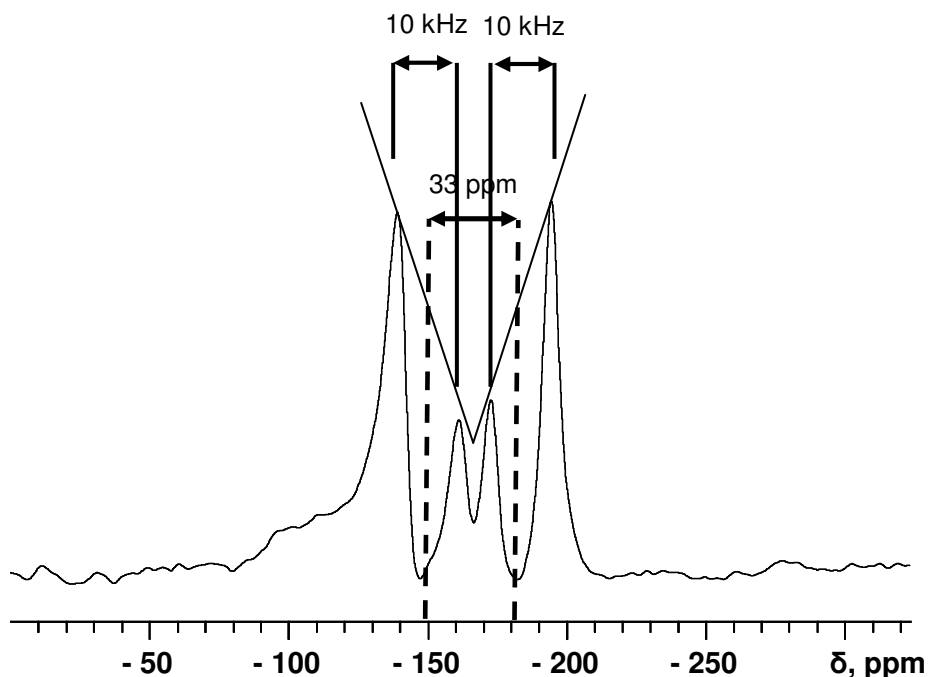


Figure 3.25. Solid state ^{19}F -NMR spectrum of I-t- $\text{F}_2\text{MePro-GS}$ in DLPC oriented sample ($p/l = 1/40$) at 20°C (fluid lipid phase).

In the case of II- $\text{F}_2\text{Pro-GS}$ the spectrum in the fluid lipid phase is composed from the two doublets with ~ 4.5 kHz coupling, 14 ppm apart. The signal has a triplet like appearance because the distance between two doublets and the splitting are of the same strength. In the corresponding spectra at 90 degree sample orientation the dipolar coupling became twice shorter (~ 2 kHz), and the chemical shift distance remained the same.

3.6.9. Influence of the GS analogues on the lipid bilayers (^{31}P -NMR)

^{31}P -NMR spectra of the oriented samples were acquired before and after the ^{19}F -NMR measurements, hydration, re-hydration or long sample storage in freezer. They were done well above the main phase transition temperature in order to control the degree of orientation and mosaic spread of the samples. On Fig. 3.26. the ^{31}P -NMR spectra of the II-B(t)-GS containing samples are shown as representative examples.

Typically, the band width at the half high was 200-300 Hz for the DLPC and 300-400 Hz for the DMPC samples. In the applied field strength (11.7 T) these values correspond to a 1-2 ppm width, whereas the size of the full tensor measured in multilamellar vesicles was about 45 ppm. Thus the mosaic spread could be estimated on the level of several degrees which is good enough for the oriented samples.

Presence of the peptides did not change neither the mosaic spread nor the degree of the lipid headgroups orientation as was judged from corresponding ^{31}P -NMR spectra. Several times after the samples were kept long time at the temperatures below 0°C a huge perpendicularly oriented part (15-20%) appeared in

the spectra of the diluted samples in DLPC (p/l 1/200 or 1/400). Systematic studies of this effect gave controversial results and the effect was assumed to be casual.

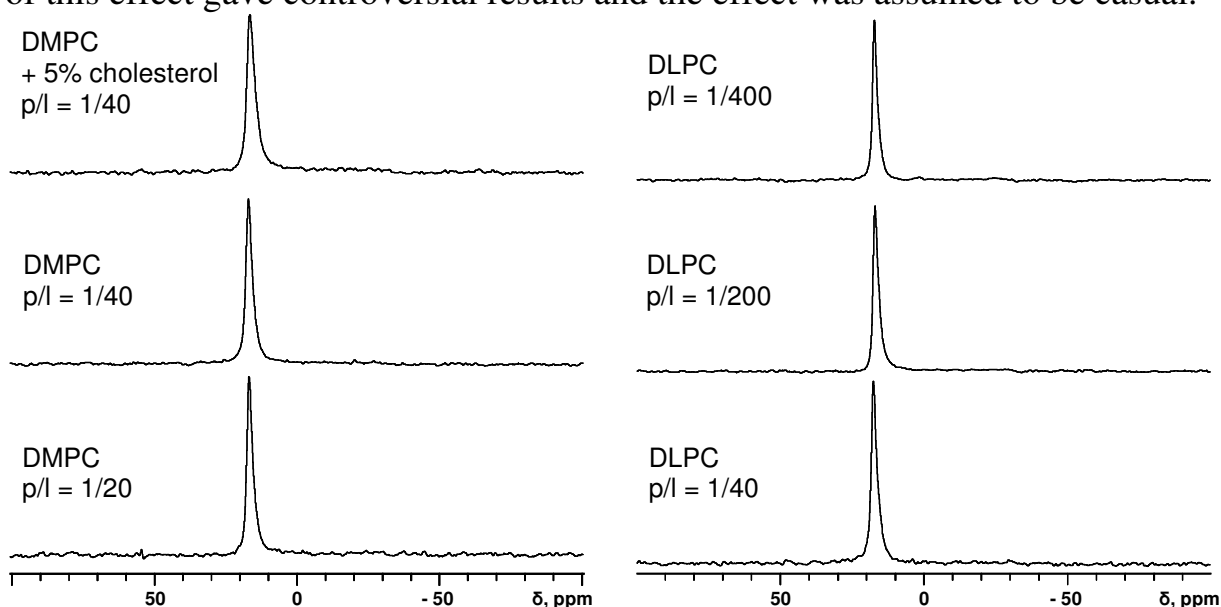


Figure 3.26. Solid state ^{31}P -NMR spectra of the oriented samples containing II-B(t)-GS reconstituted in different lipids. The spectra were acquired at 35°C for DMPC and 30°C for DLPC (in the liquid crystalline lipid phase).

The GS analogues re-alignment described above was observed near the main phase transition temperature of the lipid by ^{19}F -NMR. Corresponding ^{31}P -NMR temperature series were carried out in order to find whether the peptide re-alignment correlates with any changes in the lipid headgroups orientation or mobility. First samples with pure DMPC and DMPC containing GS peptides (at p/l = 1/40) were measured. The peptides of different re-orientation propensity were taken to make a proper comparison: II- $^{\text{L,L}}$ FPhg-GS (high re-alignment), I- $^{\text{L}}$ FPhg-GS (marginal re-alignment), II-B(t)-GS (no re-alignment) and the wild type GS (unknown re-alignment). Neither of the peptides caused any substantial changes in the spectra other than those can be attributed to the lipid phase transition. However, closer look revealed slight deviation of the chemical shift temperature dependence (Fig. 3.27.). Namely, the ^{31}P -NMR chemical shift drifted almost linearly along the temperature change for the pure lipid. II- $^{\text{L,L}}$ FPhg-GS containing sample showed visible deviation from this behavior: the chemical shift was shifted upfield in the temperature range +19 ÷ +22°C in comparison to all other samples, such that the corresponding curve has characteristic “dimple”.

The same peptides were taken for testing the phosphorus chemical shift changes in DLPC oriented samples. In this lipid the peptides re-aligned in the temperature ranges +25 ÷ -10°C for II- $^{\text{L,L}}$ FPhg-GS, +15 ÷ -10°C for I- $^{\text{L}}$ FPhg-GS and +7 ÷ -4°C for II-B(t)-GS. Corresponding temperature dependences of the ^{31}P chemical shifts for the samples contained these peptides as well as with the wild type GS and the control sample with pure DLPC sample are given on Fig. 3.28. The upfield shift caused by the presence of the peptides was more prominent as in DMPC, the “dimple” was of 3-5 ppm size. The starting temperature of the upfield

shifts was different and correlated with the re-alignment propensities of the peptides: +13 for II-^{L,L}FPhg-GS, +5 for I-^LFPhg-GS and -1 °C for II-B(t)-GS.

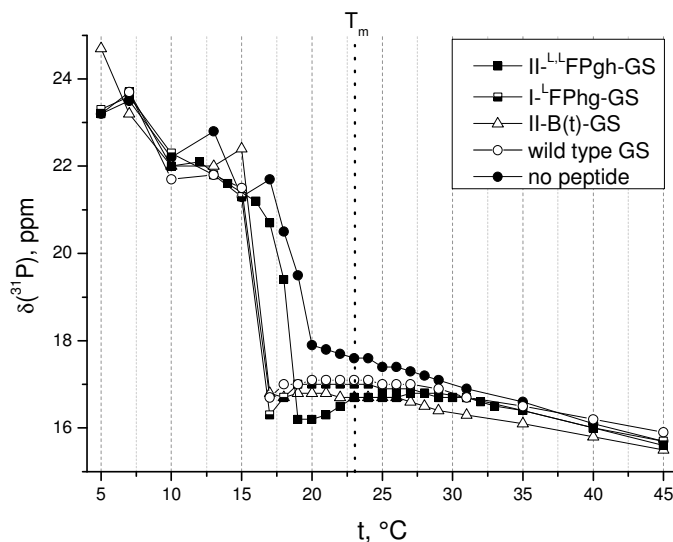


Figure 3.27. Temperature dependence of the ³¹P-NMR chemical shift in oriented samples of DMPC with (p/l = 1/40) or without peptides.

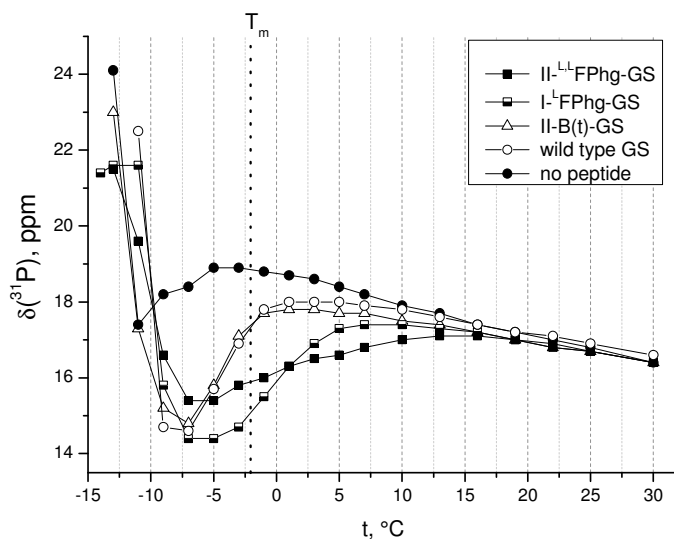


Figure 3.28. Temperature dependence of the ³¹P-NMR chemical shift in oriented samples of DLPC with (p/l = 1/40) or without peptides.

This observation leads to the conclusion that the peptide re-alignment process is indeed connected to the changes in the lipid headgroup state. The correlation between the re-alignment observed by the ¹⁹F-NMR and the upfield drift in the ³¹P-NMR is prominent and allows indirect monitoring of the re-orientation propensity for non-fluorinated peptides such as the wild type GS.

Corresponding curves of the samples with the wild type GS are very similar to that from the II-B(t)-GS. Apparently, proline substitution in this case gave minimal changes.

3.7. Conformational analysis of SAP analogues in solution

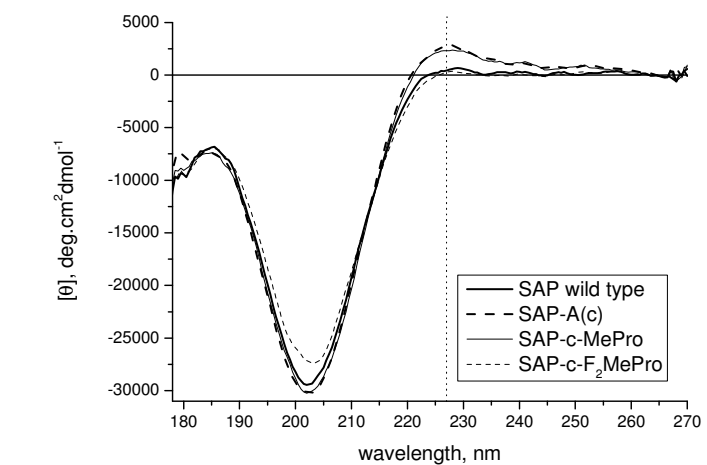
Systematic investigation of the SAP analogues was done in water solution by circular dichroism (CD) measurements with synchrotron light source¹¹⁴. CD spectra of the PPII and unordered structure (random coil) are known to be similar. The most prominent difference between them is the ellipticity at ~227 nm, where PPII shows has a small positive maximum, whereas the random coil has a negative ellipticity of the same order¹¹⁵. The CD spectrum of SAP wild type in water has the signal at 227 nm close to zero. This fact shows that the solution contains both conformations with similar populations. Substitution of proline in position 11 with the amino acids from the Table 3.1. lead to significant shift of the PPII – random coil equilibrium.

First the peptides were systematically measured at concentration 0.5 mg/ml (corresponds to ~ 0.25 mM) at 20°C. It was already known, that c-TfmMePro stabilize the PPII conformation⁹², it turned out that c-MePro sustained it as well, whereas c-F₂MePro showed no stabilization as can be judged from the different positive intensity of the band at 227 nm (Fig. 3.29., A). On the contrary, all peptides with *trans*-methano amino acids (t-TfmMePro, t-F₂MePro and t-MePro) showed very negative ellipticities at this spectral position indicating disruption of the PPII structure (Fig. 3.29., B).

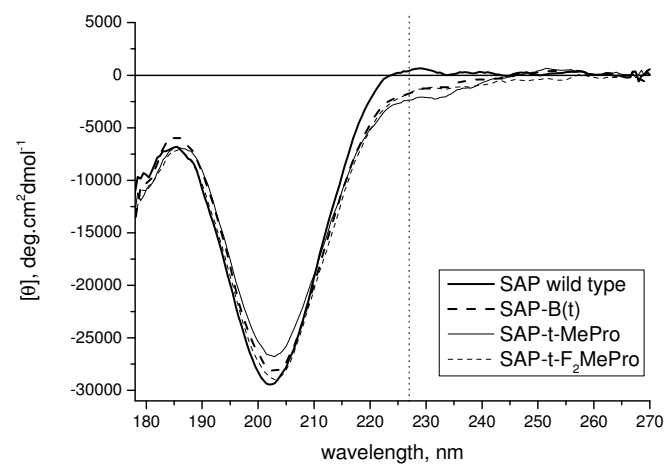
Both Flp and flp did not show any significant impact on the CD shape (Fig. 3.29., C), despite for collagen mimicking peptides⁶⁷ that two amino acids showed a significant impact to the PPII population.

The ellipticities at 227 nm are presented separately on histogram (Fig.3.29., D). This wavelength corresponds to the positive maximum in CD spectra of SAP-A(c) and SAP-c-MePro. Corresponding $[\theta]_{227}$ values were 2471 and 1915 deg·cm²·dmol⁻¹ respectively, close to those of pure PPII conformation. The negative values suggest significant contribution of the random coil structure for SAP-B(t), SAP-t-MePro and SAP-t-F₂MePro.

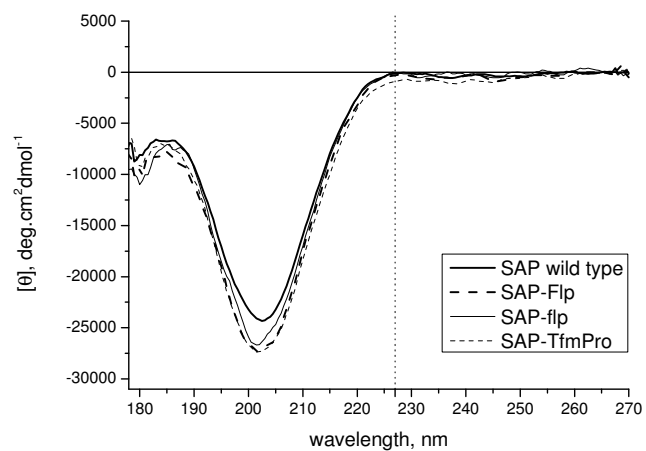
The negative maximum position in CD spectra remained almost the same for all peptides and varied in the range 202-203 nm and therefore not informative.



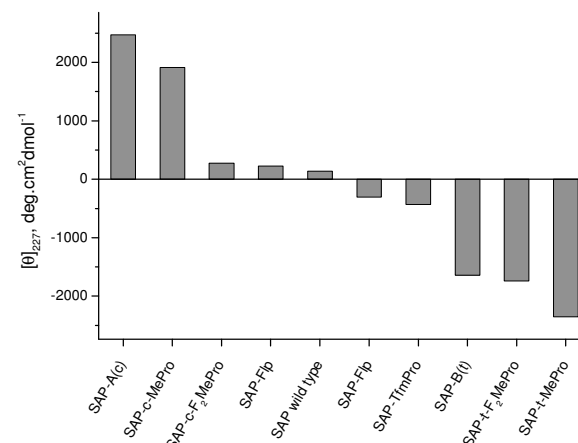
A



B



C



D

Figure 3.29. CD spectra of the SAP analogues in water at 20°C, concentration 0.5 mg/ml: A) SAP wild type, SAP-A(c), SAP-c-MePro, SAP-c-F₂MePro; B) SAP wild type, SAP-B(t), SAP-t-MePro, SAP-t-F₂MePro; C) SAP wild type, SAP-Flp, SAP-flp, SAP-TfmPro measured in another series of samples. D) histogram of ellipticities of SAP-11 substituted peptides at 227 nm.

At higher concentration 10 mg/ml (corresponds to ~ 5 mM) the positive maximum for the peptides with the sustained PPII structure appeared at the same wavelength 227 nm. Corresponding ellipticities for the investigated SAP analogues are compared on Fig. 3.30. In fact the CD curves show three “states” of the peptides: SAP-A(c) and SAP-c-MePro with high value for the positive band ($[\theta]_{227} = 2323$ and $2054 \text{ deg}\cdot\text{cm}^2\cdot\text{dmol}^{-1}$ respectively); SAP-t-F₂MePro, SAP-B-(t) and SAP-t-MePro showed negative ellipticities (-1136 , -1705 and $-2321 \text{ deg}\cdot\text{cm}^2\cdot\text{dmol}^{-1}$ respectively) and the rest of the analogs possess slight positive ellipticities, from which SAP-c-F₂MePro signal was the highest ($722 \text{ deg}\cdot\text{cm}^2\cdot\text{dmol}^{-1}$).

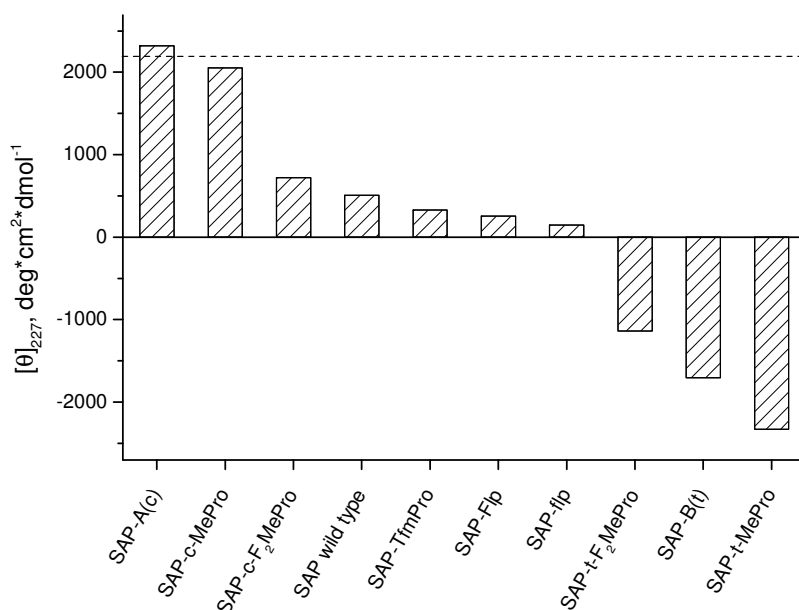


Figure 3.30. Mean residue ellipticities of SAP analogues at 227 nm. The peptides were measured in water at 20°C at concentration 10 mg/ml.

For several selected structures CD was measured in 95% n-propanol (at 4°C and concentration 0.5 mg/ml) which is known as a solvent promoting formation of PPI helical conformation. Neither of the peptides, SAP wild type, SAP-t-F₂MePro, SAP-A(c) and few others showed formation of a PPI helix conformation upon these conditions. Even after 2 days pre-incubation at 4°C the spectral shape remained unchanged.

The measurements of the SAP wild type in phosphate buffer (pH = 6.7), methanol and trifluorethanol (data not shown) showed very similar curvatures (at concentration 0.5 mg/ml and 25°C) as in water. Apparently the peptide structure is not sensitive to the solvent changes according to the expectations for PPII.

3.8. Solid state NMR of SAP analogues in lipid membranes

3.8.1. TfmMePro substituted SAP analogues

Both TfmMePro substituted peptides were investigated in solid state NMR in macroscopically oriented lipid samples. It was found that first the peptide shows an isotropic singlet which upon heating disappears and triplets of the immobilized peptide rise instead.

A typical series of SAP-A(c) is presented on Fig. 3.31. The peptide was reconstituted in DMPC at $p/l = 1/40$ and first the ^{19}F -NMR spectrum showed an isotropic signal above the phase transition of the lipid (35°C). Then the sample was heated up to 50°C and then a series of spectra was acquired. Intensity of the isotropic signal decreased and three new triplets rose instead, with $+9.5$, $+3.7$ and -4.5 kHz splitting constants.

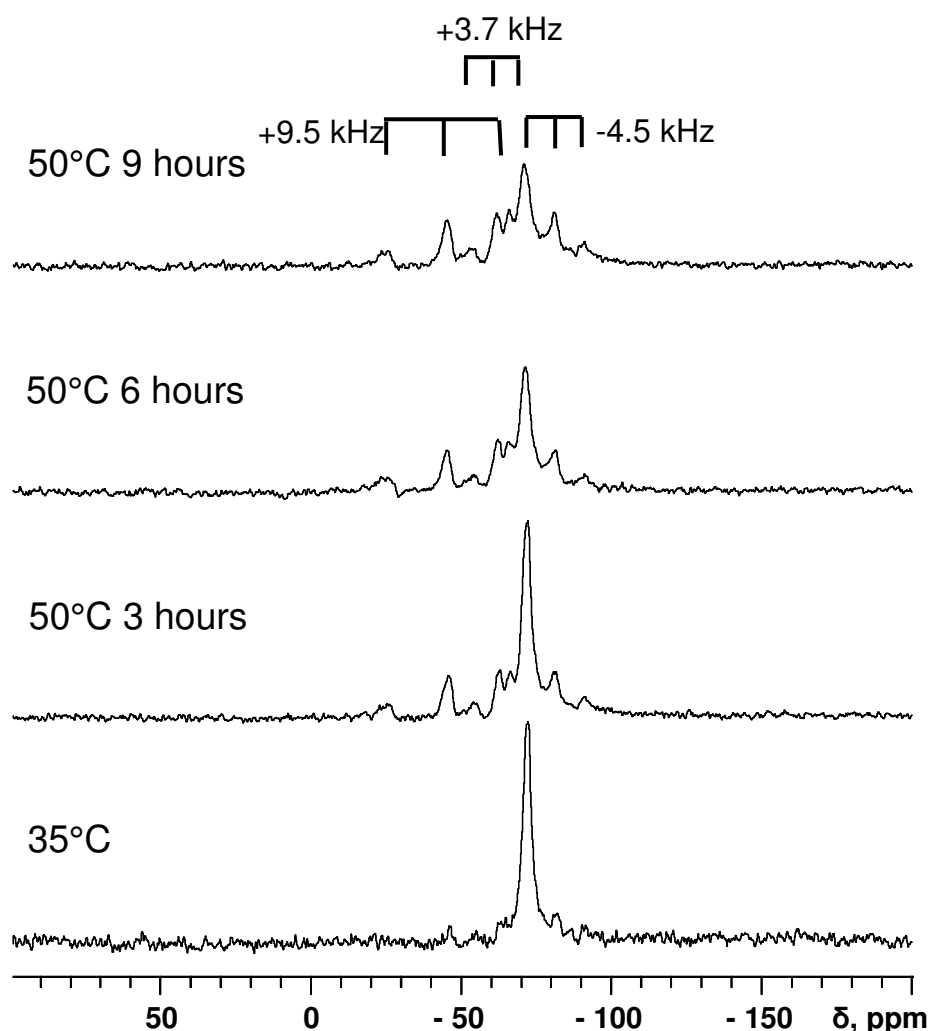


Figure 3.31. Series of solid state ^{19}F -NMR spectra of SAP-A(c) in DMPC at $p/l = 1/40$. The oriented sample was aligned parallel to the magnetic field. First a spectrum was taken at 35°C , then three spectra (3 hours per each one) were taken at 50°C .

The measurements were continued in (18:1/18:1)PC (DOPC) where the phase transition is -20°C that ensured the temperature of the measurements to be well above the phase transition temperature. The characteristic spectra are shown on Fig. 3.32.

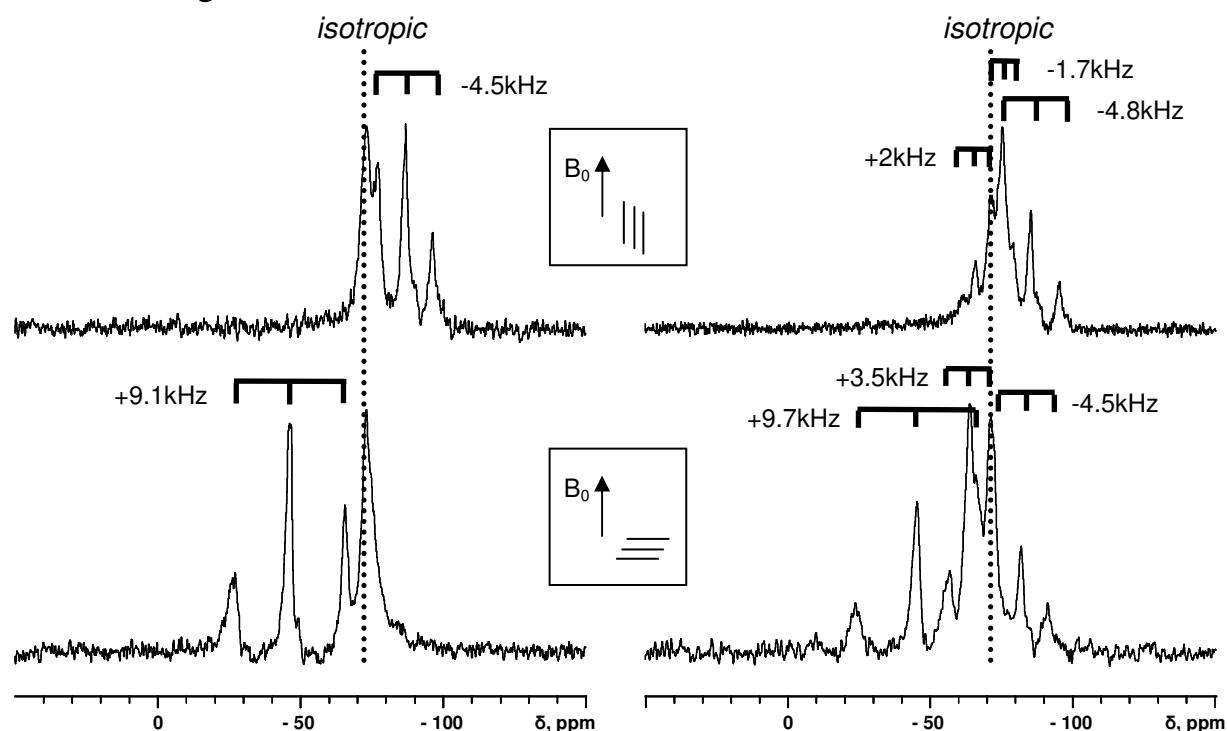


Figure 3.32. Solid state ^{19}F -NMR spectra of SAP-B(t) (left) and SAP-A(c) (right) in (18:1/18:1)PC (DOPC) at $p/l = 1/40$ and temperature 50°C . The samples aligned parallel (spectra below) and perpendicular (spectra above) to the magnetic field. Presented triplets are denoted. The dotted lines indicate the isotropic signals.

In contrast to SAP-A(c) peptide the SAP-B(t) always showed only one triplet in the corresponding ^{19}F -NMR spectra with $+9.1$ kHz splitting constant. All the signals of SAP analogues showed $-1/2$ reflection in the corresponding 90° spectra (Fig. 3.32., above), that indicated fast rotation along the lipid normal of the peptides for all peptide states represented by the triplets. The intensity of the isotropic signal increased when the samples were cooled to lower temperatures, but it was never coming back to the same domination as was before the heating.

In order to understand the role of peptide-peptide interactions in the alignment of SAP analogues in the membrane environment, the SAP-A(c) was mixed with SAP-3E* in 1:1 ratio and these mixture was reconstituted in DOPC at total $p/l = 1/40$. SAP-3E was known as not stabilizing PPII conformation as was judged from corresponding CD measurements (data not shown).

The sample was measured at 30°C and then a series of spectra was acquired at 50°C for two days. In this conditions the two triplets with the

* sequence: VELPPPVELPPPVELPPP.

splitting constants +3.5 and -4.7 kHz showed simultaneous disappearance and eventually only the triplet with +10 kHz splitting remained (Fig. 3.33.).

The result of this measurement is that presence of another peptide can change the states equilibrium for the observed peptide, thus an interaction between SAP peptides indeed takes place. Another conclusion is that two small triplets were presumably of the same conformational state of the peptide and the third one not.

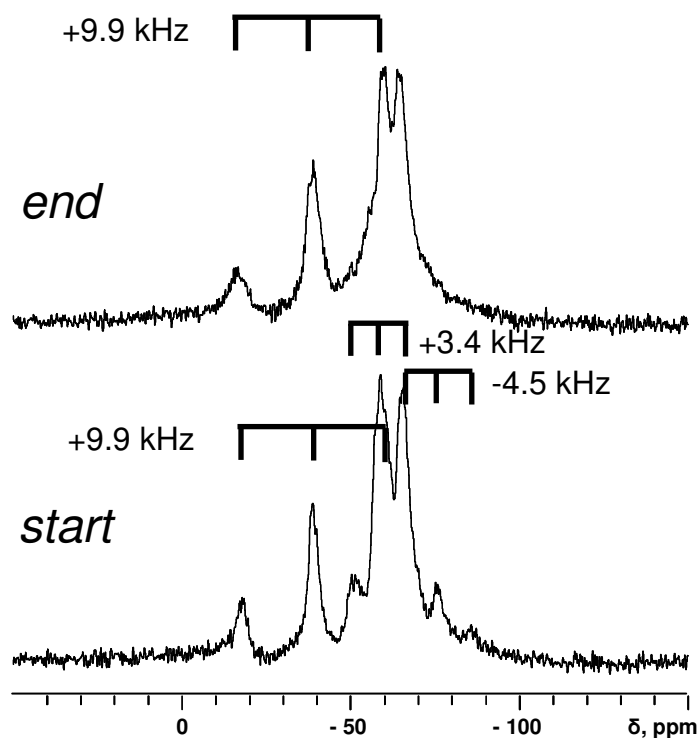


Figure 3.33. Solid state ^{19}F -NMR spectra of SAP-A(c) in mixture with SAP-3E 1:1 in DOPC at $p/l = 1/40$ (ratio 1:1:80) at 30°C before (below) and after (above) two days incubation at 50°C . The sample was aligned parallel to the magnetic field.

3.8.2. *TfmPro* substituted SAP

^{19}F -NMR spectra of SAP-TfmPro in DMPC samples ($p/l = 1/40$) were acquired. First the spectrum at 35°C showed strong isotropic signal, which upon high temperature incubation disappeared and two triplets with constants +6.4 and -3 kHz appeared instead as presented on Fig. 3.34.

In another temperature series the same sample was heated to even higher temperature and then cooled down to the room temperature. The measurements within this temperature series showed different dominant states, the two triplets mixture was observed at the beginning of the series, the downfield triplet dominated at 70°C and the upfield triplet with the significantly higher dipolar coupling constant remained after the sample was cooled down at the end. This was an indication that complicated peptide transition between different states was happening. This point requires further exploration.

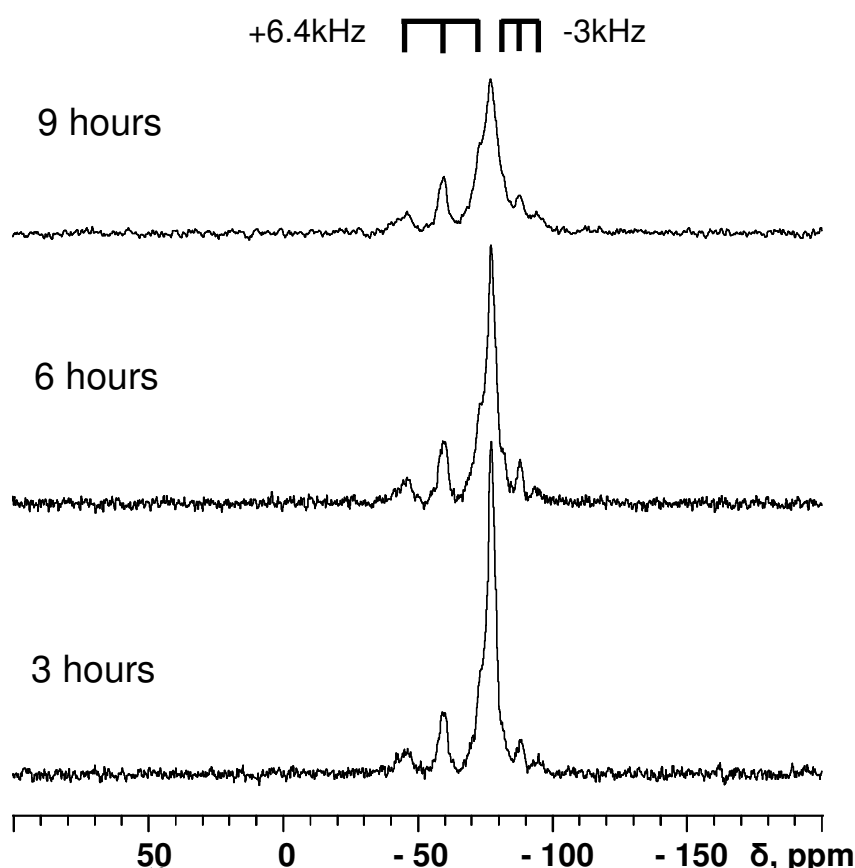


Figure 3.34. Solid state ^{19}F -NMR spectra of SAP-TfmPro in DMPC (p/l = 1/40): three spectra were done at 55°C (3 hours per each one) in a row.

3.8.3. ^{31}P -NMR spectra of the lipid oriented samples with SAP analogues

In corresponding ^{31}P -NMR spectra the samples showed good degree of orientation and good quality in terms of the band width. However, all the samples in DMPC or DOPC contained an additional peak after high temperature incubations which was $\sim 10\text{-}15\%$ of the spectral intensity and the chemical shift near the main signal as shown on Fig. 3.35. This observation can be attributed to the so-called arginine anchoring, which was previously observed with Tat samples reach of arginine¹¹⁶. The guanidine groups of the arginines interact with the phosphate lipid head groups and therefore forms another population of them.

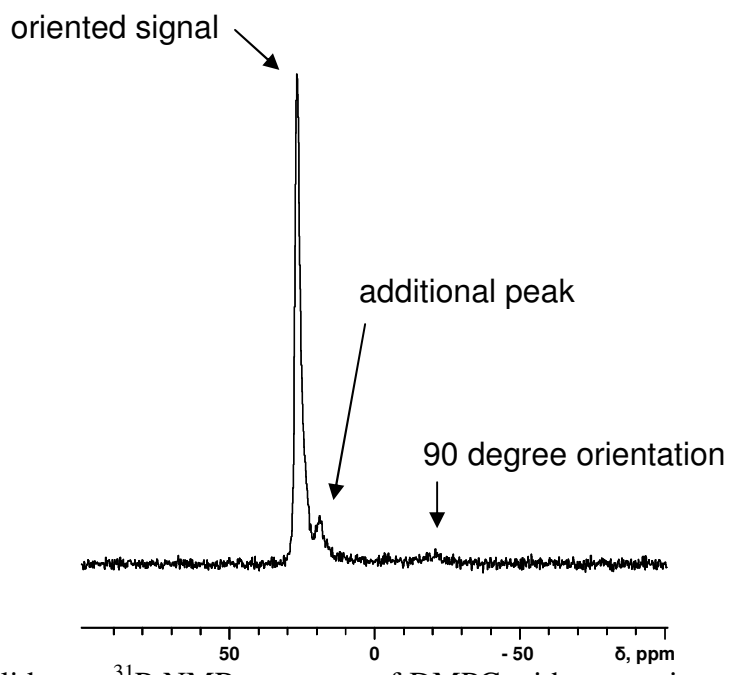


Figure 3.35. Solid state ^{31}P -NMR spectrum of DMPC with reconstituted SAP-TfmPro ($p/l = 1/50$), measured at 35°C . The sample was aligned parallel to the magnetic field.

4. Discussion

4.1. The antimicrobial peptide gramicidin S

4.1.1. Activity against Gram-positive strains

Careful analysis of the antimicrobial activity of the proline substituted GS analogues against Gram-positive bacteria reveals several unspecific tendencies. All MIC values were on the level of the wild type peptide, or 2-4 fold less for those peptides in which the fluorine content does not exceed two atoms. Trifluoromethylated peptides have further reduced activity. II-F₂Pro-GS was even less active. Eventually, for the double trifluoromethylated peptides the activity was substantially reduced.

The effect behind this observation can be considered as unspecific* *fluorous* effect. An increase of the fluorine content leads to an increase of the hydrophobicity of the substances, as was shown in chapter 3.5.1 by analysis of the RP-HPLC retention times. For GS, which is only modestly soluble in water, the solubility plays a significant role. Presumably, this parameter directly influences the ability of the peptide to reach the plasma membrane of the bacteria. Fluorination leads to an increase in the hydrophobicity and thus to a decrease in the solubility. A low rate of membrane binding for the most hydrophobic GS analogues was directly observed in CD experiments with lipid vesicles (chapter 3.5.3.), supporting this hypothesis. This effect can therefore be considered as kinetic.

Furthermore, not only the fluorine content plays significant role in the reduction of the antibacterial activity. A comparison of the MIC values for the peptides

- GS wild type, I-c-MePro-GS, II-c-MePro-GS,
- I-TfmPro-GS, I-A(c)/B(t), and
- II-TfmPro-GS, II-A(c)/B(t)

leads to the conclusion that the presence of the methano-unit slightly decreases the activity within each row. This observation correlates with the increase in the hydrophobicity within these rows.

The logic of the kinetic effect suggests that the more soluble (the less hydrophobic) the GS analogue is, the higher the membrane binding rate and thus the higher its antimicrobial activity. However, for the leucine substituted peptides the effect was completely opposite. Incorporation of the enantiomeric D-amino acids decreased both the RP-HPLC retention time (hydrophobicity) and the bacterial grow inhibition significantly.

The effect behind such apparent controversion is the reduction of the membrane affinity. Indeed, incorporation of the D-residues instead of the

* the term "unspecific" here implies that this effect does not depend from the particular amino acid sequence and will be expected in any other peptide substituted with corresponding amino acids.

hydrophobic L-ones disrupts the amphiphilic molecular *sidedness* responsible for the membrane binding ability. For instance, it was shown that incorporation of charged NH_3^+ -groups in the proline residues did not improve the antimicrobial activity but even slightly decreased it¹¹⁷.

The observation of two signals in the ^{19}F -NMR spectrum of II- $^{D,D}\text{FPhg-GS}$ in DMPC supports the latter conclusion. Apparently, in the corresponding two bans spectrum, one signal was from the membrane bound (oriented) and the other one was from the membrane detached (isotropic) peptide. Also, measurements of the hydrophilic II-Flp-GS in multilamellar DLPC vesicles showed a significant contribution of the isotropic peak in the corresponding ^{19}F -NMR spectrum, such that the anisotropic spectrum was almost completely obscured.

4.1.2. Activity against Gram-negative strains

The antimicrobial activity against the Gram-negative bacteria changes in a similar way as in the case of the Gram-positive strains. For the proline substituted GS analogues, the MIC values increase along with the fluorine content: mono CF_3 < double F_2Pro < double CF_3 .

However, for the leucine substituted GS analogues the activity was the highest in the case of the corresponding L,D-forms. This fact can be rationalized in terms of the effective peptide concentration. GS is less active against Gram-negative strains, hence corresponding MIC values are simply higher than for the Gram-positive bacteria. Thus the effective concentration of the antibiotic in the soluble form has to be considered, rather than the nominal values stated in the MIC assay. An increase in the solubility of II- $^{D,L}\text{FPhg/Phg-GS}$ leads to an increase of its antimicrobial activity, despite the fact that molecule itself possesses a reduced affinity to membranes.

Support for the given explanation was found in the results of an agar diffusion test (Table 4.1.). The diffusion of the D-forms in the LB-agar medium was apparently better than of the less soluble L-substituted peptides. The affinity to the membrane changes in the opposite direction. Eventually, unlike in the broth dilution test, II- $^{D,L}\text{FPhg-GS}$ showed the highest activity against Gram-positive strains, because better diffusion was required in this case. In contrast, when the diffusion was not that important, II- $^{L,L}\text{FPhg-GS}$ was the most active.

Peptide	bacterial strain / radius of inhibition, mm			
	Gram-positive			Gram-negative
	<i>B. subtilis</i> , ATCC 6633	<i>M. luteus</i> , DSM 1790	<i>K. rhizophila</i> , DSM 348	<i>E. helveticus</i> , DSM 18396
wild type GS	9	13	7	3
II-FPhg-GS				
L,L	5	7	3	1
L,D	9	8	1	0.5
L,D	5	3	1	0.5

Table 4.1. Results of an agar diffusion test for the wild type GS and II-FPhg-GS.

Also, for the proline substituted analogues the critical balance between solubility and membrane affinity led to a better activity of the flp/Flp containing peptides in comparison to the others.

4.1.3 Hemolytic activity

An increase of the hemolysis with increasing hydrophobicity of the GS analogues was expected⁴⁰. In this work it was shown that, in contrast to the antimicrobial activity, the solubility did not affect the results of the hemolytic tests measured by the given protocol. Any increase in the hydrophobicity directly increased the hemolytic activity (Fig. 4.1.). However, a closer look revealed secondary effects.

In the broth dilution tests (MIC), the activity values seen for c- and t-TfmMePro substituted GS were practically the same. The RP-HPLC retention times were identical. But in the hemolysis test the corresponding c-TfmMePro substituted peptides were less active than the t-TfmMePro containing analogues. The observed higher hemolysis of peptides containing t-TfmMePro, t-F₂MePro and flp than of peptides containing the corresponding closest analogues (c-TfmMePro, c-MePro, Flp, respectively) can be related to a tendency found in the CD measurements. Namely, the difference between the band ratios $[\theta]_{223}/[\theta]_{206}$ in the two mediums (PB and lipid vesicles; water and TFE) was the smallest for these peptides, suggesting a rigidification of the secondary structure as well as a pre-organization of the structure in water compared to the situation in the lipid bilayers.

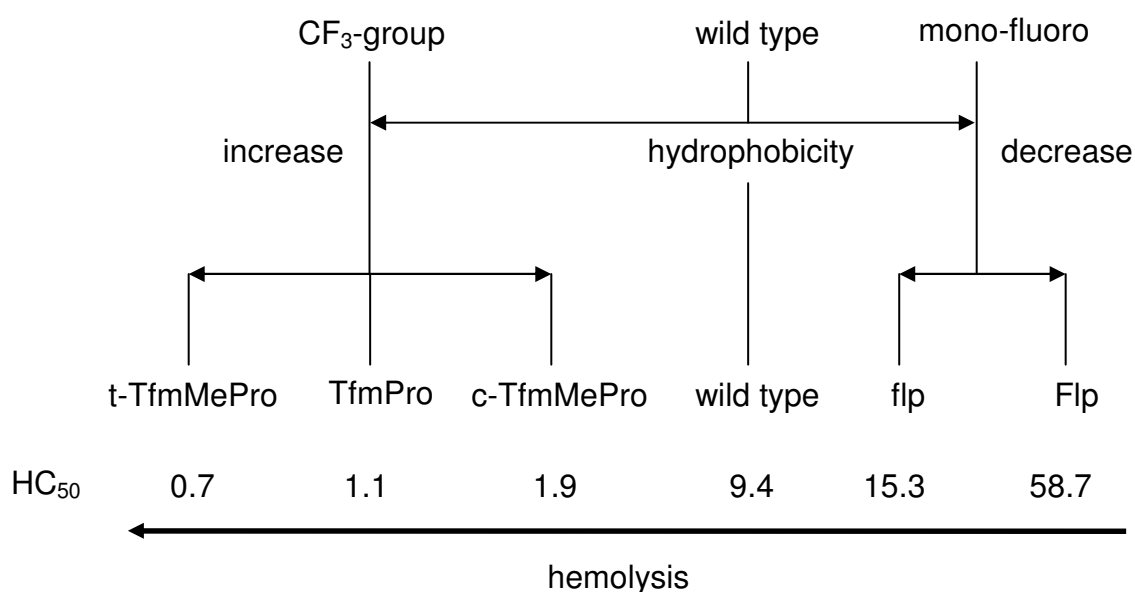


Figure 4.1. Interpretation of the hemolytic activity of the proline substituted GS analogues.

In the case of the leucine substituted peptides both the decrease in hydrophobicity and the secondary structure distortion lead to a significant decrease in hemolysis with each incorporated D-amino acid instead of an L-one¹¹⁸.

The fact that the hemolytic activity of II-^{L,L}FPhg-GS was higher than for the wild type peptide can not be explained in terms of hydrophobicity, effective concentration or secondary structure pre-organization. Furthermore, the hemolysis increased stepwise in the row wild type GS < I-^LFPhg-GS < II-^{L,L}FPhg-GS, despite the fact, that the antimicrobial activity as well as the hydrophobicity (hence, the membrane affinity) was reduced. The explanation of this phenomenon requires consideration of other parameters, such as a specific propensity, observed by solid state ¹⁹F-NMR in terms of “re-alignment”.

4.1.4. Understanding the specific oligomerization of gramicidin S

The binding of peptides to lipid bilayers can be described by eq. 3³⁷:

$$\Delta G_b = \Delta G_e + \Delta G_h + \Delta G_n + \Delta G_c + \Delta G_l \quad (\text{equation 3})$$

where the free energies correspond to: b – binding of the peptide to the membrane, e – electrostatic interaction with the membrane, h – contribution of the hydrophobic effect, n – interaction of the non-polar peptide side chains with the lipid hydrophobic core, c – conformational changes in the peptide upon binding, l – bilayer deformation caused by peptide binding. The major contributions in the total free energy for gramicidin S are believed to be electrostatic (ΔG_e), hydrophobic (ΔG_h) and non-polar (ΔG_n).

In the corresponding antimicrobial activity tests hydrophobicity indeed indirectly reflected on the values obtained. In the case of hemolysis, conformational effects played an additional role. One can presume that the contribution of conformational changes (ΔG_c) becomes significant for binding to non-charged eukaryotic membranes. However, the conformational changes upon membrane binding in the cyclic rigid GS structure are rather small, because the rigid cyclic structure is maintained in general in both, aqueous solution and lipid vesicles. Also, in the case of II-^{L,L}FPhg/Phg-GS, there was no stabilization or rigidification of the secondary structure observed in the CD correlations, but the hemolysis was still higher. This leads to the conclusion that in hemolysis a specific oligomerization of the GS molecules plays additional important role.

Oligomerization has been previously attributed to the re-alignment of LGS in model membranes, as observed by solid state ¹⁹F-NMR, based on the fact that the re-alignment was concentration dependent. In this work, an additional observation was made to support this explanation. Namely, the presence of II-^{L,L}Phg-GS in the II-B(t)-GS samples caused an increase in the re-aligned population of the observed peptide (II-B(t)-GS). Apparently, L-FPhg/Phg residues in the leucine position provide an additional motif for oligomerization, which is, however, not yet understood. Immersion of the II-

L,L -Phg-GS molecules into the lipid bilayer under conditions of the re-alignment (temperature close to the lipid phase transition, sufficiently high concentration) is apparently promoted by formation of oligomeric structures. Other GS molecules, such as II-B(t)-GS, can be incorporated into these structures to form mixed membrane bound oligomers.

The results obtained for c- and t-TfmMePro substituted GS peptides can provide significant insights into the factors important for oligomerization in the membrane immersed/re-aligned state. In solid state NMR measurements, c- and t-TfmMePro substituted structures showed different re-alignment propensities. Namely, in the ^{19}F -NMR temperature series in DLPC at $p/l = 1/40$, the re-orientation range was 13° (complete within 4°) and 4°C (never complete) for II-B(t)-GS and II-A(c)-GS, respectively. Correlation of the re-alignment in ^{19}F -NMR with the ^{31}P -NMR upfield shift provided an indirect way to observe the peptide re-alignment by sensing the lipid head groups. In the ^{31}P -NMR temperature series, II-A(c)-GS showed a “dimple” that was less deep than for II-B(t)-GS (Fig. 4.2), in agreement with the ^{19}F -NMR data. Thus, the specific re-alignment is sensitive to the secondary structure that is being distorted/sustained by the conformationally restricted amino acids, as observed in CD. The hemolysis values were also higher for the t-TfmMePro substituted peptide.

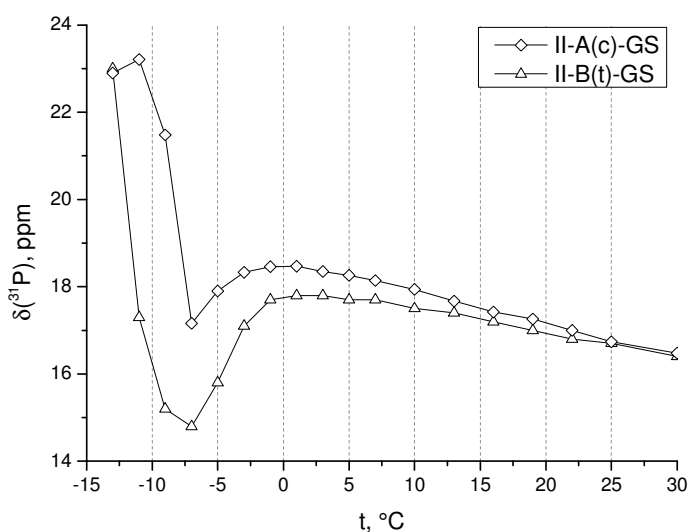


Figure 4.2. Temperature dependence of the main chemical shift in ^{31}P -NMR spectra of DLPC samples with II-A(c)-GS and II-B(t)-GS at $p/l = 1/40$.

For the leucine substituted peptides, the re-alignment propensity correlated with the hemolysis. Both increased in the row: wild type GS < I- L -FPhg-GS < II- L,L -FPhg-GS.

Previously, the formation of pores for mono- and divalent cations by gramicidin S was observed in (18:0/18:1)PG (POPG)¹¹⁹. Discrete conductive events in DPhPC/DPhPG membranes were detected after GS addition (at relatively high concentrations). It was also shown that GS caused membrane

depolarization in *E. coli* cells already at sub-MIC concentrations¹²⁰. Later the electrophysiological measurements were repeated in DPhPC/DPhPG bilayers as well as in a few other long-chains lipids¹²¹. These measurements showed an absence of regular pores, such as formed by gramicidin A or alamethicin. Rather unspecific conductive events were observed only at high concentrations of GS.

The discrepancy in the literature concerning GS pore formation can thus be explained by the wrong membrane model used for the electrophysiological measurements. Namely, the lipid composition should resemble the composition of eukaryotic cells more closely.

The ability of GS to form putative pore is apparently much relevant for the leakage/lysis of eukaryotic blood cells than for the antibacterial activity. In each case, an increase in the re-alignment propensity correlated with an increase in hemolysis induced by the given peptide. The relevance of the re-alignment for the activity against eukaryotic cells is also supported by the facts that the re-alignment was observed in phosphatidylcholines, and the population of the re-aligned peptide was increased by the presence of cholesterol, which is characteristic for animal cells.

In summary, the antimicrobial activity of the different GS analogues was shown to be sensitive unspecifically to (1) amphipathicity, and (2) the total hydrophobicity of the molecules. Introduction of D-amino acids in the leucine position led to a decrease of the membrane binding potency by distortion of the amphipathic *sidedness*. An increase in the hydrophobicity upon increase the fluorine content (*fluorous* effect) in the proline position lead to a decrease in the solubility of the peptides, and thus to a decrease in the found antibacterial activity.

In contrast, the hemolytic activity did not depend on the solubility of the peptides, but rather (1) increased with increasing total hydrophobicity. Also, hemolysis (2) increases with the propensity of the peptide to oligomerize in lipid bilayers. The latter effect was reflected in solid state NMR measurements in terms of the peptide re-alignment. The oligomerization (1) is sensitive to distortions in the secondary structure, and (2) can be promoted by specific oligomerization motifs.

4.1.5. Spectral populations with low molecular mobility

The basic solid state NMR parameters of the CF₃-containing amino acids were estimated from the ¹⁹F-NMR spectra of the corresponding double substituted peptides in the form of lyophilized powder. Visual inspection (assuming symmetric tensors) of the spectra at two different field strengths showed good agreement of the values obtained with the literature data for other CF₃-containing amino acids¹²². Remarkably, the chemical shift anisotropy (CSA) values were closer to those of aliphatic trifluoromethylated amino acids (such as TfmBpg, 52-55 ppm) and not aromatic (such as TfmPhg, 34-39 ppm).

In TfmMePro, the CF₃-group is attached to the cyclopropane ring, which possesses a partial aromatic character. However, the corresponding CSA widths were only slightly reduced.

Peptide	¹⁹ F-NMR frequency			
	470.6 MHz		282.4 MHz	
	CSA, ppm	Δ ⁰ , kHz	CSA, ppm	Δ ⁰ , kHz
II-A(c)-GS	51	16	50	16
II-B(t)-GS	52	16	51	16
II-TfmPro-GS	53	15	55	17

Table 4.2. Chemical shift anisotropy (CSA) and maximal dipolar splitting (Δ⁰) of CF₃ containing peptides (lyophilized powders; 25°C).

All measured Δ⁰ values were in good agreement with the theoretical Δ⁰_{CF₃} = 15.8 kHz. Thus, the values of the splittings given in Tables 3.7. and 3.8. can be interpreted in terms of the orientation angles of the CF₃-group (θ) relative to the membrane normal, and the parameter of the molecular wobbling (S_{mol}).

The wobbling should narrow down the ¹⁹F-NMR spectra. For instance, the CSA tensor width for II-B(t)-GS in DLPC was 18 ppm at +20°C (fluid bilayers) and 45 ppm at -20°C (frozen bilayers), which correspond to molecular wobbling S_{mol} parameters of 0.37 and 0.82, respectively. For II-^{L,L}FPhg-GS in fluid DMPC, S_{mol} was reported⁴⁷ to be 0.34±0.05. This is in good agreement with the data obtained here for the proline substituted GS analogues.

A high molecular mobility for the GS analogues can be seen already from the fact that the ¹⁹F-NMR spectra contained only one triplet in all three characteristic situations: in the gel phase, in the fluid lipids, and in the region around the lipid phase transition. This was seen regardless whether amino acids containing one or two CF₃-groups were introduced in the molecule. Remarkably, a significant degree of wobbling was observed even when the lipid was frozen. The corresponding S_{mol} parameter was in the range 0.7 ÷ 0.8.

In the “second re-aligned” state, which appears upon heating right after the frozen state, one of the splittings of the t-TfmMePro substituted peptides was +12-13 kHz. This value corresponds to S_{mol} = 0.75-0.81, as in the previous frozen state. Thus, hysteresis in the temperature series can be explained by a delayed transition of the peptide from the state with reduced mobility to the state with higher mobility.

The “second re-aligned” state characterized by the two low mobile components was already observed in the lamellar ordered state of DMPC at higher (p/l = 1/20) peptide concentration, or in the presence of cholesterol as shown in Fig. 3.19. (solid squares). In both cases the components with low mobility give only a minor contribution to the total spectra. The components with low mobility can represent either a pure peptidic aggregate, or the lipid state which governs the mobility of the accumulated peptide molecules, or the lipid phase modulations induced by presence of the peptide. The latter can not

be followed by ^{31}P -NMR so easily, because the normal lipid phase at such p/l ratios still prevails.

The effect of gramicidin S on the thermotropic phase behavior of DMPC was previously investigated^{123,124}. It was shown that in the presence of gramicidin S at $p/l > 1/100$, the pre-transition $L_{\beta} - P_{\beta}$ was eliminated. At higher peptide content ($p/l = 1/25$ and more) the main phase transition was slightly shifted towards low temperatures and a broad post-transition appeared. In phosphatidylethanolamine vesicles, gramicidin S caused the formation of non-lamellar phases.

Thus the presence of an additional lamellar phase of DMPC induced by the presence of GS can be assumed. In this phase the peptide possesses a lower mobility and two similar populations which most likely correspond to the surface-aligned and the re-aligned states of the same population. In the normal (highly mobile) state in DMPC, the re-aligned population was remarkably lower. The additional phase can be responsible for the formation of pores, such that one population (surface-aligned) is responsible for sustaining the phase, and the second one (re-aligned) for the non-specific pores in this phase. As was concluded in the previous chapter, this mechanism can be most likely responsible for the hemolytic activity. First, because zwitterionic PC is a model for uncharged eukaryotic membranes. Second, because of the correlation between specific oligomerization and hemolytic activity as discussed above. However, the low mobility state of the peptide might correspond to a completely alternative mechanism which could be responsible for the antibacterial activity as well.

4.2. Cell penetrating peptide SAP

4.2.1. Conformation in solution

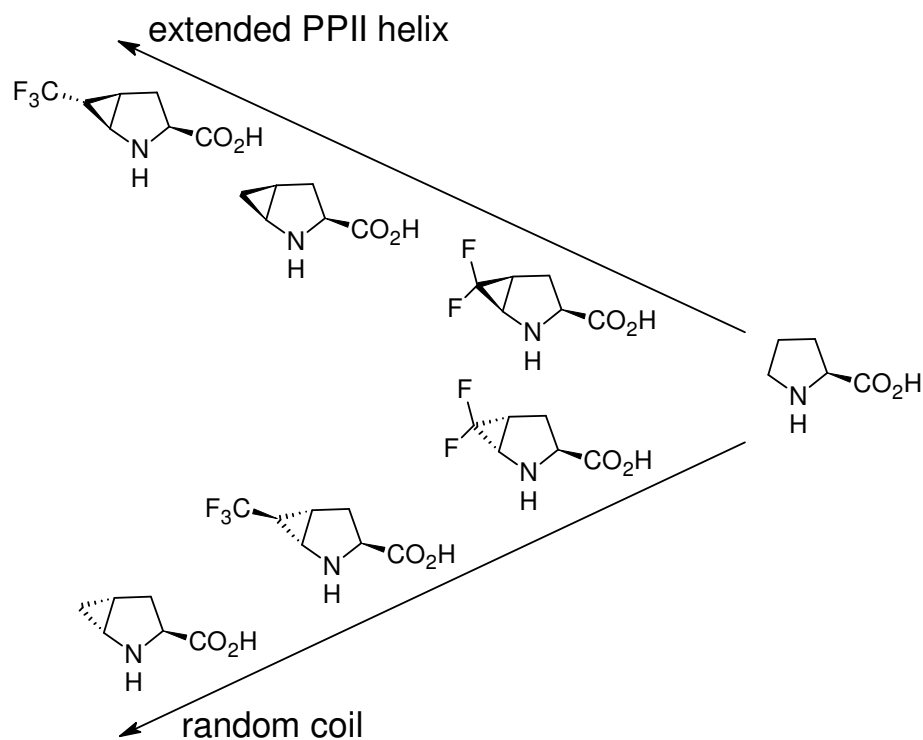
The cell penetrating proline-rich peptide SAP ($[\text{VRLPPP}]_3$) was used as a model to investigate the conformational influence of different proline analogues. Incorporation of *c*-TfmMePro in position 11 of SAP showed a significant stabilization of the PPII structure⁹². In this work, the first systematic study of this phenomenon was presented. Remarkably, the conformational effect was induced by a single substitution in the whole sequence of 18 amino acids.

The formation of an amphipathic PPII helix from the SAP sequence is accompanied by an increase in the hydrophobic moment, and therefore leads to aggregation. In SAP, the proline in position 11 is located on the hydrophilic (arginine) face of the formed polyproline II helix. This reduces the influence of the hydrophobicity substituted amino acids on aggregation. Both, *c*- and *t*-TfmMePro substitution changed the total hydrophobicity in the same way in gramicidin S, in contrast, the peptide pairs SAP-*c*-MePro – SAP-*t*-MePro and SAP-A(*c*) – SAP-B(*t*) (but not in SAP-*c*-F₂MePro – SAP-*t*-F₂MePro) were characterized by a visible differences of the RP-HPLC retention times (see

Table 7.2.). Namely, the peptides with the *cis*-methano amino acids possessed higher retention times than the corresponding *trans*-methano substituted analogues. This fact was already an indication that the hydrophobic moment was higher in the *cis*-methano case due to conformational changes.

The character of the changes was then monitored by the CD measurements. At both tested concentrations, the *trans*-methano containing amino acids showed a significant disruption of the PPII structure and domination of the random coil. Even at a concentration of ~5 mM, which is considered to be two orders of magnitude higher than the aggregation concentration (50 μ M)⁴⁵, the disrupting effect remained.

The PPII destabilization in the SAP analogues can be explained based on the following observations. In gramicidin S, where proline is enclosed in the type II' β -turn, t-TfmMePro and t-F₂MePro caused a remarkable rigidification of the peptide secondary structure, whereas c-TfmMePro and c-MePro did not. The high stabilization of the turn showed by the *trans*-methano amino acids in GS can be also expected for the other peptide structures. In SAP, proline-11 is located in the central tri-proline motif. If one amino acid forms a kink in this position, the whole structure loses the ability to form a stable long PPII helix. Thus all three *trans*-methano amino acids disrupt the PPII helix by forming a regular kink, which is most likely to be of a β -turn type, such that the whole conformation becomes disconnected in two.



Scheme 4.1. Effect of different 4,5-methanoproline derivatives on the conformational equilibrium of SAP.

All three *cis*-methano amino acids stabilized the PPII helix, as could be judged from the CD spectra. Both *c*-MePro and *c*-TfmMePro showed stabilization on a very similar level, such that the ellipticity $[\theta]_{227}$ reached the value reported for a pure PPII helix¹¹⁵. Incorporation of two fluorine atoms in the *cis*-methano unit (*c*-F₂MePro) diminished the stabilization. The latter effect can be attributed to (1) either a high electron withdrawing impact of the two fluorine atoms, or (2) additional steric effects of the endo-fluorine atom, which repels the carboxyl group of the amino acid and thereby distorts the pyrrolidine ring geometry needed for the stabilization.

In contrast to the methanoprolines, other amino acids used in this study (TfmPro, Flp, flp) did not show any significant influence on the conformation of SAP. The level of change they induced upon incorporation in position 11 was rather marginal.

Stereoelectronic effects were expected to dominate the PPII helix stabilization phenomenon. Substituents in both 4- and 5-positions of the proline ring are known to significantly affect the proline secondary structure preferences. A substituent in position 4 shifts the proline puckering equilibrium. Two puckers have different *cis/trans* populations and different isomerization rates⁶⁷. A substituent in proline position 5 affects the amide bond isomerization directly^{125,126}. However, 4,5-methanoproline can not be considered just as a combination of the 4- and 5-substituents.

The strong effect coming just from the configuration of the methano unit was surprising. From a steric perspective, the pyrrolidine ring in 4,5-methanoprolines is rather flat, such that the cyclopropane ring sticks either up or down in the corresponding amino acids. Thus, the difference of the φ, ψ angles in *c*- and *t*-MePro formed peptides should be small. Likewise, the peptide bond (angle ω) should experience a similar electronic influence from the configuration of methano unit. The collected results showed that these expectations were completely wrong. First of all, the methano unit configuration has a crucial influence at least on the *cis/trans* peptide bond equilibrium. In comparison with proline ($K_{trans/cis} = 4.6^*$), *c*-MePro possesses an increased *trans* population (5.8^{*}). The abundance of the *trans*-amide bond is believed to be crucial for the PPII folding, because in the PPII helix all peptide bonds must be *trans*. An increase in the *trans*-amide bond population would explain the stabilization effect. But surprisingly, *t*-MePro possesses an even higher *trans*-peptide bond population (10.6^{*}), even though in SAP this amino acid showed the highest disruption of the PPII conformation.

Following the systematic analysis of the conformational effects, the initially observed effect of the PPII helix stabilization by *c*-TfmMePro was attributed to the *cis*- configuration of the methano-unit. The CF₃-group was *per se* not so important. Moreover, in this work configuration of the methano-unit was shown to trigger the SAP secondary structure, such that in the case of the

* the ratios were measured in D₂O for corresponding Ac-Xaa-OMe derivatives.

trans-amino acids PPII helices were disrupted and the random coil dominated. The molecular origins of these effects are still not clear and will require further elaboration.

4.2.2. Behavior of SAP in lipids

The configuration of the methano-unit was shown to have the strongest effect on conformation, since SAP-c-MePro adopts pure PPII helix in solution, whereas SAP-t-MePro is characterized by an apparently completely disordered secondary structure. A CF₃-group in the methano-unit gave only a small effect. However, the CF₃-group allowed to monitor the peptide when bound to lipid bilayers.

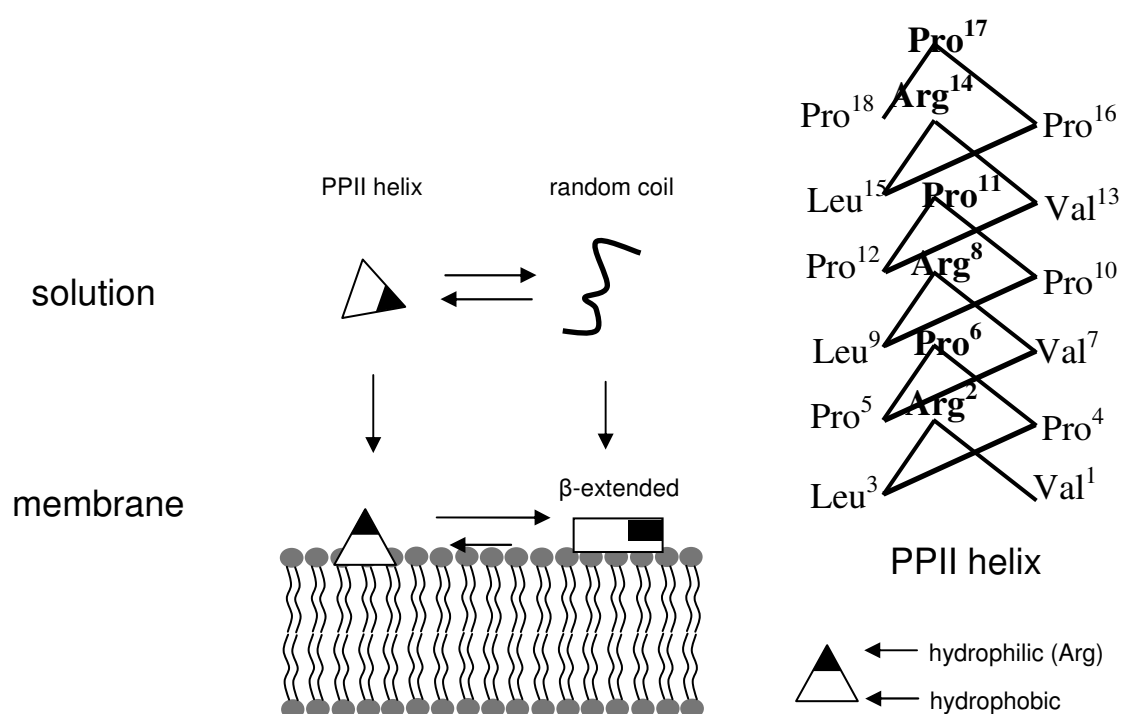


Figure 4.3. Conformations of SAP in solution and upon binding to a lipid membrane (left). PPII helix of SAP (right). Non-polar part of the peptide is shown as white and polar – in black.

The two peptides SAP-A(c) and SAP-B(t), showed presence of three (+10, +3.5, -4.5 kHz) and one (+9 kHz) triplets in oriented lipid samples, respectively. Similar values from the same conformational and orientational states were expected for the two amino acids *c/t*-TfmMePro, due to the fact that in the corresponding GS analogues they were the same. The large triplet (9-10 kHz) was therefore attributed to the same peptide state in the spectra of both SAP-A(c) and SAP-B(t). The remaining two triplets in the spectra of SAP-A(c) must correspond to another conformational state of the peptide. The simultaneous disappearance of those two small splittings detected for the SAP-A(c) peptide in the mixture with SAP-3E supports this conclusion. The SAP-TfmPro represents a marginal case and can thus be considered to represent the

wild type peptide. There, two different triplets were observed in the immobilized state, similar to the case of SAP-A(c).

The large splitting (10-9 kHz) most likely corresponds to an extended β -conformation of the peptide, lying on the surface of the lipid bilayer. The peptide binds from the random coil in solution directly to the membrane surface and remains there (“projected”) as an extended β -structure (Fig. 4.3.). A direct proof for the extended β -conformation was taken from CD measurements of wild type SAP in lipids, where the total content of β -conformations increased upon heating and reached a maximum at $\sim 40^\circ\text{C}$ (in DMPC:DMPG 3:1 mixture, $p/l = 1/200$).

The two small remaining triplets (+3.5 and -4.5 kHz) in the spectra of SAP-A(c) in lipids are apparently coming from the regular PPII helix, which is formed when SAP binds to the lipid surface, but with two different orientations of the PPII helix. Remarkably, in solution the PPII helix was practically the only form of this peptide (as judged from the corresponding ellipticity values). In lipid bilayers, the content of the PPII conformation becomes reduced when compared to the situation in solution. The fact that heating ($\sim 50^\circ\text{C}$) was required in order to achieve full binding of the peptide to the lipid bilayers can explain this observation. Presumably, the heating leads to denaturation of the PPII helix, and the random coil peptide can bind better, such that the excess of the extended β -form is eventually created.

4.3. Labeling the proline position: general remarks

4.3.1. Extrapolation of the data obtained for fluorine-substituted peptides to wild type peptides

It was clearly shown in the course of this work that substitution of proline with only one analogous amino acid in a peptide sequence is not enough to draw correct biophysical conclusions concerning the conformation and function, the mode of action etc. Instead, different proline analogues should be compared.

In investigations of antimicrobial peptides, common logic suggests that the microbiological function should be evaluated for the substituted peptides before carrying out any biophysical investigations. If the corresponding activities of a substituted peptide are significantly different from those of the wild type, the results of further biophysical explorations should not be judged as reliable. When the substitution alters the antimicrobial activity, there is no reason to perform any further investigation, because their relevance is very low.

Many observations in this work can find simple physico-chemical explanations. The biological activity of a peptide can be substantially lowered, but the behavior in solid state ^{19}F -NMR can still be representative and lead to correct conclusions about the wild type peptide. The effects behind the differences in antimicrobial activities can not be related to the parameters

observed by solid state ^{19}F -NMR, such as orientation, mobility, oligomerization state in lipid bilayers.

For instance, a double substitution with t-TfmMePro in GS (II-B(t)-GS) leads to a substantial decrease in the antimicrobial activity. After the systematic studies using different amino acids, this effect was explained by an increased hydrophobicity of the substance. The decreased activity was attributed to either a low rate of reaching the bacterial membranes or by a low effective concentration in solution due to the lowered solubility. These effects can be considered as kinetic. In contrast, the preparation of solid state NMR samples implies a reconstitution of the peptide in the lipid before any further manipulations. Thus, kinetic effects do not play any role in the latter studies.

Sometimes the above mentioned “common logic” can be even misleading. For instance, the MIC values for II- L,L FPhg-GS were closer to the corresponding values of the wild type than in the case of II-B(t)-GS. The HC_{50} values were decreased for both fluorine-labeled peptides to the same extent. However, careful exploration showed that the proline substitution was more representative for making conclusions on the wild type GS behavior in lipids. It turned out that the leucine substitution in this case created an additional motif for peptide oligomerization, whereas the proline substitution did not.

Substitution of proline with fluorine-containing amino acids for solid state ^{19}F -NMR structure analysis should be planned carefully, taking into account the inevitable changes in hydrophobicity and conformation. Different ^{19}F -NMR reporter groups also offer different opportunities for observation. These opportunities, explored so far and the corresponding problematic points will be discussed below.

4.3.2. *Flp/flp*

Substitution of proline with 4-fluorprolines leads to a reduction of the hydrophobicity. This can affect the binding of the substituted amphipathic peptides to lipid bilayers. For instance, the most hydrophilic proline substituted GS II-Flp-GS, reconstituted in multilamellar DLPC vesicles (MLVs), showed a significant contribution of an isotropic signal in the ^{19}F -NMR spectra. The isotropic signal dominated the spectra of both II-Flp-GS and II-flp-GS in the gel phase MLVs. This fact was attributed to a partial detachment of the peptide from the lipid. It was observed only for Flp/flp and not for any other proline substitution in GS.

The use of these amino acids can also lead to conformational changes. It is known that flp prefers an endo-puckered conformation, such that the amide bond isomerization constant $K_{trans/cis}$ is lowered and the energy barrier between the *trans*- and *cis*-peptide bonds is reduced. In contrast, Flp prefers an exo-pucker, hence the $K_{trans/cis}$ and the *trans/cis* barrier is higher than for proline. An overwhelming number of studies was done on these amino acids concerning the

stabilization of the collagen triple helix in collagen mimicking and other peptides^{67,127,128,129}. However, it is still difficult to predict the conformational effects on other peptide sequences using the existing literature data. The corresponding effect will significantly depend on the number of substituted prolines and an intrinsic rigidity of the substituted segment in the initial structure.

For example, in gramicidin S, double flp substitution (II-flp-GS) leads to a remarkable rigidification of the peptide conformation. In SAP, a single proline substitution with Flp/flp did not show any appreciable effect on the PPII helix – random coil equilibrium.

For solid state ¹⁹F-NMR, the only parameter which can be monitored is the chemical shift anisotropy. The referencing problem for correct interpretation of this parameter still exists. In the temperature series, where the spectra were referenced to one another, the chemical shift was plotted against the temperature in order to follow the different alignment states of gramicidin S. The chemical shift difference between the two (aligned and re-aligned) states of GS was ~3 ppm for II-flp-GS and ~8 ppm for II-Flp-GS. In contrast, the corresponding difference for II-B(t)-GS was 28 ppm. Apparently, the CSA is reduced for the flp/Flp peptides. Presumably, the proline puckering is still happening in the corresponding peptides. The side chain wobbling narrows down the spectra. The presence of wobbling makes a conversion of the CSA into orientation/wobbling parameters of the peptide a complicated task. Therefore, the Flp/flp substitution should be used only for qualitative characterization of different peptide states in the same sample.

An advantage of these amino acids is the fact that they are easily available on chemicals market.

4.3.3. *c/t-TfmMePro*

The two amino acids, *c/t-TfmMePro*, require complicated chemical synthesis. However, both amino acids were fairly compatible with the SPSS protocol. When introduced into peptides, they increase the hydrophobicity substantially. The influence of the latter effect on the activity values was discussed above.

In both studied peptides, the amino acids induced significant changes in the secondary structures. The corresponding conformational effects have been described here the first time. It was possible to compare the effect of the different substitutions and extrapolate to the properties of the wild type peptide. Comparison of the RP-HPLC retention times, biological activities, solid state ¹⁹F-NMR line shapes, etc., for the *c*- and *t*-TfmMePro substituted peptide pairs was most fruitful in the course of this work.

In the solid state ¹⁹F-NMR investigations the peptides substituted with these two amino acids gave the most representative spectral line shapes. The CF₃-group triplets were well resolved, and the resolution enabled to discriminate

between different peptide states in one spectrum, and the relatively short spectra collection times were sufficient for collecting high-quality spectra. These features were essential for making some conclusions, concerning the low mobility state in GS, concerning two orientational states of the SAP PPII helix, etc. The attachment of a CF₃-group to the restricted bicyclic skeleton makes the values of the CSA and dipolar coupling easily convertible into peptide orientation/wobbling parameters.

The use of only one amino acid for the substitution, either *c*- or *t*-TfmMePro, will give less representative results, because the conformational changes are supposed to be significant. On the other hand, a combination of both amino acids for proline substitution, combined with further solid state ¹⁹F-NMR studies, should be considered as the strategy of choice.

4.3.4. *TfmPro*

The amino acid TfmPro is not commercially available, but the synthesis is relatively simple, and the amino acid is well compatible with the SPPS protocol. An increase in the hydrophobicity upon Pro to TfmPro substitution should be expected.

However, in both of the studied peptides no substantial conformational changes were noticed. Thus, TfmPro can be considered a non-perturbing substituent concerning conformational changes.

In solid state ¹⁹F-NMR both parameters, CSA and dipolar coupling, can be measured and converted into the corresponding structural orientation/wobbling parameters. The absence of any significant spectral narrowing, as was observed for Flp/flp, indirectly proves that the anchoring of the pyrrolidine ring was indeed achieved. From a practical perspective, the spectral resolution was not as good as in the *c/t*-TfmMePro case. Therefore, not all alignment states that were clearly distinguished using *c/t*-TfmMePro, were observed in the spectra of TfmPro substituted peptides.

Marginal conformational changes and the presence of a CF₃-label make this amino acid a good choice for solid state ¹⁹F-NMR structural studies of peptides.

4.3.5. *F₂MePro and F₂Pro*

F₂Pro is very easy to synthesize and it is fully compatible with the Fmoc SPPS. Conformational changes induced by this amino acid are rather small. The hydrophobicity changed not much from a single substitution. In solid state ¹⁹F-NMR, the use of the corresponding peptides can only be affordable in the fluid lipid state and not in the gel phase.

F₂MePro is not compatible with SPPS. Incorporation of this amino acid into peptides requires prior synthesis of the corresponding dipeptides. There is also no guarantee that the synthesis will yield significant amounts of the *c*-

F₂MePro form. Use of the pair c/t-F₂MePro imposes similar advantages as use of the c/t-TfmMePro pair. Moreover, F₂MePro increases the hydrophobicity less than any CF₃-containing amino acid. In solid state ¹⁹F-NMR, the use of F₂MePro makes it possible to follow different peptide states even in the gel lipid phase.

The characteristic shape of the ¹⁹F-NMR peptide spectra in fluid lipids were shown to be defined by two parameters: (1) chemical shift difference between the two inequivalent fluorines, (2) dipolar coupling. The latter can be used for conversion into the orientation/wobbling parameters. However, such CSA and Δ^0 simulations still have to be done.

The use of the pair c/t-F₂MePro as a strategy for proline substitution should be preferred in cases where the hydrophobicity plays a substantial role.

In summary, the following strategies can be applied to substitute the proline substitution in peptides for ¹⁹F-NMR structural investigations:

- (1) Combination of c- and t-TfmMePro can be considered as the best option, as the effect of the substitution can be discriminated from the original peptide properties,
- (2) The use of TfmPro should be considered as a compromise,
- (3) A combination of c- and t-F₂MePro is a good alternative to (1), if the hydrophobicity induced by the CF₃-group is considered to be an issue.

5. Conclusions

This work has examined the incorporation of different proline analogues into peptides and their suitability for ^{19}F -NMR and biophysical studies. The amino acids were incorporated into two peptide sequences, and systematic investigations were carried out in order to reveal any induced conformational changes in the two secondary structures, namely the relevant β -turn and polyproline type-II helix. It was shown that the β -turn type II is stabilized by several amino acids, some of them containing a *trans*-4,5-methano unit. The previously observed stabilization of the PPII structure in SAP was attributed to the *cis*-configuration of the 4,5-methano unit. Moreover, the *trans*-4,5-methano prolines substantially disrupted this secondary structure.

In gramicidin S, the effects of different proline substitutions were systematically investigated. It was shown that the antibacterial activity was affected rather unspecifically by changing the hydrophobicity and amphipathicity of the peptide molecule. An increase in the hydrophobicity, first of all by increasing the fluorine content, substantially decreased the activity. This effect was explained by a reduced rate of binding of the peptide to the cell membranes. Additional studies of the leucine substituted peptides showed that a decrease in the hydrophobicity decreases the activity by lowering the membrane affinity. Thus, the native GS structure is well optimized in terms of balancing these two opposing effects. Remarkably, any conformational changes did not affect the antibacterial activity. But an additional contribution of the conformational effect was found for the hemolytic activity. This observation was rationalized in terms of a mechanism in which oligomerization of the peptide molecules in the lipid membranes was considered. This oligomerization was monitored by solid state ^{19}F -NMR in terms of the previously described GS re-alignment. An increased propensity for the re-alignment provided the only valuable explanation of the observed increase in the hemolytic activity in several cases. In fact, the antibacterial and the hemolytic activity seem to involve different mechanisms.

The use of fluorine containing amino acids as labels for solid state ^{19}F -NMR studies was demonstrated and discussed. Proline in peptides is sensitive to substitutions, hence the use of certain analogues was recommended in order to extract information on the effect of the substitution and on the properties of the wild type peptide. Based on this work, the number of the amino acids needed for investigations of other peptides can now be well adjusted and the effort reduced.

A novel amino acid, difluoro-4,5-methanoproline, was synthesized. Being N-protected, this structure was intrinsically unstable. The mechanism of its decomposition was elucidated. Finally, the amino acid was incorporated into peptides using a dipeptide strategy. Sodium chlorodifluoroacetate was used for the first time for difluorocyclopropanation of protected enamines. The preferential formation of the *trans*-methano isomer and formation of an acetylated side product were detected in this principal step.

6. Zusammenfassung

In dieser Arbeit wurde der Einbau verschiedener Prolin Analoga in Peptide, sowie deren Eignung für ^{19}F -NMR und biophysikalische Studien untersucht. Die Aminosäuren wurden in zwei verschiedene Peptidsequenzen eingebracht, die daraufhin systematisch auf jegliche induzierte Änderung der beiden Sekundärstrukturen, genauer der β -Schleife und der Polyprolin Typ II Helix, untersucht wurden. Es wurde gezeigt, dass einige Aminosäuren, unter denen manche eine *trans*-4,5-methano Einheit enthalten, die β -Schleife Typ II stabilisieren. Die bereits zuvor beobachtete Stabilisierung der PPII Struktur in SAP wurde auf die *cis*-Konfiguration der 4,5-methano Einheit zurückgeführt. Des Weiteren störten die *trans*-4,5-methano Proline diese Sekundärstruktur erheblich.

In Gramicidin S wurden die Effekte der verschiedenen Prolin-Substitutionen systematisch untersucht. Es wurde gezeigt, dass die antimikrobielle Aktivität eher unspezifisch durch Änderung der Hydrophobizität und Amphiphilie des Peptides beeinflusst wurde. Eine Erhöhung der Hydrophobizität, in erster Linie durch einen erhöhten Fluor-Gehalt, minderte die Aktivität erheblich. Dieser Effekt wurde durch eine verringerte Bindungsrate des Peptids an die Zellwand erklärt. Zusätzliche Studien Leucin substituierter Peptide zeigten, dass eine Herabsenkung der Hydrophobizität die Aktivität durch eine verringerte Membranaffinität senkte. Demnach ist die native GS Struktur in Hinsicht auf die Balance zwischen diesen beiden sich entgegenstehenden Effekten gut optimiert. Bemerkenswerterweise beeinflusste keinerlei konformationelle Änderung die Aktivität. Jedoch wurde ein zusätzlicher Beitrag des konformationellen Effekts für die hämolytische Aktivität gefunden. Diese Beobachtung wurde durch einen Mechanismus, bei welchem die Oligomerisierung der Peptid Moleküle in der Lipidmembran angenommen wurde, erklärt. Diese Oligomerisierung wurde, im Zusammenhang mit der zuvor beschriebenen GS Umorientierung, mittels ^{19}F -NMR beobachtet. Eine erhöhte Tendenz zur Umorientierung lieferte die einzige sinnvolle Erklärung der beobachteten Erhöhung der hämolytischen Aktivität in einigen Fällen. In der Tat scheinen die antibakterielle und die hämolytische Aktivität mit verschiedenen Mechanismen einherzugehen.

Die Verwendung Fluor-haltiger Aminosäuren als Markierungen für Festkörper ^{19}F -NMR Studien wurde demonstriert und diskutiert. Prolin reagiert in Peptiden sehr empfindlich auf Substitutionen, daher wurde der Gebrauch bestimmter Analoga empfohlen um Informationen über den Effekt der Substitution und die Eigenschaften des Wildtyp Peptids zu erhalten. Basierend auf dieser Arbeit, kann die Anzahl der benötigten Aminosäuren für Untersuchungen angepasst und der Aufwand reduziert werden.

Eine neue Aminosäure, Difluoro-4,5-methanoprolin, wurde synthetisiert. In ihrer N-entschützten Form war diese Struktur intrinsisch instabil. Der Mechanismus ihres Zerfalls wurde erläutert. Schließlich wurde die Aminosäure,

mittels einer Dipeptid Strategie, in Peptide eingebracht. Natriumchlorodifluoracetat wurde zum ersten Mal für Difluorocyclopropanierung von geschützten Enaminen verwendet. Die bevorzugte Bildung des *trans*-methano Isomers sowie die Entstehung eines acetylierten Nebenproduktes wurden in diesem wichtigsten Schritt detektiert.

7. Experimental part

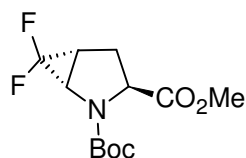
¹H-NMR spectra were recorded on Bruker Avance 400 and Bruker Avance DRX 500 spectrometers and referenced to TMS. ¹⁹F-NMR spectra in solution were recorded on Bruker Avance 300 spectrometer (282 MHz) at 23°C and referenced to TFA solution in water (-75 ppm). δ values are given in points per million. IR spectra were recorded on Bruker Alpha spectrometer with diamond-ATR module, the values are given in cm^{-1} (only bands above 1500 cm^{-1}). Optical rotation was measured on Perkin-Elmer 241 Polarimeter at 20°C in chloroform. MALDI-TOF spectra were recorded on Bruker Autoflex III Smart Beam.

RP-HPLC was done on Jasco HPLC system using (unless other stated) C18 columns: 4.6 mm x 250 mm as analytical (flow rate 1.5 ml/min), 10 mm x 250 mm as semi-preparative (6 ml/min) and 22 mm x 250 mm as preparative (20 ml/min); solvent A: 90% water, 10% acetonitrile, solvent B: 90% acetonitrile, 10% water; 5 mM hydrochloric acid was used as an ion-pairing agent. Analytical gradient from 5 to 95% of solvent B starting from 3 min ending at 18 min (15 min), the loop size was 20 μl , the temperature 40°C.

Tetrahydrofuran (THF), diglyme, DIPEA, and diethyl ether were freshly distilled under argon atmosphere from sodium/benzophenone, toluene was distilled from sodium. Trifluoroacetic anhydride was distilled over potassium carbonate. All other chemicals were of commercial grade (purchased from Merck, Acros, ABCR, Fisher, Iris Biotech, Biosolve) and used without further purification unless other stated. Compound **50** was prepared from pyroglutamic acid in three steps according to^{130,131,132}. (*S*)-*tert*-butyl pyroglutamate was prepared according to⁹⁷. **28** was prepared according to^{133,134} and finally reaction with the Ruppert-Prakash reagent was done according to⁸⁵. The wild type GS was provided by Dr. Berditsch and O. Babii; the SAP wild type and SAP-A(c) were synthesized by Dr. Mykhailiuk. Lipids were bought in Avanti Polar Lipids. The amino acids Boc-c-MePro and HCl*t-MePro were provided by Prof. Komarov.

7.1. General organic synthesis

2-*tert*-butyl 3-methyl (1*S*,3*S*,5*R*)-6,6-difluoro-2-azabicyclo[3.1.0]hexane-2,3-dicarboxylate, **51**.

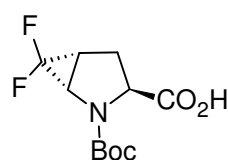


A 250 ml three necked reactor equipped with a dropping funnel and a Liebig condenser was charged with **50** (1 g, 4.4 mmol) and dry diglyme (60 ml) under argon. The mixture was heated to 177 °C in an oil bath, and slurry of sodium chlorodifluoroacetate (10.1 g, 66.4 mmol, 15 eq.) in diglyme (40 ml) was added under stirring through the dropping funnel within 15 min. After the addition, the mixture was heated with stirring for 5 min, keeping the temperature strictly within the range of 175-178 °C over this period. Then the mixture was cooled to the room temperature and filtered through a paper

filter. The solid on the filter was washed with ether, the combined filtrate and washings were evaporated under reduced pressure. The residue was purified by column chromatography (silica gel, eluent – hexane-ethyl acetate 2:1, $R_f = 0.5$). 0.860 g (71% yield) of the product **51** was obtained as a pale yellow oil.

$^1\text{H-NMR}$ (CDCl_3 , 400 MHz) – (Boc-rotamers): 4.39 (major) and 4.17 (minor) (m, 1H, N-CH-CO₂Me), 3.99 (minor) and 3.80 (major) (m, 1H, N-CH-CF₂), 3.76 (s, 3H, CO₂CH₃), 2.62 (m, $J = 10\text{-}11\text{Hz}$, 1H, CHH), 2.34 and 2.28 (two m, 2H, CH-CH-CHH), 1.48 (major) and 1.43 (minor) (s, 9H, (CH₃)₃C). $^{19}\text{F-NMR}$ (CDCl_3 , 282 MHz) – (Boc-rotamers): -129.7 (major) and -130.0 (minor) (dd, $J_{\text{F-F}} = 160\text{ Hz}$, $J_{\text{F-H}} = 10\text{ Hz}$, exo-F), -155.7 (minor) and -156.2 (major) (d, $J_{\text{F-F}} = 160\text{Hz}$, endo-F). IR: 2978, 1750, 1704. $[\alpha]_{\text{D}} = 105^\circ$ ($c = 1.01$).

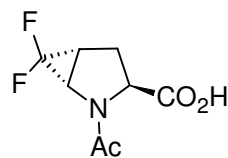
(1S,3S,5R)-2-(tert-butoxycarbonyl)-6,6-difluoro-2-azabicyclo[3.1.0]hexane-3-carboxylic acid, 52.



51 (0.5 g, 1.8 mmol) was dissolved in methanol (15 ml). A sodium hydroxide solution (1M in water, 7.3 ml, 4 eq.) was added to the solution within two minutes upon stirring. The solution was stirred for 6 h at room temperature, and then methanol was evaporated under reduced pressure (keeping the bath temperature below 40 °C). The residue was taken up in water (15 ml), extracted with diethyl ether (2 x 15 ml), and the ethereal extracts were discarded. The water layer was then acidified by 1 M hydrogen chloride solution until acidic pH (1-2) and the product was extracted with dichloromethane (4 x 15 ml). The combined extracts were dried over magnesium sulfate, filtered and evaporated to give 0.433 g (91% yield) of the product as pale fluffy crystals.

$^1\text{H-NMR}$ (CDCl_3 , 500 MHz) – (Boc-rotamers): 8.80 (broad s, 1H, CO₂H), 4.39 (major) and 4.24 (minor) (m, 1H, CH-CO₂Me), 4.02 and 3.76 (m, 1H, N-CH-CF₂), 2.73 (m, 1H), 2.61 (major) and 2.47 (minor) (m, 1H, both CH₂), 2.36 (m, 1H, CH-CH-CH₂); the assignment was accomplished using HMQC experiment. $^{19}\text{F-NMR}$ (CDCl_3) – (Boc-rotamers): -129.9 (minor) and -130.8 (major) (dd, $J_{\text{F-F}} = 162\text{Hz}$, $J_{\text{F-H}} = 12\text{ Hz}$, exo-F), -155.9 (minor) and -156.3 (major) (d, $J_{\text{F-F}} = 161\text{ Hz}$, endo-F). IR: broad 3300-2500, 2981, 2935, 1747, 1632. $[\alpha]_{\text{D}} = -126^\circ$ ($c = 1.00$).

Methyl (1S,3S,5R)-2-acetyl-6,6-difluoro-2-azabicyclo[3.1.0]hexane-3-carboxylate.

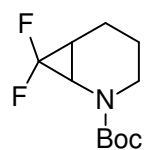


To **51** (0.6 g) trifluoroacetic acid-dichloromethane mixture (3 ml : 9 ml) was added quickly upon stirring. After 30 min stirring at room temperature volatilities were evaporated (temperature in bath < 30°C) within 5 min and acetic anhydride (25 ml) was added. The mixture was stirred for 12 h. Liquids were removed under reduced pressure (temperature ≤ 60°C), the residue was taken up in ethyl acetate (50 ml), washed with 1M hydrogen chloride (3 x 25ml), 1M sodium hydroxide (3 x 25ml) and brine (2 x 25ml). Solution was dried over

magnesium sulphate, filtered and evaporated. The crude product was purified via gradient silica gel chromatography (ethyl acetate – chloroform 8.5:1.5 to 5:5 ratio) to give 41mg (9%) of the product as colorless oil.

$^1\text{H-NMR}$ (CDCl_3 , 400MHz): 4.59 (d, $J = 8.3\text{Hz}$, 1H, N-CH-CO₂Me), 3.78 (m, 1H, N-CH-CF₂), 3.69 (s, 3H, CO₂CH₃), 2.55-2.28 (m, 3H, CH-CH-CH₂), 2.12 (s, 3H, N-C(=O)CH₃). $^{19}\text{F-NMR}$ (CDCl_3): -128.3 (dm, $J_{\text{F-F}} = 159\text{Hz}$, 1F), -155.7 (d, $J_{\text{F-F}} = 159\text{Hz}$, 1F).

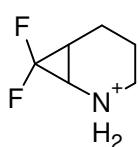
7,7-difluoro-2-aza-bicyclo[4.1.0]heptane-2-carboxylic acid tert-butyl ester, **55**.



The starting compound was prepared in two steps from valerolactame analogous to **50**. The synthesis was done analogous to synthesis of **51**. The charged amounts were: 1.5 g (8.1 mmol) of the starting Boc-enamine and 12.5 g (82 mmol, 10eq.) of the salt. The reaction time was 35 min. The product **55** was purified by column chromatography (silica gel, eluent – hexane:diethyl ether 2:1, $R_f = 0.5$). Resulting compound was pale yellow oil.

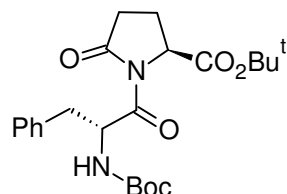
$^1\text{H-NMR}$ (CDCl_3 , 400 MHz) – (Boc-rotamers): 3.78 (major) and 3.54 (minor) (dt, $J = 13, 4\text{Hz}$, 1H, CF₂-CH-N), 3.21 (minor) and 3.12 (major) (m, 1H), 2.67 (minor) and 2.48 (major) (m, 1H), 1.82-1.62 (m, 3H), 1.49 (m, 2H), 1.41 (s, 9H, CH₃). $^{19}\text{F-NMR}$ (CDCl_3) – (Boc-rotamers): -130.0 (minor) and -130.5 (major) (ddd, $J_{\text{F-F}} = 163\text{Hz}$, $J_{\text{F-H}} = 14, 8\text{ Hz}$, exo-F), -152.3 (major) and -152.9 (minor) (d, $J_{\text{F-F}} = 163\text{Hz}$, endo-F). IR: 2976, 2940, 2870, 1699.

7,7-difluoro-2-azonia-bicyclo[4.1.0]heptane trifluoroacetate, **56**.



55 (129 mg) was mixed with trifluoroacetic acid in dichloromethane (6 ml; 1:9 vol) for 1 h. The volatiles were evaporated and the product was obtained as yellow viscous liquid. $^1\text{H-NMR}$ (CDCl_3 , 400 MHz): 9.76 and 7.90 (to broad s, 2H, NH₂), 3.46 (t, $J = 9\text{ Hz}$, 1H, CF₂-CH-N), 3.30 (m, 1H), 3.04 (m, 1H), 2.15 (m, 1H), 2.06 (m, 2H), 1.89-1.69 (m, 2H). $^{19}\text{F-NMR}$ (CDCl_3): -129.0 (dt, $J_{\text{F-F}} = 176\text{Hz}$, $J_{\text{F-H}} = 11\text{Hz}$). IR: 3300-2150 (broad), 1779, 1662, 1617.

tert-Butyl (2S)-1-{(2R)-2-[(tert-butoxycarbonyl)amino]-3-phenylpropanoyl}-5-oxopyrrolidine-2-carboxylate, **57**.

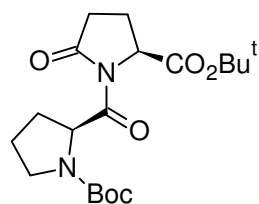


Sodium hydride (60% in paraffin, 512 mg, 12.8 mmol) was washed with dry toluene (2 x 5 ml) under argon, 70 ml of dry toluene (70 ml) was added following by *tert*-butyl pyroglutamate (2.26 g, 12.2 mmol) upon stirring. After 30 min Boc-^DPhe-ONp (4.5 g, 11.6 mmol) suspension in toluene (40 ml) was added quickly and the stirring was continued for the next 16 h. The reaction mixture was filtrated and the filtrate was concentrated in vacuum. 4.69 g of pure **57** (89%) was obtained after column

chromatography (silica gel, eluent – hexane:ethyl acetate 3:1, $R_f = 0.3$) as white crystals.

$^1\text{H-NMR}$ (CDCl_3 , 400MHz) – (rotamers): 7.32-7.17 (m, 5H, Ph), 5.78 and 5.70 (m and broad m, 1H, CH-C(=O)-N), 5.19 and 4.99 (d and broad m, $J = 8.5\text{Hz}$, 1H, NH), 4.49 (d, $J = 9.3\text{Hz}$, 1H, $\text{CH-CO}_2\text{Bu}^t$), 3.16 and 3.08 (two m, 1H, CHH-N) and 2.90 (m, 1H, CHH-N), 2.76 (two m, 1H, CHH in Phe), 2.51 (ddd, $J = 17.8, 9.2$ and 2.1Hz , 1H, CHH in Phe), 2.24 (m, 1H, $\text{N-CH}_2\text{-CHH}$), 2.07 (m, 1H, $\text{N-CH}_2\text{-CHH}$), 1.47, 1.40 and 1.31 (three s, CH_3). IR: 3422, 2981, 2934, 1730, 1717, 1702. $[\alpha]_D = -75.7^\circ$ ($c = 1.00$).

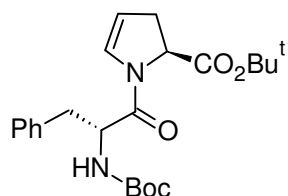
***tert*-Butyl (2S)-2-[[*(2S)*-2-(*tert*-butoxycarbonyl)-5-oxopyrrolidin-1-yl]carbonyl]pyrrolidine-1-carboxylate.**



Was prepared analogous to **57** starting from 2.60 g (14 mmol) of *tert*-butyl pyroglutamate and 4.5 g of Boc-Pro-ONp (13.4 mmol). 4.25 g (83%) of the product was obtained as white crystals after chromatography (silica gel, eluent – toluene:ethyl acetate 9:2, $R_f = 0.4$).

$^1\text{H-NMR}$ (CDCl_3 , 400 MHz) – (rotamers): 5.37 (m, 1H, N-CH-C=O), 4.70 (m, 1H, N-CH-C=O), 3.58 (m, 1H, N-CHH), 3.44 (m, 1H, N-CHH), 2.76-2.49 (m, 2H), 2.43-2.29 (m, 2H), 2.13-1.96 (m, 2H), 1.89 (m, 2H), 1.47, 1.46, 1.45 and 1.38 (four s, 18H, $\text{C}(\text{CH}_3)_3$). IR: 2976, 2940, 2891, 1740, 1691. $[\alpha]_D = -116^\circ$ ($c = 1.01$).

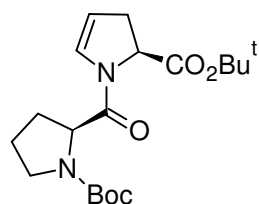
***tert*-Butyl (2S)-1-[(2R)-2-[(*tert*-butoxycarbonyl)amino]-3-phenylpropanoyl]-2,3-dihydro-1H-pyrrole-2-carboxylate, **58**.**



Was prepared according to the protocol¹³⁴ starting from **57** (3 g). 2.20 g (76%) of the product **58** was obtained after chromatography (silica gel, eluent – hexane:ethyl acetate 4:1, $R_f = 0.3$).

$^1\text{H-NMR}$ (CDCl_3 , 400MHz) – (rotamers): 7.33-7.15 (m, 5H, Ph), 6.39 (m, 1H, N-CH=CH), 5.39 (d, $J = 9\text{Hz}$, 1H, NH), 5.02 (m, 1H, N-CH=CH), 4.76 (m, 1H, CH-C(=O)-N), 4.52 (dd, $J = 5, 11\text{Hz}$, 1H, $\text{CH-CO}_2\text{Bu}^t$), 3.03 (d, $J = 7\text{Hz}$, 2H, CH=CH-CH_2), 2.90 (m, 1H, CHH in Phe), 2.52 (two m, 1H, CHH in Phe), 1.47 and 1.43 (two s, 18H, CH_3). IR: 3307 (broad), 2977, 2931, 1736, 1705, 1649, 1621. $[\alpha]_D = -115^\circ$ ($c = 1.00$).

***tert*-Butyl (5S)-1-[[*(2S)*-1-(*tert*-butoxycarbonyl)pyrrolydin-2-yl]carbonyl]-2-pyrrolidine-5-carboxylate, **62**.**

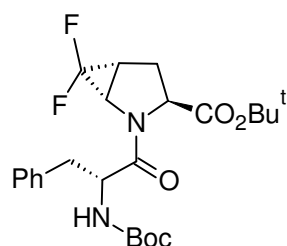


Was prepared according to the protocol¹³⁴ starting from the corresponding Pro-Pyr derivative (3 g). 2.00 g (70%) of the product was obtained after chromatography (silica gel, eluent – toluene:ethyl acetate 9:2, $R_f = 0.6$).

$^1\text{H-NMR}$ (CDCl_3 , 400 MHz) – (rotamers): 6.55 (m, 1H, N-CH=CH), 5.07 (m, 1H), 4.70 (m, 1H), 4.52 and 4.39 (two

m, 1H), 3.53 (m, 1H), 3.42-3.28 (m, 1H), 2.97-2.86 (m, 1H), 2.55-2.43 (three m, 1H), 2.18-2.05 (m, 1H), 2.05-1.91 (m, 2H), 1.86-1.74 (m, 1H), 1.39, 1.38, 1.38 and 1.31 (four s, 18H). IR: 2971, 2926, 2870, 1746, 1698, 1660, 1625. $[\alpha]_D = -160^\circ$ (c = 1.01).

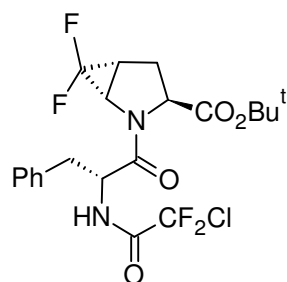
***tert*-Butyl (1S,3S,5R)-6,6-difluoro-2-{(2R)-2-[(*tert*-butoxycarbonyl)amino]-3-phenylpropanoyl}-2-azabicyclo[3.1.0]hexane-3-carboxylate, **59**.**



Was synthesized according to the protocol for **51**. The charged amounts were 1 g (2.4 mmol) of **58** and 9.2 g (60.3 mmol, 25 eq.) of the salt. The total reaction time was 40 min. After chromatography (silica gel, eluent – hexane:ethyl acetate, $R_f = 0.6$) 400 mg (36%) of transparent glass fractions was obtained out of the column from which the first part was **60** and the last (main) part was pure **59**. The ratio was estimated as 2:9 after analysis of the NMR spectra of all fractions.

$^1\text{H-NMR}$ (CDCl_3 , 400MHz) – two N-Boc rotamers, δ , ppm: 7.31-7.18 (m, 5H, Ph), 5.20 (m, 1H, NH), 4.83 (q, $J = 7\text{Hz}$, 1H, CH-CH₂-Ph), 4.36 (dd, $J = 10, 4\text{Hz}$, CH-CO₂Bu^t), 4.30 (dd, $J = 9, 5\text{Hz}$, N-CH-CF₂), 3.13 (dd, $J = 14, 6\text{Hz}$, 1H, CHH in Phe), 2.86 (dd, $J = 14, 7\text{Hz}$, 1H, CHH in Phe), 2.59-2.49 (m, 2H, CF₂-CH-CHH), 2.33 (m, 1H, CF₂-CH-CHH), 1.47 and 1.40 (two s, 9H, CH₃). $^{19}\text{F-NMR}$ (CDCl_3) – (rotamers): -127.9 (minor) and -128.7 (major) (ddd, $J_{\text{F-F}} = 160\text{Hz}$, $J_{\text{F-H}} = 15, 4\text{Hz}$, exo-F), -153.9 (major) and -157.0 (minor) (d, $J_{\text{F-F}} = 160\text{Hz}$, endo-F). IR: 3319, 2981, 2936, 1738, 1705, 1658. $[\alpha]_D = -113^\circ$ (c=1.19).

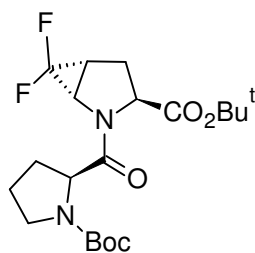
***tert*-Butyl (1S,3S,5R)-6,6difluoro-2-{(2R)-2-[chlorodifluoroacetilamino]-3-phenylpropanoyl}-2-azabicyclo[3.1.0]hexane-3-carboxylate, **60**.**



$^1\text{H-NMR}$ (CDCl_3 , 400MHz), δ , ppm: 7.33-7.13 (m, 5H, Ph), 5.11 (q, $J = 7\text{Hz}$, 1H, CH-CH₂-Ph), 4.54 (dd, $J = 9, 4\text{Hz}$, 1H, CH-CO₂Bu^t), 4.24 (dd, $J = 5, 9\text{Hz}$, 1H, N-CH-CF₂), 3.30 (dd, $J = 14, 5\text{Hz}$, 1H, CHH in Phe), 3.00 (dd, $J = 14, 7\text{Hz}$, 1H, CHH in Phe), 2.63 (m, 2H, CF₂-CH-CHH), 2.40 (m, 2H, CF₂-CH-CHH), 1.47 (s, 9H, CH₃). $^{19}\text{F-NMR}$ (CDCl_3) – (rotamers): -63.8 (s, 2F, CF₂), -128.3 (ddd, $J_{\text{F-F}} = 160\text{Hz}$, $J_{\text{F-H}} = 14, 4\text{Hz}$, exo-F), -153.2 (d, $J_{\text{F-F}} = 160\text{Hz}$, endo-F). IR: 3255, 3073, 2984, 2931, 2859, 1748, 1718, 1654, 1553. $[\alpha]_D = -121^\circ$ (c=1.33).

***tert*-Butyl (1S,3S,5R)-6,6-difluoro-2-[(2S)-1-(*tert*-butoxycarbonyl)pyrrolidin-2-yl]carbonyl}-2-azabicyclo[3.1.0]hexane-3-carboxylate, **63**.**

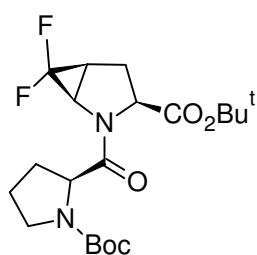
Was synthesized according to the protocol for **51**. The charged amounts were 1 g (2.7 mmol) of the starting enamine and 11.3 g (74 mmol, 27 eq.) of the



¹⁹F-NMR spectra and analytical HPLC. Pure **63** was a white solid.

¹H-NMR (CDCl₃, 400 MHz, two rotamers, δ, ppm): 4.53 (m, both N-CH-C=O of the minor isomer, both amino acid residues), 4.47 (m, N-CH-C=O major isomer, the F₂MePro residue), 4.40 (m, N-CH-C=O, major isomer, the Pro residue) – 2H in total, 3.72 (m, 1H, N-CH-CF₂), 3.53-3.30 (m, 2H, N-CH₂), 2.44 (m, 2H, CF₂-CH-CHH), 2.24 (m, 2H, CF₂-CH-CHH and N-C(=O)-CH-CHH), 2.01 (m, 1H, N-C(=O)-CH-CHH), 1.96-1.77 (m, 2H, N-CH₂-CH₂), 1.39 and 1.33 (two s, C(CH₃)₃). ¹⁹F-NMR (CDCl₃) – (rotamers): -126.7 (minor), -127.0 (major) (ddd, J_{F-F} = 158 Hz, J_{F-H} = 14, 3 Hz, exo-F), -154.2 (major), -154.5 (minor) (d, J_{F-F} = 158 Hz, endo-F). IR: 2973, 2931, 2877, 1718, 1688, 1662. [α]_D = -138° (c = 1.01).

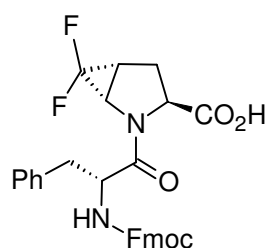
tert-Butyl (1R,3S,5S)-6,6-difluoro-2-[(2S)-1-(tert-butoxycarbonyl)pyrrolidin-2-yl]carbonyl}-2-azabicyclo[3.1.0]hexane-3-carboxylate, **64.**



Was obtained after preparative RP-HPLC using water and methanol as solvents A and B respectively. **64** was collected after **63** as a mixture of **64** and **63** ~ 9:1 (estimated from analytical HPLC and ¹⁹F-NMR).

¹H-NMR (CDCl₃, 300 MHz, two rotamers, δ, ppm): 4.78 (m, 1H, N-CH-CO₂Bu^t), 4.55 and 4.45 (two m, 1H, N-CH-C(=O)-N), 4.19 and 3.91 (two m, 1H, N-CH-CF₂), 3.60-3.29 (m, 2H, N-CH₂), 2.57 and 2.21 (two m, 2H, CH₂, the F₂MePro residue), 2.32 (m, 1H, CF₂-CH-CH₂), 2.05 (m, 3H, CH-CH₂-CHH-CH₂), 1.81 (m, 1H, CH-CH₂-CHH-CH₂), 1.38, 1.35 and 1.34 (three s, 18H, two C(CH₃)₃). ¹⁹F-NMR (CDCl₃) – (rotamers): -126.0 (minor) and -126.3 (major) (dd, J_{F-F} = 162 Hz, J_{F-H} = 14 Hz, exo-F), -151.7 (major) and -151.9 (minor) (d, J_{F-F} = 162 Hz, endo-F). IR: 2973, 2939, 2882, 1746, 1681. [α]_D = -48° (c = 0.98).

(1S,3S,5R)-6,6difluoro-2-[(2R)-2-[(9H-fluoren-9-ylmethoxy)amino]-3-phenylpropanoyl]-2-azabicyclo[3.1.0]hexane-3-carboxylic acid, **61.**

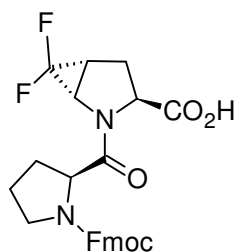


59 (206 mg, 0.44 mmol) was dissolved in dichloromethane (5 ml) and trifluoroacetic acid (1.5 ml) was added upon stirring. After 1.5 h the volatilities were removed under reduced pressure, the residue was additionally evaporated from dichloromethane (5 ml) twice and then taken up in 10% solution of sodium carbonate (1.2 ml) until pH become 8-9. Acetone (2 ml) was added followed by Fmoc-

OSu (164 mg, 0.49 mmol) in acetone (2 ml). The mixture was stirred for the next 27 h at room temperature and then volatilities were removed under vacuum (temperature in bath was $\leq 30^{\circ}\text{C}$), the water solution was diluted with water (50 ml). Water layer was extracted with diethyl ether (2 x 20 ml), the water fraction was acidified with hydrogen chloride solution (1M) until pH was ~ 1 . The water layer was extracted with ethyl acetate (4 x 30 ml). The ethyl acetate fractions were dried over sodium sulphate and concentrated under vacuum. The residue was lyophilized from acetonitrile-water mixture to give 193 mg (82%) of **61** as a white powder.

$^1\text{H-NMR}$ (CDCl_3 , 400MHz) – (rotamers only the major rotamer signals are denoted, minor rotamer content is less than 20%): 7.76 (d, $J= 7.6\text{Hz}$, 2H), 7.53 (t, $J= 8\text{Hz}$, 2H), 7.40 (t, $J= 7\text{Hz}$, 2H), 7.34-7.18 (m, 7H), 7.04 (broad s, CO_2H), 5.80 (d, 1H, NH), 4.91 (m, 1H), 4.70-4.05 (m, 5H), 3.17 (dd, $J= 5.7, 14\text{Hz}$, 1H, CHH in Phe), 2.93 (dd, $J= 7.8, 14\text{Hz}$, 1H, CHH in Phe), 2.64-2.48 (m, 3H). $^{19}\text{F-NMR}$ (CDCl_3) – (rotamers): -128.2 (minor) and -128.8 (major) (dd, $J= 12, 161\text{Hz}$, exo-F), -153.0 (minor) and -153.4 (major) (d, $J= 160\text{Hz}$, endo-F). IR: 3500-2200 (broad), 3304, 3064, 2954, 1714, 1659, 1520. $[\alpha]_{\text{D}} = -89.7^{\circ}$ ($c=1.00$).

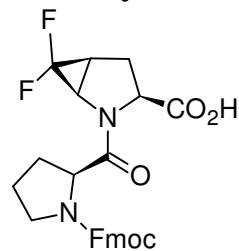
(1S,3S,5R)-6,6-difluoro-2-([(2S)-1-(9H-fluoren-9-ylmethoxy)carbonylpyrrolidin-2-yl]carbonyl)-2-azabicyclo[3.1.0]hexane-3-carboxylic acid.



Was synthesized analogous to **61**. 141 mg (94%) of the product was obtained out of 130 mg of **63** as white powder.

$^1\text{H-NMR}$ (CDCl_3 , 400 MHz) – (rotamers): 7.67 (m, 2H), 7.56-7.44 (m, 2H), 7.31 (m, 2H), 7.23 (m, 2H), 7.07 (broad s, 1H), 4.70-4.10 (m, 5H), 3.73-3.44 (m, 3H), 2.57-1.83 (m, 7H). $^{19}\text{F-NMR}$ (CDCl_3) – (rotamers): -128.0 (dm, $J = 161\text{ Hz}$, exo-F), -153.9 (minor) and -154.1 (major) (two d, $J = 160\text{ Hz}$, endo-F). IR: 3600-2400 (broad), 2958, 2889, 1706, 1674, 1522. $[\alpha]_{\text{D}} = -109^{\circ}$ ($c = 1.00$).

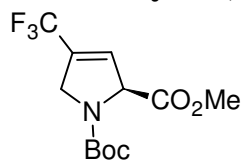
(1R,3S,5S)-6,6-difluoro-2-([(2S)-1-(9H-fluoren-9-ylmethoxy)carbonylpyrrolidin-2-yl]carbonyl)-2-azabicyclo[3.1.0]hexane-3-carboxylic acid.



This compound was prepared analogous to **61**, starting from **64** (42 mg, 0.1 mmol). As the amount of the compound synthesized (33 mg, 67% yield) was too small for its full characterization, only $^{19}\text{F-NMR}$ spectrum was run and the compound was immediately used for the peptide synthesis.

$^{19}\text{F-NMR}$ (CDCl_3) – (rotamers): -126.9 (minor) and -127.4 (major) (dm, $J_{\text{F-F}} = 162\text{ Hz}$, exo-F), -151.4 (major) and -151.8 (minor) (d, $J_{\text{F-F}} = 163\text{ Hz}$, endo-F).

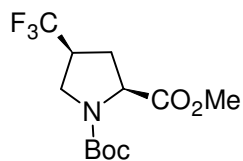
2-tert-butyl 2-methyl (2S)-4-trifluoromethyl-3-pyrrolin-1,2-dicarboxylate, 66.



Thionyl chloride (7 ml) was added to a stirred solution of **28** (2.34 g, 7.5 mmol) in dry pyridine (100 ml). The mixture was heated up until reflux for 25 min in total. Water (25 ml) was carefully added in order to quench the reaction. The dark mixture was extracted by pyridine (100 ml) and ether (3 x 150 ml). Combined organic fractions were evaporated, diethyl ether (300 ml) was added and resulting solution was washed with hydrogen chloride (2 M, 2 x 150 ml), saturated sodium hydrocarbonate (150 ml), water (150 ml) and brine (150 ml), dried over sodium sulphate and evaporated to give 1.59 g (72%) of **66** as wine oil.

$^1\text{H-NMR}$ (CDCl_3 , 400MHz) – (Boc-rotamers): 6.19 (td, $J = 19, 2$ Hz, 1H, $\text{CH}=\text{CCF}_3$), 5.08 (two m, 1H, N- $\text{CH}-\text{CO}_2\text{Me}$), 4.33 (m, 2H, N- CH_2), 3.71 (two s, 3H, CO_2CH_3), 1.42 and 1.37 (two s, 9H, $\text{C}(\text{CH}_3)_3$). $^{19}\text{F-NMR}$ (CDCl_3): -65.3 (d, $J_{\text{F-H}} = 19\text{Hz}$, CF_3). IR: 3093, 2983, 2876, 1748, 1703, 1667. $[\alpha]_{\text{D}} = -202^\circ$ ($c = 0.55$).

2-tert-butyl 2-methyl (2S,4S)-4-trifluoromethylpyrrole-1,2-dicarboxylate, 67.

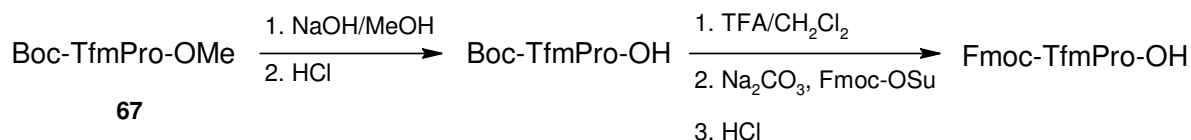


A mixture of **66** (790 mg, 2.7 mmol) and palladium on carbon (10%, 0.5 g) in methanol (15 ml) was stirred under hydrogen atmosphere (1 atm) at room temperature for 21 h. The mixture was filtered and evaporated giving 744 mg of **67** (94%) as colourless oil.

$^1\text{H-NMR}$ (CDCl_3 , 400MHz) – (Boc-rotamers): 4.42 and 4.33 (two t, $J = 8$ Hz, 1H), 3.92 and 3.84 (two t, $J = 10\text{Hz}$, 1H), 3.77 (s, 3H), 3.51 (t, $J = 10\text{Hz}$), 2.96 (m, 1H), 2.56 (m, 1H), 2.14 (m, 1H), 1.49 and 1.43 (two s, 9H). $^{19}\text{F-NMR}$ (CDCl_3): -70.4 (d, $J_{\text{H-F}} = 8.4$ Hz, CF_3). IR: 2987, 2870, 1747, 1695. $[\alpha]_{\text{D}} = -70^\circ$ ($c = 2.1$).

7.1.1. Procedures towards Fmoc-amino acids

Miscellaneous Fmoc-amino acids were synthesized according to Scheme 3.7. in chapter 3.3. After the synthesis purity of the Fmoc-Xaa-OH was checked on analytical HPLC and the substances were launched in peptide synthesis without characterization. The syntheses were performed analogously, few procedures are described below. Fmoc-OSu was preferred for small amounts and Fmoc-Cl for bulk syntheses.

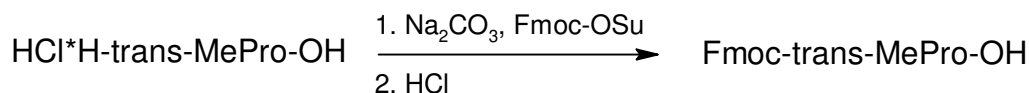


Boc-TfmPro-OH.

67 (711 mg, 2.4 mmol) was dissolved in methanol (10 ml), sodium hydroxide solution in methanol (1M, 5 ml) was added and the solution was stirred at room temperature for two hours. Methanol was removed under reduced pressure (temperature in bath $\leq 36^\circ\text{C}$), the rest was dissolved in water (20 ml) and extracted with diethyl ether (2 x 10 ml). The water layer was acidified by hydrogen chloride solution (1M) to pH = 1 and extracted with dichloromethane (3 x 30 ml). Combined dichloromethane fractions were dried over magnesium sulphate, filtered and concentrated in vacuum giving 657 mg (97%) of **Boc-TfmPro-OH** as colourless crystals.

Fmoc-TfmPro-OH.

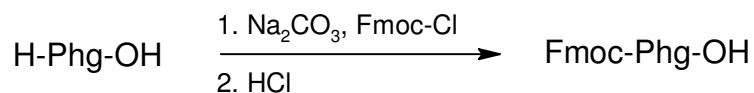
To a solution of **Boc-TfmPro-OH** (569 mg, 2.0 mmol) in dichloromethane (10 ml) trifluoroacetic acid (3 ml) was added, the solution was stirred at room temperature for 2 hours. Volatilities were removed under reduced pressure (temperature in bath 30°C), the residue was evaporated from dichloromethane (10 ml) once again. Water (10 ml), 10% sodium carbonate (7 ml, to pH ~ 8-9) and acetone (5 ml) were subsequently added until clear solution was obtained, resulting mixture was cooled down in an ice bath. Suspension of Fmoc-OSu (745 mg, 2.2 mmol) in acetone (2 ml) was added within 1 min upon stirring, and then acetone (~ 10 ml) was added to the reaction mixture. 4 hours after adding the reagent the ice bath was removed and stirring was continued for 25 hours at ambient temperature. Acetone was removed under reduced pressure (temperature in bath $\leq 31^\circ\text{C}$), the transparent solution was poured in water (100 ml), and resulting suspension was extracted with diethyl ether (4 x 30 ml). The water layer was acidified by hydrogen chloride (1M) until pH ~ 1 and extracted by ethyl acetate (4 x 50 ml), the ethyl acetate fractions were dried over magnesium sulphate, filtered and evaporated, the residue was lyophilized from acetonitril-water mixture to give 813 mg (quant.) of **Fmoc-TfmPro-OH** as pale fawny powder.



Fmoc-trans-MePro-OH.

HCl \cdot *H-trans-MePro-OH* (99 mg, 0.61 mmol) was dissolved in water (3 ml), 10% sodium carbonate (1.5 ml) was added until pH reached 8-9. Acetone (1.5 ml) was added, the mixture was cooled down in an ice bath and Fmoc-OSu (227 mg, 0.67 mmol) in acetone (2 ml) suspension was added over 0.5 min. Acetone (3 ml) and water (3 ml) were added in order to get clear solution and the mixture was stirred at ambient temperature 16h. Acetone was removed under reduced pressure and the residue was poured in water (50 ml). Water was extracted with diethyl ether (2 x 20 ml) and acidified with hydrogen chloride solution (1M, 3 ml) until pH ~ 1-2. The water was extracted with ethyl acetate (5

x 30 ml), the ethyl acetate fractions were dried over sodium sulphate, filtered and concentrated in vacuum. Lyophilization out of acetonitril-water mixture gave 213 mg (quant.) of Fmoc-*trans*-MePro-OH as fawny powder.



Fmoc-Phg-OH.

H-Phg-OH (5 g, 33 mmol) was dissolved in 10% sodium carbonate solution (60 ml), acetone (25 ml) and additional water (30 ml) mixture. This mixture was cooled down in an ice bath. Fmoc-Cl (9.41 ml, 36.4 mmol) in acetone (35 ml) was added over 7 min upon stirring. The mixture was stirred for 43h and was allowed to warm to room temperature. Acetone was removed under reduced pressure (temperature $\leq 30^\circ\text{C}$) and the residue was diluted with water (600 ml), extracted with diethyl ether (4 x 100 ml) and acidified by hydrogen chloride solution (1M, 70 ml) until acidic pH. The mixture was extracted with ethyl acetate (3 x 250 ml), the ethyl acetate fractions were dried over magnesium sulphate, filtered and evaporated. The product was lyophilized out of acetonitril-water. 10.26 g (83%) of Fmoc-Phg-OH was obtained as white powder.

7.2. Peptide synthesis

7.2.1. Synthesis of gramicidin S analogues

Was performed manually according to¹⁰² as described in chapters 3.4. The RP-HPLC purification was done on either semi-preparative or preparative columns. The synthesis type and analytical data for the peptides obtained is summarized in Table 7.1. HPLC was done as described above, only analytical biphenyl column of the same size was used instead of a C18, injected amount was 5 μl of 1 mg/ml solutions in acetonitrile-water. ¹⁹F-NMR of fluorine containing peptides was done in acetonitril-water (1:1) solution. Analytical data for the peptides is summarized in Table 7.1.

7.2.2. Synthesis of SAP analogues

Was performed manually according to⁴⁴ as described in chapters 3.4. The RP-HPLC purification was done on either semi-preparative or preparative columns. The synthetic rout was denoted in Table 3.5. Analytical data for the peptides obtained is summarized in Table 7.2. HPLC was done as usual, 15 μl of 1-3 mg/ml solutions in methanol were injected. ¹⁹F-NMR of fluorine containing peptides was done in water solution.

name	starting amino acid	ornithine protection group	Mass		HPLC retention time, min	¹⁹ F-NMR data
			calculated, Da	MALDI-TOF, Th		
proline substituted						
I-flp-GS	^D Phe	ivDde	1159.5	1160.3	15.35	m, -170.1
II-flp-GS	Val	Boc	1177.5	1177.5	15.18	m, -170.1
I-Flp-GS	^D Phe	ivDde	1159.5	1161.2	15.25	m, -177.8
II-Flp-GS	^D Phe	ivDde	1177.5	1178.3	15.00	m, -177.8
I-F ₂ Pro-GS	^D Phe	ivDde	1177.5	1178.3	15.63	dm, J= 235 Hz, -91.6; d, J= 234 Hz, -102.8
II-F ₂ Pro-GS	^D Phe	Boc	1213.4	1214.6	15.79	dm, J= 234 Hz, -91.5; d, J= 236 Hz, -102.7
I-c-MePro-GS	^D Phe	Boc	1153.5	1154.0	15.74	-
II-c-MePro-GS	Val	Boc	1165.5	1166.0	15.90	-
I-TfmPro-GS	^D Phe	Boc	1209.5	1211.2	15.86	d, J= 10Hz, -70.5
II-TfmPro-GS	Val	Boc	1277.5	1278.3	16.16	d, J= 9Hz, -70.5
I-A(c)-GS	^D Phe	ivDde	1221.5	1222.6	15.94	m, -64.7
II-A(c)-GS	Val	Boc	1301.5	1302.8	16.36	d, J= 7 Hz, -64.8
I-B(t)-GS	^D Phe	Boc	1221.5	1222.5	15.99	d, J= 7 Hz, -64.1
II-B(t)-GS	Val	Boc	1301.5	1302.2	16.36	d, J= 7 Hz, -64.1
I-t-F ₂ MePro-GS	^D Phe	Boc	1189.5	1191.5	15.78	dd, J= 158, 12 Hz, -127.8; d, J= 159 Hz, -152.7
leucine substituted						
I- ^D FPhg-GS	^D Phe	Boc	1179.5	1180.0	14.71	s, -106.8
I- ^L Phg-GS				1180.1	15.36	s, -108.4
II- ^{D,D} FPhg-GS		Boc	1217.4	1218.0	13.27	s, -112.5
II- ^{D,L} FPhg-GS				1218.5	14.63	s, -112.1; s, -113.3
II- ^{L,L} FPhg-GS (LGS)				1217.5	15.12	s, -113.5
II- ^{D,D} Phg-GS		Boc	1181.5	1182.0	13.06	-
II- ^{D,L} Phg-GS				1182.0	14.54	-
II- ^{L,L} Phg-GS				1182.3	15.27	-

Table 7.1. Analytical data for the gramicidin S analogues.

Name	Mass		HPLC retention time, min	¹⁹ F-NMR data
	calculated, Da	MALDI-TOF, Th		
SAP-TfmPro	2065.5	2066.1	9.08	d, J= 8 Hz, -69.7
SAP-c-MePro	2009.5	2010.0	8.82	-
SAP-t-MePro	2009.5	2009.4	8.60	-
SAP-flp	2015.5	2016.0	8.59	m, -176.2
SAP-Flp	2015.5	2016.1	8.58	m, -170.5
SAP-B(t)	2077.5	2077.5	9.23	d, J= 7 Hz, -64.4
SAP-t-F ₂ MePro	2045.5	2045.6	8.87	dd, J= 162, 13 Hz, -129.2; d, J= 161 Hz, -152.9
SAP-c-F ₂ MePro	2045.5	2046.1	8.82	dd, J= 159, 12 Hz, -125.6; d, J= 159 Hz, -151.7

Table 7.2. Analytical data for the SAP analogues.

7.3. Antimicrobial activity test

Serial broth dilution test was done with all gramicidin S analogues according to the protocol¹⁰⁷ modified as described¹³⁵. The peptides concentration after weighting was calibrated to the wild type GS concentration via HPLC and corrected by aliquotzing.

7.4. Circular dichroism measurements

CD spectra of gramicidin S analogues were recorded on Jasco J-815 Spectrophotometer. The measurements were done in a suprasil® 1 mm cell. The samples in trifluoroethanol and deionized water were of 50 µM peptide concentration and were measured at 25°C. The phosphate buffer was of 20 mM concentration and pH 7.2 (at 30°C). The lipid vesicles were prepared according to the following protocol: the lipid (DLPC) was dissolved in methanol, and aliquotized by portions of 50 µl. For the samples with the reconstituted peptides the peptide 50 µl aliquote in methanol was added on this step. The methanol solution was dried by nitrogen current and then additionally dried under vacuum for at least 2 h. 300 µl portion of the PB was added such that the final peptide concentration was 37 mM and the lipid 0.92 mg/ml (resulting p/l was 1/40). The mixture was vortexed for 10 min, 8-10 times freeze-thaw cycles were performed by freezing in liquid nitrogen and warming in warm water. Resulting mixture was sonicated 4 x 4 min and the CD spectra were recorded at 30°C. For the mixed samples, the resulting suspension of the lipid vesicles was added to a dry peptide aliquote which was prepared accordingly. The mixture was vortexed for 1 min before the measurements.

CD spectra of SAP analogues were done on CD12 beamline at synchrotron facility at the Karlsruhe Institute of Technology¹³⁶. Measurements in solution were done in deionized water at 20°C. The peptides were aliquotized from the stock solutions in methanol and dried before being dissolved in water. Measurements at 10 mg/ml concentration were done in demountable 13 µm

CaF₂ cell. Measurements at concentration 0.5 mg/ml were done in a suprasil® 0.1 mm cell.

7.5. Hemolysis assays

Human blood conserves were obtained in Städtisches Klinikum Karlsruhe. Two buffers were employed: “buffer 1” 160 mM Tris* with pH 7.6 at 4°C, “buffer 2” 160 mM Tris with pH 7.6 at 37°C.

5 ml of the blood conserves was diluted with 45 ml of buffer 1, centrifuged 10 min at 231 g (1,500 rpm) and 4°C and the supernatant (~ 45 ml) was discarded. This operation was repeated twice. 1 ml of the residue was diluted with 9 ml of buffer 1 and the resulting suspension was then stored on ice as the stock suspension. Hemolytic tests of GS wild type which were done at the beginning at the end of the measurements (~ 5 h in between) showed fully consistent curves. 0.5 ml of the stock suspension was diluted with 9.5 ml of buffer 2 and 200 µl were aliquotized in each one vial with buffer 2 and peptides in different concentrations (200 µl of solution in each one) as well as with buffer 2 only (negative control) and 0.2% solution of Triton X-100® (positive control). The mixtures of the blood cells and peptides in buffer 2 in corresponding vials were incubated 30 min at 37°C with gentle discrete shaking. Then the mixtures were centrifuged 10 min at 13,000 rpm, 320 µl of supernatant solution from each one vial was taken and absorption at 540 nm was measured at SmartSpec spectrophotometer. Buffer 2 was used as blank. Values from the negative control vial were controlled to be low and were taken in analysis as 0%, corresponding values from the positive control vials were taken as 100% hemolysis value. There were two rows of 2-fold dilution for each one peptide:

- 1) 64-0.5 (8 values) and 50-1.6 (6 values) µg/ml for the medium hemolytic;
- 2) 32-0.25 (8 values) and 25-0.4 (7 values) µg/ml for the high hemolytic;
- 3) 150-2.3 (7 values) and 128-2 (7 values) µg/ml for the peptides with the homolysis lower as induced by the wild type GS.

The peptides were originally dissolved in buffer 2:dimethylsulfoxide mixture (9:1 vol) and then titrated in the vials with the buffer 2 such that the DMSO content was 5% in the vial with the 64 µg/ml starting concentration.

Few values with enormously high absorption (>> with Triton X-100®) were not taken in the analysis. These samples apparently contained blood cell ghosts, which caused scattering.

* tris(hydroxymethyl)aminomethane

Peptide	hemolytic concentration, $\mu\text{g/ml}$		
	HC ₂₅	HC ₅₀	HC ₇₅
GS wild type	6.9	9.4	11.9
I-Flp-GS	20.2	23.7	27.8
II-Flp-GS	42.0	58.7	71.2
I-flp-GS	13.3	17.2	22.5
II-flp-GS	10.3	15.3	20.6
I-F ₂ Pro-GS	3.4	4.5	5.7
II-F ₂ Pro-GS	1.2	2.0	2.7
I-c-MePro-GS	4.1	6.1	7.4
II-c-MePro-GS	3.5	4.8	6.3
I-t-F ₂ MePro-GS	4.0	5.0	6.4
I-TfmPro-GS	1.6	2.2	2.8
II-TfmPro-GS	0.6	1.1	2.0
I-A(c)-GS	3.4	4.7	6.1
II-A(c)-GS	1.1	1.9	2.6
I-B(t)-GS	1.4	2.8	4.1
II-B(t)-GS	0.5	0.7	1.2

Table 7.3. Hemolytic concentrations of proline substituted gramicidin S analogues.

7.6. Solid state NMR studies in lipid bilayers

7.6.1. Instruments and pulses

¹⁹F- and ³¹P-NMR spectra of peptide in lipid samples were recorded at:

- Bruker Avance 500 NMR system with a wide bore magnet equipped with:
 - 1) for ¹⁹F spectra (470.6 MHz) ¹H/¹⁹F double resonance variable angle flat coil probe (Doty Scientific), 90 deg pulse of 2.1 μs and 126 W, decoupling 8 W; 2) for ³¹P spectra (202.5 MHz) ¹H/¹⁹FX variable angle flat coil probe (Bruker), 90 deg pulse 7.1 μs and 125 W, decoupling 13 W.
- Bruker Avance 500 III NMR system with a wide bore magnet equipped with:
 - 1) for ¹⁹F spectra (470.6 MHz) ¹H/¹⁹F lowE¹³⁷ coil probe (home built), 90 deg pulse of 3.4 μs and 75 W, decoupling 16 W; 2) for ³¹P spectra (202.5 MHz) ¹HXY lowE flat coil probe (home built), 90 deg pulse of 5 μs and 48 W, decoupling 16 W.
- Bruker Avance 300 NMR system with wide bore magnet equipped with:
 - 1) for ¹⁹F spectra (282.4 MHz) ¹H/¹⁹F lowE coil probe (home-built), 90 deg pulse of 3.0 μs and 158 W, decoupling 8 W.

The proton decoupling power corresponded to the 15-20kHz actual decoupling strength.

For ³¹P-NMR spectra hahnecho pulse sequence with decoupling was applied (30 μs echo delay, 10-20 ms acquisition time and 2 s recycling delay). For ¹⁹F spectra: 1) for mono fluorine system hahnecho sequence with decoupling (30 μs echo delay, 20 ms acquisition time and 2 s recycling delay); 2) for

geminal difluoro substituted peptides single pulse sequence with decoupling was applied (2 μ s acquisition time, and 3 s recycling delay); 3) for trifluoromethyl substituted peptides composite aring sequence with decoupling was applied (2 μ s acquisition time, and 1 s recycling delay).

7.6.2. Peptide-lipid samples preparation

Typical procedure for a sample with p/l = 1/40.

Peptide (0.5-0.7 mg) was co-dissolved with the lipid (10-14 mg) in either methanol or methanol-chloroform (2:1) mixture and spread over 12-17 glass plates (Marienfeld Laboratory Glassware) such that the amount per a glass plate was 0.7-0.8 mg for 18 x 7.5 mm and 0.6-0.7 mg for 15 x 7.5 mm glass plates (30-50 μ l per a glass plate). The solvent was allowed to dry out for 30-60 min and the glass plates were dried in vacuum for at least 4 hours. They were then stacked and hydrated in chambers with saturated potassium sulphate (96% relative humidity) for 12-24 hours and finally wrapped in Nescofilm® and Sarogold® films. The samples were stored at -20°C between the measurements.

7.6.3. Miscellaneous experimental parameters

The samples were thermostated by gas flow 1200, 1600 or 2000 l/h depending on the temperature range. The pre-acquisition delay used for the proper thermostating was 5-10 min (also within temperature series).

Processing was done in Topspin 2.1. Exponential window function (em) was taken with different Lorentzian broadening (lb) parameters, typically 100-300 Hz for the liquid-crystalline and ~500 Hz for the gel lipid states. Within temperature series lb was always taken the same.

The solid state NMR spectra were not externally referenced.

Curriculum Vitae

Personal data:

Name: Volodymyr S. Kubyshkin (Vladimir S. Kubyshkin)
Date of birth: October 12, 1986
Place of birth: Yalta, Ukraine
Citizenship: Ukrainian
Address: Schützenstr., 35, Karlsruhe, Germany, 76137
Phone (work): +49(0)72160847223
Mob.: +49(0)15124270897
E-mail: kyblo14@rambler.ru (personal), vladimir.kubyshkin@kit.edu (work)
Member of the Fluorine division of the American Chemical Society (since 2011)



Education:

1993-2001: basic secondary (school) education (completion grade “excellent”), Yalta school No. 6;
2001-2003: complete secondary (school) education (completion grade “excellent”), Yalta school No. 6;
2003-2008: highest (university) education at Chemistry Dept., T. Shevchenko National University of Kyiv, Kyiv, Ukraine;
2007: B.S. in chemistry (degree with honour);
2008: M.S. in chemistry (degree with honour); specialization: organic chemistry; thesis: “Consecutive ester enolate bis-alkylation in synthesis of new amino acids”;
2009 – 2012: PhD student at Karlsruhe Institute of Technology (KIT), Karlsruhe, Germany;

Awards:

2001-2003: participation in the Ukrainian Chemistry Olympiads of scholars: 3rd prizes 2001 and 2002, 2nd prize 2003;
2007: personal stipend of the city major of Kyiv “For the best students”;
2010-2012: two years stipend from the land Baden-Württemberg (Landesgraduiertenförderung).

Teaching experience:

2005-2008: Judging of the Crimean Chemistry Olympiads of scholars, Simferopol
2008: Supervision of the “Advanced NMR practical training”, T. Shevchenko University, Kyiv;
2009: Supervision of the “Organic chemistry advanced practical training”, KIT, Karlsruhe;
2010: Supervision of two student’s profound practicum projects, KIT, Karlsruhe;
2010-2012: Supervision of microbiological practicum for students in Chemical Biology, KIT, Karlsruhe.

List of publications:

1. V. S. Kubyshkin, P. K. Mikhailiuk, I. V. Komarov. Synthesis of 7-azabicyclo[2.2.1]heptane-1,4-dicarboxylic acid, a rigid non-chiral analogue of 2-aminoadipic acid. *Tetrahedron Letters*, 2007 (48): 4061–4063.
2. V. S. Kubyshkin, P. K. Mykhailiuk, A. S. Ulrich, I. V. Komarov. Synthesis of a conformationally rigid analogue of 2-aminoadipic acid - containing an 8-azabicyclo[3.2.1]octane skeleton. *Synthesis*, 2009 (19): 3327-3331.

3. V. S. Kubyshkin, I. V. Komarov, S. Afonin, P. K. Mykhailiuk, S. L. Grage, A. S. Ulrich. Trifluoromethyl-substituted α -amino acids as solid state ^{19}F -NMR labels for structural studies of membrane peptides. Book chapter in *Fluorine in pharmaceutical and medicinal chemistry. From biophysical aspects to clinical applications*. Edited by V. Gouverneur and K. Müller. Imperial college press, 2012. [Review]
4. V. S. Kubyshkin, P. K. Mykhailiuk, S. Afonin, A. S. Ulrich, I. V. Komarov. Incorporation of novel cis- and trans-4,5-difluoromethanoprolines into polypeptides. *Organic Letters*, 2012 (14): 5254-5257.
5. A. N. Tkachenko, S. Afonin, P. K. Mykhailiuk, D. S. Radchenko, V. S. Kubyshkin, A. S. Ulrich, I. V. Komarov. First ^{19}F -NMR peptide label with a polar side chain: a CF_3 -substituted analogue of serine and threonine. *Angewandte Chemie International Edition*, 2013 (52): 1486-1489.
6. V. S. Kubyshkin, P.K. Mykhailiuk, S. Afonin, S. L. Grage, I. V. Komarov, A. S. Ulrich. Incorporation of labile trans-4,5-difluoromethanoproline into a peptide as a stable label for ^{19}F -NMR structure analysis. *Journal of Fluorine Chemistry*, 2013, online <http://dx.doi.org/10.1016/j.jfluchem.2013.03.002>

Conference reports:

1. Synthesis of new bicyclic Pro-Glu chimeras by consecutive ester enolate alkylation. *11th International Congress on Amino Acids, Peptides and Proteins*. Vienna, Austria, August 3-7, 2009. [Oral talk]
2. Fluorine-labeled amino acids as labels for ^{19}F -NMR structure analysis of membrane-active peptides. *20th Winter Fluorine Conference (ACS)*. St. Pete Beach, FL, January 9-14, 2011. [Oral talk]
3. Re-alignment of the antimicrobial peptide gramicidin S in lipid membranes: probing different sites of the molecule. *8th EBSA European Biophysics Congress*. Budapest, Hungary, August 23-27, 2011. [Poster]

References

- ¹ S. Purser, P. R. Moore, S. Swallow, V. Gouverneur. Fluorine in medicinal chemistry. *Chem Soc Rev*, **2008**, 37, 320-330.
- ² K. Müller, C. Faeh, F. Diederich. Fluorine in pharmaceuticals: looking beyond intuition. *Science*, **2007**, 317, 1881-1886.
- ³ D. O'Hagan. Understanding organofluorine chemistry. An introduction to the C-F bond. *Chem Soc Rev*, **2008**, 37, 308-319.
- ⁴ S. L. Cobb, C. D. Murphy. ¹⁹F NMR applications in chemical biology. *J Fluor Chem*, **2009**, 130, 132-143.
- ⁵ J. L. Kitevski-LeBlanc, R. S. Prosser. Current applications of ¹⁹F NMR to studies of protein structure and dynamics. *Prog Nuc Mag Res Spec*, **2012**, 62, 1-33.
- ⁶ M. A. Danielson, J. J. Falke. Use of ¹⁹F NMR to probe protein structure and conformational changes. *Annu Rev Biophys Biomol Struct*, **1996**, 25, 163-195.
- ⁷ P. A. Luchette, R. S. Prosser, C. R. Sanders. Oxygen as a paramagnetic probe of membrane protein structure by cysteine mutagenesis and ¹⁹F NMR spectroscopy. *J Am Chem Soc*, **2002**, 124, 1778-1781.
- ⁸ C. Li, G.-F. Wang, Y. Wang, R. Creager-Allen, E. A. Lutz, H. Scronce, K. M. Slade, R. A. S. Ruf, R. A. Mehl, G. J. Pielak. Protein ¹⁹F NMR in *Escherichia coli*. *J Am Chem Soc*, **2010**, 132, 321-327.
- ⁹ S. Capone, I. Kieltsch, O. Flögel, G. Lelais, D. Seebach. Electrophilic S-trifluoromethylation of cysteine side chains in α - and β -peptides: isolation of trifluoro-methylated *Sandostatin*® (Octreotide) derivatives. *Helv Chim Acta*, **2008**, 91, 2035-2056.
- ¹⁰ A. Sutherland, C. L. Willis. Synthesis of fluorinated amino acids. *Nat Prod Rep*, **2000**, 17, 621-631.
- ¹¹ X.-L. Qiu, W.-D. Meng, F.-L. Qing. Synthesis of fluorinated amino acids. *Tetrahedron*, **2004**, 60, 6711-6745.
- ¹² C. Jäckel, B. Koksche. Fluorine in peptide design and protein engineering. *Eur J Org Chem*, **2005**, 4483-4503.
- ¹³ X.-L. Qiu, F.-L. Qing. Fluorinated amino acids. *Eur J Org Chem*, **2011**, 3261-3278.
- ¹⁴ M. Zanda. Trifluoromethyl group: an effective xenobiotic function for peptide backbone modification. *New J Chem*, **2004**, 28, 1401-1411.
- ¹⁵ E. Parisini, P. Metrangolo, T. Pilati, G. Resnati, G. Terraneo. Halogen bonding in halocarbon-protein complexes: a structural survey. *Chem Soc Rev*, **2011**, 40, 2267-2278
- ¹⁶ M. Cametti, B. Crousse, P. Metrangolo, R. Milani, G. Resnati. The fluorous effect in biomolecular applications. *Chem Soc Rev*, **2012**, 41, 31-42.
- ¹⁷ Y. T. Lim, M. Y. Cho, J.-H. Kang, Y.-W. Noch, J.-H. Cho, K. S. Hong, J. W. Chung, B. H. Chung. Perfluorodecalin/[InGaP/ZnS quantum dots] nanoemulsions as ¹⁹F MR/optical imaging nanoprobe for the labeling of phagocytic and nonphagocytic immune cells. *Biomaterials*, **2010**, 31, 4964-4971.
- ¹⁸ V. Gouverneur, K. Müller (Eds). *Fluorine in Pharmaceutical and medicinal chemistry*, **2012**, Imperial College Press.
- ¹⁹ R. G. Dubos, C. Cattaneo. Studies of a bactericidal agent extracted from a soil bacillus. *J Exp Med*, **1939**, 70, 249-256.
- ²⁰ M. Zasloff. Antimicrobial peptides of multicellular organisms. *Nature*, **2002**, 415, 389-395.
- ²¹ R. E. Koeppe II, O. S. Andersen. Engineering of gramicidin channels. *Annu Rev Biophys Biomol Struct*, **1996**, 25, 231-258.
- ²² K. A. Brogden. Antimicrobial peptides: pore formers or metabolic inhibitors in bacteria? *Nat Rev Microbiol*, **2005**, 3, 238-250.
- ²³ Y. Shai. Mode of action of membrane active antimicrobial peptides. *Biopolymers*, **2002**, 66, 236-248.
- ²⁴ K. Matsuzaki. Control of cell selectivity of antimicrobial peptides. *Biochim Biophys Acta*, **2009**, 1788, 1687-1692.
- ²⁵ S. L. Grage, S. Afonin, A. S. Ulrich „Dynamic transitions of membrane-active peptides“ in *Antimicrobial peptides, methods in molecular biology* (Eds.: A. Giuliani, A. C. Rinaldi), Springer Science, **2010**, 183-207.
- ²⁶ M. C. Morris, S. Deshayes, F. Heitz, G. Divita. Cell-penetrating peptides: from molecular mechanism to therapeutics. *Biol Cell*, **2008**, 100, 201-217.
- ²⁷ F. Heitz, M. C. Morris, G. Divita. Twenty years of cell-penetrating peptides: from molecular mechanism to therapeutics. *British J Pharmacol*, **2009**, 157, 195-206.
- ²⁸ S. B. Fonseca, M. P. Pereira, S. O. Kelley. Recent advances in the use of cell-penetrating peptides for medical and biological applications. *Adv Drug Deliv Rev*, **2009**, 61, 953-964.
- ²⁹ A. S. Ulrich. Solid state ¹⁹F NMR methods for studying biomembranes. *Prog Nuc Mag Res Spec*, **2005**, 46, 1-21.
- ³⁰ A. Ulrich, P. Wadhvani, U.H.N. Dürr, S. Afonin, R.W. Glaser, E. Strandberg, P. Tremouilhac, C. Sachse, M. Berditchevskaia, S.L. Grage “Solid-state ¹⁹F-Nuclear magnetic resonance analysis of membrane-active peptides” in *NMR spectroscopy of biological solids* (Ed.: A. Ramamoorthy), CRC Press, **2006**, 215-236.
- ³¹ G. F. Gause, M. G. Brazhnikova. Gramicidin S and its use in the treatment of infected wounds. *Nature*, **1944**, 154, 703.

- ³² N. Izumiya, T. Kato, H. Aoyagi, M. Waki, M. Kondo. *Synthetic aspects of biologically active cyclic peptides – gramicidin S and tyrocidines*, **1979**, Wiley.
- ³³ L. H. Kondejewski, S. W. Farmer, D. S. Wishart, R. E. W. Hancock, R. S. Hodges. Gramicidin S is active against both gram-positive and gram-negative bacteria. *Int J Pept Protein Res*, **1996**, 47, 460-466.
- ³⁴ T. Kato, N. Izumiya. Conformations of di-Nmethylleucine gramicidin S and N-methylleucine gramicidin S compatible with the sidedness hypothesis. *Biochem Biophys Acta*, **1977**, 493, 235-238.
- ³⁵ D. C. Hodgkin, B. M. Oughton. Possible molecular models for gramicidin S and their relationship to present ideas of protein structure. *Biochem J*, **1957**, 65, 752-756.
- ³⁶ S. E. Hull, R. Karlsson, P. Main, M. M. Woolfson, E. J. Dodson. The crystal structure of a hydrated gramicidin S-urea complex. *Nature*, **1978**, 275, 206-207.
- ³⁷ M. Jelokhani-Niaraki, R. S. Hodges, J. E. Meissner, U. E. Hassenstein, L. Weaton. Interaction of gramicidin S and its aromatic amino-acid analog with phospholipid membranes. *Biophys J*, **2008**, 95, 3306-3321.
- ³⁸ P. Kupres, K. Pagel, J. Oomens, N. Polfer, B. Koksich, G. Meijer, G. von Helden. Amide-I and -II vibrations of the cyclic β -sheet model peptide gramicidin S in the gas phase. *J Am Chem Soc*, **2010**, 132, 2085-2093.
- ³⁹ R. N. A. H. Lewis, M. Kiricsi, E. J. Prenner, R. S. Hodges, R. N. McElhaney. Fourier transform infrared spectroscopic study of the interaction of a strongly antimicrobial but weakly hemolytic analogue of gramicidin S with lipid micelles and lipid bilayer membranes. *Biochemistry*, **2003**, 42, 440-449.
- ⁴⁰ D. L. Lee, R. S. Hodges. Structure-activity relationship of de novo designed cyclic antimicrobial peptides based on gramicidin S. *Biopolymers*, **2003**, 71, 28-48.
- ⁴¹ G. M. Grotenberg, M. D. Witte, P. A. V. van Hooft, E. Spalburg, P. Reiß, D. Noort, A. J. de Neeling, U. Koert, G. A. van der Marel, H. S. Overkleeft, M. Overhand. Synthesis and biological evaluation of gramicidin S dimers. *Org Biomol Chem*, **2005**, 3, 233-238.
- ⁴² M. Tamaki, K. Fujinuma, T. Harada, K. Takanashi, M. Shindo, M. Kimura, Y. Uchida. Fatty acyl-gramicidin S derivatives with both high antibiotic activity and low hemolytic activity. *Bioorg Med Chem Lett*, **2012**, 22, 106-109.
- ⁴³ A. D. Knijnenburg, E. Spalburg, A. J. de Neeling, R. H. Mars-Groenendijk, D. Noort, G. M. Grotenberg, G. A. van der Marel, H. S. Overkleeft, M. Overhand. Ring-extended derivatives of gramicidin S with furanoid sugar amino acids in the turn region have enhanced antimicrobial activity. *ChemMedChem*, **2009**, 4, 1976-1979.
- ⁴⁴ J. Fernández-Carneado, M. J. Kogan, S. Castel, E. Giralt. Potential peptide carriers: amphipathic proline-rich peptides derived from the N-terminal domain of γ -zein. *Angew Chem Int Ed*, **2004**, 43, 1811-1814.
- ⁴⁵ S. Pujals, E. Giralt. Proline-rich, amphipathic cell-penetrating peptides. *Adv Drug Delivery Reviews*, **2008**, 60, 473-484.
- ⁴⁶ I. Llop-Tous, S. Madurga, E. Giralt, P. Marzabal, M. Torrent, M. D. Ludevid. Relevant elements of a maize γ -zein domain involved in protein body biogenesis. *J Biol Chem*, **2010**, 285, 35633-35644.
- ⁴⁷ J. Salgado, S. L. Grage, L. H. Kondejewski, R. S. Hodges, R. N. McElhaney, A. S. Ulrich. Membrane-bound structure and alignment of the antimicrobial β -sheet peptide gramicidin S derived from angular and distance constraints by solid state ^{19}F -NMR. *J Biomol NMR*, **2001**, 21, 191-208.
- ⁴⁸ S. Afonin, R. W. Glaser, M. Berditschewskaia, P. Wadhvani, K. H. Gührs, U. Möllmann, A. Perner, A. S. Ulrich. 4-Fluorophenylglycine as a label for ^{19}F NMR structure analysis of membrane-associated peptides. *ChemBioChem*, **2003**, 7, 1151-1163.
- ⁴⁹ R. W. Glaser, A. S. Ulrich. Susceptibility corrections in solid-state NMR experiments with oriented membrane samples. Part I: applications. *J Mag Res*, **2003**, 164, 104-114.
- ⁵⁰ R. W. Glaser, C. Sachse, U. H. N. Dürr, P. Wadhvani, A. S. Ulrich. Orientation of the antimicrobial peptide PGLa in lipid membranes determined from ^{19}F -NMR dipolar couplings of 4-CF₃-phenylglycine labels. *J Mag Res*, **2004**, 168, 153-163.
- ⁵¹ P. K. Mikhailiuk, S. Afonin, A. N. Chernega, E. B. Rusanov, M. O. Platonov, G. G. Dubinina, M. Berditsch, A. S. Ulrich, I. V. Komarov. Conformationally rigid trifluoromethyl-substituted α -amino acid designed for peptide structure analysis by solid-state ^{19}F NMR spectroscopy. *Angew Chem Int Ed*, **2006**, 45, 5659-5661.
- ⁵² S. Afonin, P. K. Mikhailiuk, I. V. Komarov, A. S. Ulrich. Evaluating the amino acid CF₃-bicyclopentylglycine as a new label for solid-state ^{19}F -NMR structure analysis of membrane-bound peptides. *J Pept Sci*, **2007**, 13, 614-623.
- ⁵³ J. F. Lontz, M. S. Raasch. Alpha-amino acids containing alpha, fluorinated-alkyl or cycloalkyl groups. *US Pat 2662915*, **1953**, *Chem Abstr*, 4871849.
- ⁵⁴ D. Maisch, P. Wadhvani, S. Afonin, C. Böttcher, B. Koksich, A. S. Ulrich. Chemical labeling strategy with (R)- and (S)-trifluoromethylalanine for solid state ^{19}F NMR analysis of peptaibols in membranes. *J Am Chem Soc*, **2009**, 131, 15596-15597.
- ⁵⁵ A. N. Tkachenko, P. K. Mykhailiuk, S. Afonin, D. S. Radchenko, V. S. Kubyschkin, A. S. Ulrich, I. V. Komarov. *Angew Chem Int Ed*, **2012**, accepted.
- ⁵⁶ S. Afonin. personal communication.

- ⁵⁷ V. S. Kubyshkin, I. V. Komarov, S. Afonin, P. K. Mikhailiuk, S. L. Grage, A. S. Ulrich “Trifluoromethyl-substituted α -amino acids as solid-state ^{19}F NMR labels for structural studies of membrane-bound peptides” in *Fluorine in Pharmaceutical and medicinal chemistry* (Ed.: V. Gouverneur, K. Müller), Imperial College Press, **2012**, 91-138.
- ⁵⁸ S. A. Hollingsworth, P. A. Karplus. A fresh look at the Ramachandran plot and the occurrence of standard structures in proteins. *Biomol Concepts*, **2010**, 1, 271-283.
- ⁵⁹ I. V. Komarov, A. O. Grigorenko, A. V. Turov, V. P. Khilya. Conformationally rigid cyclic α -amino acids in the design of peptidomimetics, peptide models biologically active compounds. *Russian Chem Rev*, **2004**, 73, 785-810.
- ⁶⁰ Y. K. Kang, H. Y. Choi. *Cis-trans* isomerization and puckering of proline residue. *Biophysical Chemistry*, **2004**, 111, 135-142.
- ⁶¹ I. K. Song, Y. K. Kang. Puckering transition of 4-substituted proline residues. *J Phys Chem B*, **2005**, 109, 16982-16987.
- ⁶² J. E. Hodges, R. T. Raines. Stereoelectronic and steric effect in the collagen triple helix: toward a code for strand association. *J Am Chem Soc*, **2005**, 127, 15923-15932.
- ⁶³ W. J. Wedemeyer, E. Welker, H. A. Scheraga. Proline *cis-trans* isomerization and protein folding. *Biochemistry*, **2002**, 41, 14637-14644.
- ⁶⁴ C. Melis, G. Bussi, S. C. R. Lummi, C. Molteni. *Trans-cis* switching mechanisms in proline analogues and their relevance for the gating of the 5-HT₃ receptor. *J Phys Chem B*, **2009**, 113, 12148-12153.
- ⁶⁵ Y. K. Kang. *Cis-trans* isomerization of N-acetyl-N'-methylamides of 5-methylproline and 5,5-dimethylproline. *J Mol Struct (Theochem)*, **2002**, 585, 209-221.
- ⁶⁶ S. K. Holmgren, K. M. Taylor, L. E. Bretscher, R. T. Raines. Code for collagen's stability deciphered. *Nature*, **1998**, 392, 666-667.
- ⁶⁷ M. D. Shoulders, R. T. Raines. Collagen structure and stability. *Annu Rev Biochem*, **2009**, 78, 929-958.
- ⁶⁸ G. Fischer. Chemical aspects of peptide bond isomerization. *Chem Soc Rev*, **2000**, 29, 119-127.
- ⁶⁹ G. Fischer. Peptidyl-prolyl *cis/trans* isomerases and their effectors. *Angew Chem Int Ed*, **1994**, 33, 1415-1436.
- ⁷⁰ T. H. Lee, L. Pastorino, K. P. Lu. Peptidyl-prolyl *cis-trans* isomerase Pin1 in ageing, cancer and Alzheimer disease. *Expert Rev Mol Med*, **2011**, 13, e21.
- ⁷¹ H.-L. Hyryläinen, B. C. Marciniak, K. Dahncke, M. Pietiäinen, P. Courtin, M. Vitikainen, R. Seppala, A. Otto, D. Becher, M.-P. Chapot-Chartier, O. P. Kuipers, V. P. Kontinen. Penicillin-binding protein folding is dependent on the PrsA peptidyl-prolyl *cis-trans* isomerase in *Bacillus subtilis*. *Molecular Microbiology*, **2010**, 77, 108-127.
- ⁷² G. Bissoli, R. Niñoles, S. Fresquet, S. Palombieri, E. Bueso, L. Rubio, M. J. García-Sánchez, J. A. Fernández, J. M. Mulet, R. Serrano. Peptidyl-prolyl *cis-trans* isomerase ROF2 modulates intracellular pH homeostasis in Arabidopsis. *The Plant Journal*, **2012**, 70, 704-716.
- ⁷³ G. Chaume, M.-C. Van Severen, S. Marinkovic, T. Brigaud. Straightforward synthesis of (S)- and (R)- α -trifluoromethyl proline from chiral oxazolidinones derived from ethyl trifluoropyruvate. *Org Lett*, **2006**, 8, 6123-6126.
- ⁷⁴ C. Caupène, G. Chaume, L. Richard, T. Brigaud. Iodocyclization of chiral CF₃-allylmorpholinones: a versatile strategy for the synthesis of enantiopure α -Tfm-prolines and α -Tfm-dehydroprolines. *Org Lett*, **2009**, 11, 209-212.
- ⁷⁵ G. Chaume, N. Lensen, C. Caupène, T. Brigaud. Convenient synthesis of N-terminal Tfm-dipeptides from unprotected enantiopure α -Tfm-proline and α -Tfm-alanine. *Eur J Org Chem*, **2009**, 5717-5724.
- ⁷⁶ K. Burger, K. Gaa. Eine effiziente Synthese für α -Trifluormethyl-substituierte ω -Carboxy- α -amino-säuren, *Chemiker-Zeitung*, **1990**, 114, 101-104.
- ⁷⁷ B. Koksche, D. Ullmann, H.-D. Jakubke, K. Burger. Synthesis, structure and biological activity of α -trifluoromethyl-substituted thyrotropin releasing hormone. *J Fluor Chem*, **1996**, 80, 53-57.
- ⁷⁸ S. N. Osipov, A. F. Kolomiets, A. V. Fokin. Methyl 2-N-trifluoroacetylaminotrifluoropropionate in reactions of (2+4)-cycloaddition. *J Fluor Chem*, **1989**, 45, 159.
- ⁷⁹ S. N. Osipov, O.I. Artyushin, A. F. Kolomiets, C. Bruneau, M. Picquet, P. H. Dixneuf. Synthesis of fluorine-containing cyclic α -amino acid and α -amino phosphonate derivatives *Eur J Org Chem*, **2001**, 3891-3897.
- ⁸⁰ A. V. Gulevich, I. V. Shpilevaya, V. G. Nenajdenko. The passerini reaction with CF₃-carbonyl compounds – multicomponent approach to trifluoromethyl depsipeptides. *Eur J Org Chem*, **2009**, 3801-3808.
- ⁸¹ D. Gestmann, A. J. Laurent, E. J. Laurent. Synthesis of pure enantiomers of *cis*- and *trans*-3-(trifluoromethyl)pyroglutamic esters. *J Fluor Chem*, **1996**, 80, 27-30.
- ⁸² L. Antolini, A. Forni, I. Moretti, F. Prati. Synthesis, enzymatic resolution and absolute configuration of ethyl *trans*-3-(trifluoromethyl)pyroglutamate. *Tetrahedron: Asymmetry*, **1996**, 7, 3309-3314.
- ⁸³ V. A. Soloshonok, C. Cai, V. J. Hruby, L. V. Meervelt, N. Mischenko. Stereochemically defined C-substituted glutamic acids and their derivatives. 1. An efficient asymmetric synthesis of (2S,3S)-3-methyl- and -3-trifluoromethylpyroglutamic acids. *Tetrahedron*, **1999**, 55, 12031-12044.

- ⁸⁴ J. R. Del Valle, M. Goodman. Stereoselective synthesis of Boc-protected *cis* and *trans*-4-trifluoromethylprolines by asymmetric hydrogenation reaction. *Angew Chem Int Ed*, **2002**, 41, 1600-1602.
- ⁸⁵ X.-l. Qiu, F.-l. Qing. Practical synthesis of Boc-protected *cis*-4-trifluoromethyl and *cis*-4-difluoromethyl-L-prolines. *J Org Chem*, **2002**, 67, 7162-7164.
- ⁸⁶ X.-l. Qiu, F.-l. Qing. Synthesis of Boc-protected *cis*- and *trans*-trifluoromethyl-D-prolines. *J Chem Soc, Perkin Trans 1*, **2002**, 2052-2057.
- ⁸⁷ R. Nadano, Y. Iwai, T. Mori, J. Ichikawa. Divergent chemical synthesis of prolines bearing fluorinated one-carbon units at the 4-position via nucleophilic 5-endo-*trig* cyclization. *J Org Chem*, **2006**, 71, 8748-8754.
- ⁸⁸ X.-L. Qiu, F.-L. Qing. Synthesis of *cis*-4-trifluoromethyl- and *cis*-4-difluoromethyl-L-pyrroglutamic acids. *J Org Chem*, **2003**, 68, 3614-3617.
- ⁸⁹ H. Yin, R. J. Crowder, J. P. Jones, M. W. Anders. Reaction of trifluoroacetaldehyde with amino acids, nucleotides, lipid nucleophiles, and their analogs. *Chem Res Toxicol*, **1996**, 9, 140-146.
- ⁹⁰ W. B. Jatoi, A. Bariau, C. Esparcieux, G. Figueredo, Y. Troin, J.-L. Canet. Asymmetric synthesis of (trifluoromethyl)piperidines: preparation of high enantioenriched α' -(trifluoromethyl)pipecolic acid. *Synlett*, **2008**, 1305-1308.
- ⁹¹ J. Jiang, H. Shah, R.J. DeVita. Synthesis of 4-trifluoromethylated 2-alkyl and 2,3-dialkyl-substituted azetidines. *Org Lett*, **2003**, 5, 4101-4103.
- ⁹² P. K. Mykhailiuk, S. Afonin, G. V. Palamarchuk, O. V. Shishkin, A. S. Ulrich, I. V. Komarov. Synthesis of trifluoromethyl-substituted proline analogues as ¹⁹F NMR labels for peptides in the polyproline II conformation. *Angew Chem Int Ed*, **2008**, 47, 5765-5767.
- ⁹³ J. Yu, V. Truc, P. Riebel, E. Hierl, B. Mudryk. One-pot synthesis of cyclic enecarbamates from lactam carbamates. *Tetrahedron Lett*, **2005**, 46, 4011-4013.
- ⁹⁴ P. Crabbe, A. Servantes, A. Cruz, E. Galeazzi, J. Iriarte, E. Velarde. Chemistry of difluorocyclopropyl acetates. Application of difluorocarbene chemistry to homologation reactions. *J Am Chem Soc*, **1973**, 95, 6655-6665.
- ⁹⁵ I. Nowak, J. F. Cannon, M. J. Robins. Synthesis and properties of *gem*-(difluorocyclopropyl)amine derivatives of bicyclo[n.1.0]alkanes. *Org Lett*, **2004**, 6, 4767-4770.
- ⁹⁶ E. S. Eberhardt, N. Panasik, Jr., R. T. Raines. Inductive effects on the energetics of prolyl peptide bond isomerization: implications for collagen folding and stability. *J Am Chem Soc*, **1996**, 118, 12261-12266.
- ⁹⁷ A. L. Johnson, W. A. Price, P. C. Wong, R. F. Vavala, J. M. Stump. Synthesis and pharmacology of the potent angiotensin-converting enzyme inhibitor N-[1(S)-(ethoxycarbonyl)-3-phenylprolyl]-(S)-alanyl-(S)-pyrroglutamic acid. *J Med Chem*, **1985**, 28, 1596-1602.
- ⁹⁸ X. Zhang, W. Jiang, A. C. Schmitt. A convenient and versatile synthesis of 6,5- and 7,5-fused bicyclic lactams as peptidomimetics. *Tetrahedron Lett*, **2001**, 42, 4943-4945.
- ⁹⁹ M. Bordeau, F. Frébault, M. Gobet, J.-P. Picard. Ethyl difluoro(trimethylsilyl)acetate and difluoro(trimethylsilyl)acetamides – precursors of 3,3-difluoroazetidionones. *Eur J Org Chem*, **2006**, 4147-4154.
- ¹⁰⁰ S. Hanessian, U. Reinhold, G. Gentile. The synthesis of enantiopure ω -methanopipecolic acid by a novel cyclopropanation reaction: the “flattering” of proline. *Angew Chem Int Ed*, **1997**, 36, 1881-1884.
- ¹⁰¹ L. Demange, A. Ménez, C. Dugave. Practical synthesis of Boc and Fmoc protected 4-fluoro and difluoroproline from *trans*-4-hydroxyproline. *Tetrahedron Lett*, **1998**, 39, 1169-1172.
- ¹⁰² P. Wadhvani, S. Afonin, M. Ieronimo, J. Buerck, A. S. Ulrich. Optimized protocol for synthesis of cyclic gramicidin S: starting amino acid is key to high yield. *J Org Chem*, **2006**, 71, 55-61.
- ¹⁰³ P. Wadhvani, personal communication.
- ¹⁰⁴ P. K. Mykhailiuk. PhD Thesis, **2008**, University of Karlsruhe.
- ¹⁰⁵ L. A. Carpino, H. Shroff, S. A. Triollo, E.-S. M. E. Mansour, H. Wenschuh, F. Albericio. The 2,2,4,6,7-pentamethyldihydrobenzofuran-5-sulfonyl group (Pbf) as arginine side chain protectant. *Tetrahedron Lett*, **1993**, 34, 7829-7832.
- ¹⁰⁶ A. Eisele. Diploma thesis. **2007**. University of Karlsruhe.
- ¹⁰⁷ I. Wiegand, K. Hilpert, R. E. W. Hancock. Agar and broth dilution methods to determine the minimal inhibitory concentration (MIC) of antimicrobial substances. *Nat Protoc*, **2008**, 3, 163-175.
- ¹⁰⁸ R. W. Woody. Circular dichroism. *Meth Enzymol*, **1995**, 246, 34-63
- ¹⁰⁹ N. J. Greenfield. Using circular dichroism spectra to estimate protein secondary structure. *Nat Protoc*, **2006**, 1, 2876-2890.
- ¹¹⁰ L. H. Kondejewski, M. Jelokhani-Niaraki, S. W. Farmer, B. Lix, C. M. Kay, B. D. Sykes, R. E. W. Hancock, R. S. Hodges. Dissociation of antimicrobial and hemolytic activities in cyclic peptide diastereomers by systematic alteration in amphipathicity. *J Biol Chem*, **1999**, 274, 13181-13192.
- ¹¹¹ M. Ieronimo. Diploma thesis, **2004**, University of Karlsruhe.
- ¹¹² S. Afonin, U. H. N. Dürr, P. Wadhvani, J. Salgado, A. S. Ulrich. Solid state NMR structure analysis of the antimicrobial peptide gramicidin S in lipid membranes: concentration-dependent re-alignment and self-assembly as a beta-barrel. *Top Curr Chem*, **2008**, 273, 139-154.

- ¹¹³ S. Afonin. PhD Thesis, **2004**, University of Karlsruhe.
- ¹¹⁴ A. J. Miles, B. A. Wallace. Synchrotron radiation circular dichroism spectroscopy of proteins and applications in structural and functional genomics. *Chem Soc Rev*, **2006**, 35, 39-51
- ¹¹⁵ F. Rabanal, M. D. Ludevid, M. Pons, E. Giralt. CD of proline-rich polypeptides: application to the study of the repetitive domain of maize glutelin-2. *Biopolymers*, **1993**, 33, 1019-1028.
- ¹¹⁶ S. Afonin, A. Frey, S. Bayerl, D. Fischer, P. Wadhvani, S. Weinkauff, A. S. Ulrich. The cell-penetrating peptide TAT(48-60) induces a non-lamellar phase in DMPC membranes. *ChemPhysChem*, **2006**, 7, 2134-2142.
- ¹¹⁷ M. Kawai, R. Tanaka, H. Yamamura, K. Yasuda, S. Narita, H. Umemoto, S. Ando, T. Katsu. Extra amino group-containing gramicidin S analogs possessing outer membrane-permeabilizing activity. *Chem Comm*, **2003**, 1264-1265.
- ¹¹⁸ M. Ieronimo. Diploma thesis, **2004**, University of Karlsruhe.
- ¹¹⁹ F. Heitz, F. Kaddari, N. van Mau, J. Verducci, H. Raniri Sehen, R. Lazaro. Ionic pores formed by cyclic peptides. *Biochimie*, **1989**, 71, 71-76.
- ¹²⁰ M. Wu, E. Maier, R. Benz, R. E. W. Hancock. Mechanism of interaction of different classes of cationic antimicrobial peptides with planar bilayers and with the cytoplasmic membrane of *Escherichia coli*. *Biochemistry*, **1999**, 38, 7235-7242.
- ¹²¹ Md. Ashrafuzzaman, O. S. Andersen, R. N. McElhaney. The antimicrobial peptide gramicidin S permeabilizes phospholipid bilayer membranes without forming discrete ion channels. *Biochim Biophys Acta*, **2008**, 1778, 2814-2822.
- ¹²² S. L. Grage, U. H. N. Dürr, S. Afonin, P. K. Mikhailiuk, I. V. Komarov, A. S. Ulrich. Solid state ¹⁹F NMR parameters of fluorine-labelled amino acids. Part II: aliphatic substituents. *J Mag Res*, **2008**, 191, 16-23.
- ¹²³ E. J. Prenner, R. N. A. H. Lewis, K. C. Neuman, S. M. Gruner, L. H. Kondejewski, R. S. Hodges, R. N. McElhaney. Nonlamellar phases induced by the interaction of gramicidin S with lipid bilayers. A possible relationship to membrane-disrupting activity. *Biochemistry*, **1997**, 36, 7906-7916.
- ¹²⁴ E. J. Prenner, R. N. A. H. Lewis, R. N. McElhaney. The interaction of the antimicrobial peptide gramicidin S with lipid bilayer model and biological membranes. *Biochim Biophys Acta*, **1999**, 1462, 201-221.
- ¹²⁵ N. G. Delaney, V. Madison. Unusual *cis-trans* isomerism in N-acetyl, N'-methylamide derivatives of *syn*- and *anti*-5-methylproline. *Int J Pept Prot Res*, **1982**, 19, 543-548.
- ¹²⁶ E. Beausoleil, W. D. Lubell. An examination of the steric effects of 5-*tert*-butylproline on the conformation of polyproline and the cooperative nature of type II to type I helical interconversion. *Biopolymers*, **2000**, 53, 249-256.
- ¹²⁷ Y. Nishi, S. Uchiyama, M. Doi, Y. Nishiuchi, T. Nakazawa, T. Ohkubo, Y. Kobayashi. Different effects of 4-hydroxyproline and 4-fluoroproline on the stability of collagen triple helix. *Biochemistry*, **2005**, 44, 6034-6042.
- ¹²⁸ R. Improta, C. Benzi, V. Barone. Understanding the role of stereoelectronic effects in determining collagen stability. 1. A quantum mechanical study of proline, hydroxyproline, and fluoroproline dipeptide analogues in aqueous solution. *J Am Chem Soc*, **2001**, 123, 12568-12577.
- ¹²⁹ P. Ruzza, G. Siligardi, A. Donella-Deana, A. Calderan, R. Hussain, C. Rubini, L. Cesaro, A. Osler A. Guiotto, L. A. Pinna, G. Borin. 4-fluoroproline derivative peptides: effect on PPII conformation and SH3 affinity. *J Pept Sci*, **2006**, 12, 462-471.
- ¹³⁰ M. P. Doyle, W. R. Winchester, M. N. Protopopova, A. P. Kazala, L. J. Westrum. *Org Synth*, **1996**, 73, 13.
- ¹³¹ E. Coudert, F. Acher, R. Azerad. A convenient and efficient synthesis of (2S,4R)- and (2S,4S)-4-methylglutamic acid. *Synthesis*, **1997**, 863-865.
- ¹³² <http://cssp.chemspider.com/Article.aspx?id=302>
- ¹³³ K. K. Schumacher, J. Jiang, M. M. Joullié. Synthetic studies towards astins A, B and C. Efficient synthesis of *cis*-3,4-dihydroxyprolines and (-)-(3S,4R)-dichloroproline esters. *Tetrahedron: Asymmetry*, **1998**, 9, 47-53.
- ¹³⁴ O. O. Gryorenko, I. V. Komarov, C. Cativiela. A novel approach towards 2,4-ethanoproline. *Tetrahedron: Asymmetry*, **2009**, 20, 1433-1436.
- ¹³⁵ http://www.ibg.kit.edu/nmr/downloads/MICprotocoll_30_Jan2012.pdf
- ¹³⁶ <http://ankaweb.fzk.de/>
- ¹³⁷ P. L. Gor'kov, E. Y. Chekmenev, C. Li, M. Cotten, J. J. Buffy, N. J. Traaseth, G. Veglia, W. W. Brey. Using Low-E resonators to reduce RF heating in biological samples for static solid-state NMR up to 900 MHz. *J Mag Res*, **2007**, 185, 77-93.